Universitat Autònoma de Barcelona

Dissecting KIT-downstream signaling pathways to uncover new oncogenic effectors responsible for adaptive resistance in gastrointestinal stromal tumors

Luis Alfonso García Valverde

Doctoral Thesis

Dissecting KIT-downstream signaling pathways to uncover new oncogenic effectors responsible for adaptive resistance in gastrointestinal stromal tumors

Author:

Luis Alfonso García Valverde

Directors:

Dr. César Serrano García

Dr. Joaquín Arribas López

Dr. Joan Carles Galcerán

Tutor:

Joaquín Arribas López

Program:
Biochemistry, Molecular Biology, and Biomedicine

Vall d'Hebron Institute of Oncology (VHIO)

Universitat Autònoma de Barcelona (UAB)

2022

The work presented in this thesis has been published in Oncogene (*Oncogene*) journal, form Springer Nature with DOI: 10.1038/s41388-021-02049-0.

García-Valverde A, Rosell J, Sayols S, Gómez-Peregrina D, Pilco-Janeta DF, Olivares Rivas I, et al. E3 ubiquitin ligase Atrogin-1 mediates adaptive resistance to KIT-targeted inhibition in gastrointestinal stromal tumor. Oncogene [Internet]. 2021 Oct 7 [cited 2022 Jan 24];40(48):6614–26. Available from: https://www.nature.com/articles/s41388-021-02049-0.

ABSTRACT

Introduction: The oncogenic signaling of KIT/PDGFRA is pivotal to the biology of GIST, a human malignant mesenchymal neoplasm that features myogenic differentiation. Despite targeted inhibition of these receptors provides a major clinical benefit, GIST cells adapt to KIT/PDGFRA driver suppression and eventually develop resistance, which usually occurs due to the polyclonal expansion of tumor subpopulations bearing KIT/PDGFRA secondary mutations. Remarkably, the molecular mechanisms underlying adaptive resistance in GIST remain unclear. Interestingly, KIT oncogenic signaling is largely driven by PI3K/mTOR and RAS/MAPK pathways regardless of KIT primary or secondary mutations.

Hypothesis: The dissection of KIT-downstream pathways will allow the identification of critical elements involved in the process of the adaptation to treatment, thus emerging as potential therapeutic targets to enhance the clinical efficacy of KIT/PDGFRA inhibitors.

Methods: Clinically representative GIST cell models were used, *in vitro* and *in vivo*, throughout. KIT-downstream pathways were characterized through pharmacological screenings. RNA sequencing studies identified Atrogin-1 as a critical gene co-regulated by KIT-downstream pathways. Functional studies were performed on viral gene overexpression and knock-down models to elucidate Atrogin-1 regulation and role in GIST. Proof-of-concept studies evaluated the preclinical impact of co-targeting KIT and the ubiquitin-pathway (UP) in GIST.

Results: *In vitro* and *in vivo* studies revealed PI3K/mTOR and MEK1/2 as the most essential KIT-downstream mediators. RNA sequencing underscored Atrogin-1 (aka FBXO32, a SCF E3 ubiquitin-ligase and the main effector of muscular atrophy in cachexia) as the most differentially expressed gene co-regulated by PI3K/mTOR and MEK1/2, resulting in increased expression upon inhibition of KIT, or KIT-downstream pathways. Functional studies and ChIP demonstrated that KIT and/or KIT-downstream signaling regulates Atrogin-1 expression through FOXO3a. Atrogin-1 proved to have a pro-survival role in GIST leading to apoptosis evasion and treatment adaptation upon KIT or KIT-downstream pathways inhibition through induction of cell quiescence. Atrogin-1 function was restricted to GIST cell lineage, being absent in other KIT- and kinase-driven neoplasms. Moreover, a significant increase in Atrogin-1 expression was shown in post-imatinib (IM) GIST tumor samples compared to pre-IM and also by IHC in a tissue microarray from pre- and post-IM GIST samples. Finally, combined inhibition of KIT and the UP with imatinib and TAK-243 (an UAE specific inhibitor), respectively, showed enhanced anti-tumor activity compared to single-agent IM.

Conclusions: Atrogin-1 emerges as a crucial KIT-dependent and GIST cell lineage-specific pro-survival factor, which drives adaptation to KIT targeted inhibition through induction of cell quiescence. Atrogin-1 highlights the ubiquitin proteome system as a therapeutic vulnerability. Accordingly, combined KIT and UP inhibition results in a novel therapeutic strategy to overcome tumor cell adaptation in the treatment of GIST patients.

RESUMEN

Introducción: La señalización oncogénica de KIT/PDGFRA es fundamental para la biología del GIST, una neoplasia mesenquimal maligna humana que presenta diferenciación miogénica. A pesar de que la inhibición selectiva de estos receptores proporciona un importante beneficio clínico, las células de GIST se adaptan a la supresión de KIT/PDGFRA y acaban desarrollando resistencias, que suelen producirse debido a la expansión policlonal de subpoblaciones tumorales portadoras de mutaciones secundarias en KIT/PDGFRA. Cabe destacar que el mecanismo molecular subyacente a la resistencia adaptativa en GIST sigue sin estar claro. Es importante señalar que la señalización oncogénica de KIT se canaliza en gran medida por las vías PI3K/mTOR y RAS/MAPK, independientemente del tipo de mutación primaria o secundaria en KIT.

Hipótesis: El estudio de las vías activadas por KIT permitirá identificar elementos críticos implicados en el proceso de adaptación al tratamiento, emergiendo así como potenciales dianas terapéuticas para potenciar la acción anti-tumoral de los inhibidores de KIT/PDGFRA.

Métodos: A lo largo de todo proyecto se utilizaron modelos celulares *in vitro* e *in vivo* de GIST clínicamente representativos. Se caracterizaron las vías de señalización de KIT mediante estudios farmacológicos. Los estudios de secuenciación de ARN identificaron a Atrogin-1 como un gen crítico corregulado por las vías de KIT. Se realizaron estudios funcionales en modelos de sobreexpresión y silenciamiento de genes mediante vectores virales para dilucidar la regulación de Atrogin-1 y su papel en GIST. Se realizaron estudios de prueba de concepto para evaluar el impacto preclínico de inhibición conjunta de KIT y de la cascada ubiquitinización (CU) en GIST.

Resultados: Estudios *in vitro* e *in vivo* revelaron que PI3K/mTOR y MEK1/2 son los mediadores más esenciales de las vías activadas por KIT. La secuenciación del ARN puso de manifiesto que Atrogin-1 (también conocido como FBXO32, una SCF ubiquitina-ligasa E3, y el principal efector de la atrofia muscular en la caquexia) es el gen más expresado de forma diferencial de entre todos los corregulados por las vías PI3K/mTOR y RAS/MAPK, lo que resulta en un aumento de la expresión tras la inhibición de KIT o de las vías activadas por KIT. Estudios funcionales demostraron que KIT y/o las vías activadas por KIT regulan la expresión de Atrogin-1 a través de FOXO3a. Atrogin-1 demostró tener un papel pro-supervivencia en el GIST ya que ayuda a las células de GIST a evitar la apoptosis, permitiendo la adaptación al tratamiento tras la inhibición de KIT o sus vías, todo ello a través de la inducción de la quiescencia celular. Está función de Atrogin-1 está restringida al linaje celular del GIST, ya que no se observó en otros tumores con alteraciones en KIT o en otros receptores tirosina quinasa. Además, se demostró, mediante inmunohistoquímica y datos de microarray de expresión, un aumento significativo de la expresión de Atrogin-1 en muestras tumorales de GIST tras el tratamiento con imatinib en comparación con las muestras previas al tratamiento. Por último, la inhibición combinada de KIT y la CU usando imatinib y TAK-243 (un inhibidor específico de UAE), respectivamente mostró una mayor actividad antitumoral en comparación con el tratamiento únicamente con imatinib.

Conclusiones: Atrogin-1 es un factor pro-supervivencia crucial, dependiente de KIT y específico del linaje celular de GIST, que participa en la adaptación a la inhibición dirigida de KIT a través de la inducción de la quiescencia celular. Atrogin-1 subraya la relevancia del sistema de ubiquitin-proteosoma como potencial diana terapéutica. Así, la inhibición combinada de KIT y la CU es una nueva estrategia terapéutica para revertir la adaptación de las células tumorales al tratamiento en los pacientes de GIST.

ABBREVIATIONS

4-OHT: 4-hydroxy-tamoxifen
ABL: ABL proto-oncogene non-receptor tyrosine kinase
ANO1: Anoctamin 1
ARF: alternate open reading frame
ASCO: American Society of Clinical Oncology
ATP: Adenosine triphosphate
AVA: Avapretinib
BL: baseline
Cas 3: Caspase 3
CDK4: cyclin dependent kinase 4
CDKN2A: Cyclin Dependent Kinase Inhibitor 2A
ChIP: Chromatin immunoprecipitation
CMB: Combination
CML: Chronic myeloid leukemia
CRL: cullin-RING-ub ligases
CSF1R: Colony stimulating factor 1 receptor
CT → Computed tomography
CTG: Cell-titer Glo
Cys: Cysteine
DEPDC5: DEP domain containing 5, GATOR1 subcomplex subunit
DFG: Asp-Phe-Gly
DMSO: Dimethyl sulfoxide
DNA: Deoxidribonucleic acid
DREAM complex: Dimerization partner, RB-like, E2F and multi-vulval class B
DUB: deubiquitinases enzymer
DUSP: Dual specificity protein phosphatase
EGFR: Epidermal growth factor receptor
ERK: Extracellular signal-regulated kinases
ESMO: European Society of Medical Oncology
ETV1: ETS variant transcription factor 1
EUS: Endoscopic ultrasonography
EZH2: Enhancer of zeste homolog 2
FGFR1: Fibroblast growth factor receptor 1
FLT3: FMS related receptor trysoine kinase 3
FNA: Fine-needle aspiration
FOXO: Forkhead box O
GDP: Guanosine diphosphate
GIST: Gastrointestinal stromal tumor
GRB2: Growth factor receptor bound protein 2
GTP: Guanosine triphosphate
H2AX: Histone H2AX
HBSS: Hank's balanced salt solution
HECT: Homologous to E6-AP carboxil
HIF: Hypoxia inducible factor
HSP90: Heat shock protein 90
i.v.p: Itravenous administration
ICCs: Interstitial cells of cajal
IGF: Insulin growth factor
IGFR: Insulin growth factor receptor
IM: Imatinib
INK4A: INhibitors of CDK4
KIT: KIT proto-oncogene receptor tyrosine kinase
Lys: Lysine

MAX: MYC associated factor X 1
mDOR: Median duration of response
MMR: Miss-match repair
MRI: Magnetic resonance imaging
mTOR: Mechanistic target of rapamycin Kinase
myoD: Myogenic differentiation 1
NCCN: National Comprehensive Cancer Network
NF1: Neurofibromin 1
OS: Overall survival
p.o: Oral administration
PARP: Poly(ADP-Ribose) polymerase
PCA: Principal component analysis
PDGFRA: Platelet derived growth factor A
PET: Positron emission tomography
PFS: Progression-free survival
PI3K: Phosphatidylinositol-4,5-Bisphosphate 3-Kinase
PVDF: Polyvinilydene
q.d: Every day
RBR: RING-between-RING
RE: Regorafenib
RI: Ripretinib
RING: Really interesting new gene
RNA: Ribonucleis acid
SCF: Stem cell factor
SDH: Succinate dehydrogenase
Ser: Serine
SHC: Src Homology 2 domain-containing transforming protein 1
shRNA: Shor-harpin RNA
SKP2: S-Phase kinase associated protein 2
SPRY: Sprouty
STAT3: Signal transducer and activator of transcription 3
SU: Sunitinib
Thr: threonine
TKI: Tyrosine kinase inhibitor
TNBC: Triple negative breast cancer
TP53: tumor protein 53
TRAM: Trametinib
UAE: Ubiquitin activating enzyme
Ub: Ubiquitin
UPS:Ubiquitin proteosome system
WD: withdrawn
WT: Wildtype

TABLE OF CONTENT

INDEX OF FIGURES

INDEX OF TABLES

1. INTRODUCTION

Cancer is a group of diseases, which can arise in almost any organ or tissue of the body as a result of an uncontrolled division of abnormal cells. Cancer cells are capable to grow in a self-autonomous manner and create a mass, named neoplasia or tumor, that eventually cause the death if the patient does not receive specific anti-cancer treatments. Tumors can be classified in benign or malign. Benign tumors are generally characterized by lower proliferation rates and, especially, lack of invasion of adjacent tissues. On the other hand, malign tumors are defined by their potential to spread not only to adjacent tissues, but also to distant organs.

There exist different types of cancer depending on their cell of origin. Accordingly, malignant tumors can be categorized in 4 different types, based on the embryonic origin of the cells that form the neoplasm: 1) epithelial, 2) mesenchymal, 3) hematological, and 4) derived from nervous system:

1) Epithelial malignant tumors are called carcinomas, which comes from Greek -*carcinos* (crab) and -*oma* (tumor). They are the most frequent, representing 80% of the total malignant cancers.

2) Mesenchymal malignant tumors are called sarcomas, which comes from -*sarcos* (flesh) and -*oma* (tumor). They come from non-epithelial tissues derived from embryonic mesoderm, such as bone, muscle, and blood vessel among others. They represent approximately 1% of adult cancers and 12% of pediatric tumors.

3) Hematological neoplasms are essentially leukemias and lymphomas, which derived from myeloid and lymphoid tissues, respectively.

4) Finally, malignancies derived from nervous system arise from glia cells and represent a small proportion of neoplasms.

This thesis is focused on sarcomas, and particularly, in a specific subtype of sarcoma named gastrointestinal stromal tumor (GIST).

Before 1998, GIST was commonly misclassified as leiomyosarcoma, a malignant neoplasm derived from the smooth muscle, arising in the gastrointestinal tract. In 1998,

the identification of *KIT* expression as a common feature of GISTs enabled their classification as an independent entity (1).

GIST is the most common tumor of mesenchymal origin in the gastrointestinal tract and the most common malignant sarcoma subtype. It arises from the Interstitial Cells of Cajal (ICCs). The oncogenic activation of KIT or platelet-derived growth factor receptor-α (PDGFRA) is a pivotal and shared event by most of GISTs. This dependency on KIT/PDGFRA signaling has made of this tumor a paradigmatic model of oncogenic addiction and an example of success for targeted therapy.

1.1. Epidemiology

Despite of being the most common mesenchymal tumor in the gastrointestinal tract, GIST only account for 1% of all gastrointestinal malignancies and 2.2% of gastric tumors (2–4). The annual incidence of GIST is ~1-1.3 cases/100,000, without significant differences between American and European studies (5). Of note, a French study ascertained that GIST is the most frequent histological subtype among sarcomas (6).

Overall, clinically malignant GIST displays a low incidence compared to other cancer types. However, several studies have reported the presence of micro-GISTs in up to one third of the population, after the analysis of resected whole stomachs from patients of gastric cancer (7). These micro-GISTs are smaller than 1 cm and, although they bear the same oncogenic mutations present in larger symptomatic GISTs, they rarely transform to GIST. However, micro-GISTs are mitotically inactive, frequently calcified, and they are present as a nodular ICCs overgrowth. Thus, although fundamental, other molecular alterations beyond KIT mutations are required for a micro-GIST to evolve to a malignant tumor with metastatic potential (8).

GISTs largely affect middle-aged people, with the most frequent age of diagnosis being between 60s and 70s. Furthermore, GISTs do not exhibit any predilection for sex, race, or ethnicity. Their location is predominantly in the stomach and the small bowel, although they can emerge in any portion of the gastrointestinal tract (2,5,6,9).

1.2. Origin

During the late 1990s, it was demonstrated first, the pivotal role of KIT in ICCs, and second, the broad expression of KIT by GISTs cells (1,10–12). These coetaneous findings led to the hypothesis that GISTs arise from ICCs. This hypothesis spanned and gained strength thanks to subsequent transgenic mice studies, in which it was demonstrated that KIT mutation leads to ICCs hyperplasia and GIST-like tumors development (13). Later studies further underpinned this idea with the identification of the ETS family member ETV1 as a master regulator in ICCs and GISTs cells (14). ICCs are cells of mesenchymal origin distributed along the gastrointestinal tract, mostly located surrounding the myenteric plexus, between circular and longitudinal muscular layer. They are thought to originate from a common progenitor that also gives rise to smooth muscle cells of the longitudinal muscular layer (11). They act as pacemaker controlling the peristaltic movements of the gastrointestinal tract. As previously mentioned, KIT signaling is vital in these cells. Accordingly, although it is not required for linage decision, or ICCs differentiation during embryogenesis, it is critical for the postnatal ICCs proliferation and to undertake their physiological function (12). Likewise, oncogenic KIT signaling is not only fundamental for GIST cells to originate the tumor, but it is also essential throughout the entire curse of the disease, until the most advanced stages.

1.3. Diagnosis

GISTs patients do not exhibit specific symptoms that facilitate the diagnosis. In early stages of the disease, patients are asymptomatic or present very mild symptoms. Consequently, early diagnoses are rare, and manly occur during a medical intervention due to tumor unrelated reasons (15). This is because GISTs largely affect stomach and small bowel, which are cavities susceptible to certain degree of distension without giving rise to any kind of symptoms. Nonetheless, tumor overgrowth can be sometimes associated with the emergence of related symptoms. The most frequent is gastrointestinal bleeding (overt or occult), which is associated with anemic syndrome. Abdominal mass or abdominal pain are also relatively common. Finally, neoplasm growth may cause intestinal obstruction in some cases (15,16).

Approximately, 15% of GISTs are diagnosed when they have already disseminated to distant organs or tissues forming metastases (5). As in other cancers, metastases are

the main responsible of the clinical complications, eventually causing the death of the patient. GISTs predominantly disseminate to liver and peritoneum, which can cause abdominal pain, liver failure, ascites, and intestinal obstruction, among others (17).

The utility of laboratory tests for the diagnosis is limited due to the lack of sensitive and specific findings. Blood test, although important to assess the general performance of the patient, is not helpful for the diagnosis.

The habitual procedure is to perform a computed tomography (CT). Specifically, an abdominopelvic CT using contrast (intravenous and oral) is critical to delimit the tumor size and to detect possible metastases. GISTs typically are shown as a well-delimited mass arising from the muscular layer. It is also common to observe necrotic areas due to an exacerbated growth and the lack of vascularity (18). Nevertheless, despite being certainly useful, CT imaging is not sufficiently specific for the diagnosis of GISTs, which necessarily requires of a tumor biopsy. Therefore, the use of CT imaging, together with other imaging techniques, such as magnetic resonance imaging (MRI) or positron emission tomography (PET), is restricted to initial staging, surgery monitoring and disease follow-up (19). In turn, if the tumor is accessible, the standard procedures to obtain the tumor biopsy necessary for the diagnosis are the endoscopic ultrasonography (EUS) guided biopsy or fine-needle aspiration (FNA). Tumor sample is then fixed in paraformaldehyde 4% for tissue preservation and histological analysis (18,19).

In most cases, GIST cells have spindle-cell appearance (77%). However, they can also have epithelioid morphology (8%), which is more frequent when they arise in the stomach, or mixed morphology (15%). One relevant aspect at the time of diagnosis is the mitotic rate, which is obtained counting the number of mitoses in 5 mm^2. The mitotic rate, together with the tumor size and tumor site, are the 3 prognosis features to classify GISTs according to the risk of recurrence (20) (**Table 1**).

Table 1. Risk stratification system used in GIST according to National Institute of Health criteria.

Risk category	Tumor size (cm)	Mitotic index	Primary tumor site
Very low risk	2.0	≤5	any
Low risk	2.1-5.0	≤5	any
Intermediate risk	2.1-5.0 <5 5.1-10.0	>5 0 6-10 ≤5	gastric any gastric

High risk	any >10 cm any >5.0 2.1-5.0 5.1-10.0	any any >10 >5 >5 ≤5	tumor rupture any any any non-gastric non-gastric

Histological morphology-based diagnosis is always supported by the immunohistological stain for KIT receptor (CD117). Approximately, 95% of GISTs stains for KIT, largely showing a cytoplasmatic pattern, and less frequently, a membranous or perinuclear expression (20–22). Beyond KIT, DOG1 is frequently expressed, and it is extremely helpful in the diagnosis of KIT negative GISTs, in which it is expressed in one third of the cases (23). DOG1 is calcium-activated chloride channel encoded by the gene *ANO1*, that is required for the function of ICCs. Furthermore, 80% also express CD34, a membrane protein commonly present in hematopoietic progenitors and endothelial cells, but also in some stromal mesenchymal cells, such as fibroblast (24,25).

Finally, mutational analysis of KIT and PDGFRA is highly recommended because it has a predictive value of response to tyrosine kinase inhibitors (TKIs). Additionally, the detection of mutations in KIT or PDGFRA can have a diagnostic value in those GIST negative for the immunohistochemical stain of KIT or DOG1. Although some evidence indicates the prognosis role of specific GIST molecular subtypes in the determining the course of the disease, guidelines do not recommend mutational assessment with this purpose (26–28).

1.4. Treatment

1.4.1. Localized disease

Complete surgical resection is the standard and the only potentially curative treatment for localized GIST. The objective of the procedure is the entire removal of the tumor mass with microscopically negative margins. This often entails the complete or partial removal of the stomach or intestine. Incomplete resection is associated with worse outcome and increased risk of recurrence (29). Lymphadenectomy is not of routine because nodal metastases are unusual. All GISTs greater than 2 cm must be removed as they cannot be considered benign. However, there is not a consensus about GISTs smaller than 2 cm, and it depends on other characteristics such as tumor location or mitotic rate (18,29).

Despite a complete macroscopically excision of the tumor bulk, nearly 50% of patients eventually experience disease recurrence (30). Hence, the need to reduce the size of larger tumors before surgery, together with the risk of relapse after tumor excision, especially in high-risk neoplasm, motivate the perioperative (pre- and post-) use of the specific KIT inhibitor imatinib.

1.4.2. Metastatic disease

Before 2000, there were scarce treatment options for GIST patients. The response rate to conventional agents, such as doxorubicin, was below 5% (31,32). The median overall survival (OS) of patients with advanced GIST was 18 months, with progression-free survival (PFS) of 9-12 months. Remarkably, the approval of imatinib in 2002 constituted a milestone in the treatment of advanced GIST patients.

1.4.3. Imatinib

During 1990s, the tyrosine kinase inhibitor STI-571, later known as imatinib mesylate, was developed for the treatment of chronic myelogenous leukemia (CML) as a specific inhibitor of the *Abelson Tyrosine-Protein Kinase 1* (*ABL*), which is the oncogenic driver of the disease upon gene fusion with *BCR* (33,34). The structural similarities of ABL with KIT led to explore the activity of imatinib in the latter. *In vitro* experiments showed a robust inhibition activity, which prompted further clinical studies in GISTs patients (35,36). Imatinib binds to the amino-terminal site of the kinase domain (ATP binding pocket) in the inactive conformation of the receptor. In particular, imatinib binds to the amino acids Cys673, Glu640, Asp810 and Phe811 in the Asp-Phe-Gly (DFG) motif of the activation loop. When it is bound, imatinib prevents the conformational change that enables the switch to the active conformation (32,37).

A phase I, phase II, and two phase III clinical trials evaluating the efficacy of imatinib in GIST patients yielded striking results. Overall, more than 70% of patients with advanced KIT-positive GIST experienced disease control, with a median PFS of 20-24 months. Hereby, imatinib was approved in 2001 for the treatment of metastatic or unresectable GIST, becoming the first approved TKI (17,38–40). Later studies reported that up to 30% of the patients remained progression-free for 5 years after treatment initiation, and 7-9% achieved a long-lasting response for more than 10 years (41,42). A subsequent phase

III clinical trial studied the efficacy of higher doses of imatinib, and determined that GIST patients with *KIT* exon 9 mutation benefit from higher doses of imatinib leading to increased PFS (38,43).

1.4.4. Adjuvant imatinib

As previously mentioned, nearly 50% of GIST patients develop recurrent disease after macroscopically complete resection of the tumor. For this reason, two randomized phase III clinical trials evaluated the post-surgery use of imatinib in high-risk GIST patients. Z9001 trial from the American College of Surgeons found a recurrence-free survival (RFS) of 98% after 1 year of adjuvant imatinib, compared to 83% of placebo (44). Likewise, XVIII/AIO trial from the Scandinavian Sarcoma Group ascertained a 5-year PFS of 65.6% after 36 months of adjuvant imatinib, compared to 47.9% in the 12-months group. Of note, the 5-year overall survival was 92% and 81.7%, respectively (45). Results of this study led the National Comprehensive Cancer Network (NCCN) and the European Society of Medical Oncology (ESMO) guidelines to recommend the use of adjuvant imatinib for 3 years after surgery in high and intermediate-risk patients (18,19).

1.4.5. Neoadjuvant imatinib

Based on the excellent response observed in metastatic GISTs, preoperative or neoadjuvant imatinib intends to decrease tumor size, and thus to facilitate surgical resection minimizing organ excision. Hence, it is recommended in GIST patients with large gastric GIST, or in those who have rectal and duodenal neoplasm in order to preserve the maximum quality of life. Nonetheless, there are not randomized clinical trials evaluating the neoadjuvant imatinib, and all the evidence come from the retrospective evaluation of phase II clinical trials, in which the optimal duration of treatment prior surgery was estimated in 6-12 months. (46–49). Therefore, the decision of using preoperative imatinib should be addressed on an individual basis considering different aspects, such as the specific characteristics of the tumor. The determination of KIT/PDGFRA primary mutation is also extremely useful because not all of them are equally sensitive to imatinib (49–52).

1.4.6. Resistance to imatinib

Resistance to imatinib, and other TKIs, can be divided in two types: primary and secondary. Primary resistance to imatinib, defined as disease progression within the first 6 months after initiating the therapy, occurs in 10% of cases (17). Results from clinical trials determined that it exists a correlation between genotyping and resistance. Thus, the probability of resistance to imatinib in *KIT* exon 11, *KIT* exon 9 and *KIT* wild-type (WT) GISTs is 5%, 16% and 23%, respectively (28,32). As aforementioned, GISTs harboring *KIT* exon 9 mutation require higher doses of imatinib to achieve a response. This probably accounts for some of the resistance observed in this subset of tumors (43,53). On the other hand, WT GISTs include tumors in which KIT/PDGFRA are not the tumor drivers, which might be the responsible of the resistant cases. Moreover, there are a subset of GISTs which are driven by the mutation D842V, affecting exon 18 of *PDGFRA*. This mutation renders tumor cells a strong resistance to imatinib binding by stabilizing the active conformation of the receptor (27,28,37,53,54).

Nonetheless, most patients experience an initial clinical benefit after the treatment with imatinib. Unfortunately, up to 85-90% these patients eventually develop resistance, which more commonly occur within the first 3 years. The most common mechanism of resistance is the polyclonal expansion of tumor subpopulations harboring acquired secondary mutations in KIT or PDGFRA. They occur almost exclusively in the same allele as the primary mutation (32). Secondary mutations in KIT are substitutions that fundamentally affect two domains: the ATP-binding pocket and the activation loop (32,55). Secondary mutations in the ATP-binding pocket emerge in *KIT* exons 13 and 14, although strictly, the exon 14 encodes for the 'gatekeeper' region of the kinase. These mutations are the most common at the onset of imatinib failure and confer biochemical resistance to imatinib by directly hindering drug binding to the receptor. Conversely, secondary mutations in the activation loop include a broad range of amino acid changes across *KIT* exons 17 and 18. These mutations stabilize the active conformation of the receptor hampering drug binding (21,56–58). Drug development in GIST after imatinib-failure has consisted in the investigation and successful approval of multikinase inhibitors with a broader activity against KIT oncoproteins. Notably, there exists a considerable heterogeneity in secondary resistance mutations across different patients, and within single patients and single lesions (56,59,60). This heterogeneity entails a challenge after first-line imatinib failure, as approved drugs in the second and

third lines are not effective against the entire resistance spectrum, which in turn results in modest clinical benefit (57). (Figure 1).

1.4.7. Sunitinib

Following imatinib failure, sunitinib, a multitargeted TKI with strong activity against KIT and PDGFRA, is approved as second-line treatment for metastatic GIST patients with imatinib-resistant disease. Approximately, 50% of patients yield a clinical benefit after the treatment with sunitinib, with a median PFS of 5-6 months (61,62). Importantly, the exons affected by the secondary mutations determine the response to sunitinib. Herein, *KIT* ATP-binding pocket mutations (encoded by exons 13 and 14) are extraordinarily sensitive to sunitinib, while the activity against mutations affecting the activation loop domain is scarce (53,59).

1.4.8. Regorafenib

Regorafenib is a multikinase inhibitor with activity against KIT and PDGFRA that hold the approval in the third line of treatment for metastatic GIST after sunitinib failure, depicting a PFS of 4.8 months. Like in the case of sunitinib, secondary mutations in KIT limit the activity of regorafenib (63). Thus, most mutations affecting activation loop (encoded by exons 17 and 18) are sensitive, while drug activity against mutations in the ATP-binding pocket is minimal (59).

Beyond sunitinib and regorafenib, several other multikinase inhibitors have been clinically investigated in the past for the treatment of metastatic imatinib-resistant GIST. Nilotinib, dasatinib, sorafenib or pazopanib are some of them. However, the overall clinical benefit of these agents is modest, achieving median PFS of 4-5 months. Moreover, the spectrum of activity against different KIT secondary mutations is limited in these agents (21,57).

The mechanism of action of most approved TKIs consists in directly binding to the catalytic site in the ATP-binding pocket of the phosphorylated, or the unphosphorylated inactive conformation of the kinase (type I and type II kinase inhibitors, respectively). Nonetheless, the emergence of KIT mutations prompting the transition of the receptor toward the active conformation or hampering drug binding constitute the most common resistance mechanism. This transition from the unphosphorylated inactive conformation

to the active conformation is mediated by specific amino acids within the switch pocket domain of the protein that interact and stabilize the activation loop. Thus, using drugs capable of inducing the inactive state of the protein would overcome conformational resistance mechanism rendered by KIT secondary mutations.

1.4.9. Ripretinib

Ripretinib (DCC-2618) is a type II switch-control TKI designed to target the full spectrum of KIT and PDGFRA mutations, potentially overcoming resistance due to heterogeneity of secondary KIT mutations (64). The positive results obtained in the phase III INVICTUS trial led to its approval in fourth line of treatment and beyond. In this trial, ripretinib achieved a remarkable median PFS of 6.3 months. Although response rate was approximately 10% (in line with previous TKIs), most patients experienced a clinical benefit through stabilization of the disease (65).

Ripretinib binds to both the switch pocket and the activation loop, locking KIT and PDGFRA in the inactive conformation and therefore achieving a broad inhibition of most primary and secondary mutations of these receptors. However, *in vitro* studies revealed higher IC_{50} values for multiresistant KIT D816V and its homologous PDGFRA D842V compared to other secondary mutants. Likewise, ATP-binding pocket mutations may also display lower sensitivity to ripretinib. Moreover, the low response rate observed in the clinical trial (<10%) hints scarce apoptosis induction. In this context, preliminary results of the phase III trial INTRIGUE, in which ripretinib was compared to sunitinib in second-line of treatment in advanced GIST patients, was recently reported. In the study, ripretinib did not demonstrate improvement in PFS compared to sunitinib, thereby missing the end point of the study. Whereas the PFS was 8.3 months in the intent-to-treat population and 7 months in *KIT* exon 11 mutant GIST, ripretinib achieved 8 and 8.3 months respectively (66,67). Further studies are warranted to explore whether resistance mutations may be the underlying mechanisms of resistance to this drug.

1.4.10. Avapritinib

The development of avapritinib (BLU-285) is conceptually the opposite to ripretinib. Whereas ripretinib seeks to target the full spectrum of mutations, avapritinib is specifically designed as a potent and highly selective inhibitor of all activation loop mutants. Type II inhibitors (such as imatinib, sunitinib or regorafenib, among others) bind

to KIT/PDGFRA in the inactive conformational state. However, mutations in the activation loop stabilize the active conformation. Avapritinib is a type I kinase inhibitor able to bind to the active conformation (68,69). Phase I NAVIGATOR trial evaluated the activity of avapritinib in GIST patients harboring PDGFRA D842V multiresistant mutation. Results of the trial showed a response rate of 88%, with a median duration of response (mDOR) of 27.6 months and a 12 months PFS of 81%. Given the substantial activity achieved, avapritinib was approved for the treatment of metastatic PDGFRA D842V mutant GIST, becoming the first agent ever effective in this subset of patients (70).

The NAVIGATOR trial also evaluated avapritinib in non-PDGFRA D842V GIST patients in ≥ fourth line of treatment showing overall response rate of 17%, mDOR of 10.2 months and median PFS of 3.7 months. These results led to the phase III VOYAGER trial, which compared avapritinib with regorafenib in the third line of treatment. Results did not meet primary endpoint (median PFS) as avapritinib showed a median PFS of 4.2 months, compared to 5.6 months of regorafenib (71). The similar activity of both drugs is probably due to mutational heterogeneity, with the emergence of mutations affecting other regions of the kinase domain (such as ATP-binding pocket or the gatekeeper). In this regard, a recent study highlighted mutations in the kinase domain of PDGFRA involving exons 13, 14 and 15, as the responsible for the resistance and tumor progression in D842V PDGFRA mutant GIST patients from NAVIGATOR trial (72).

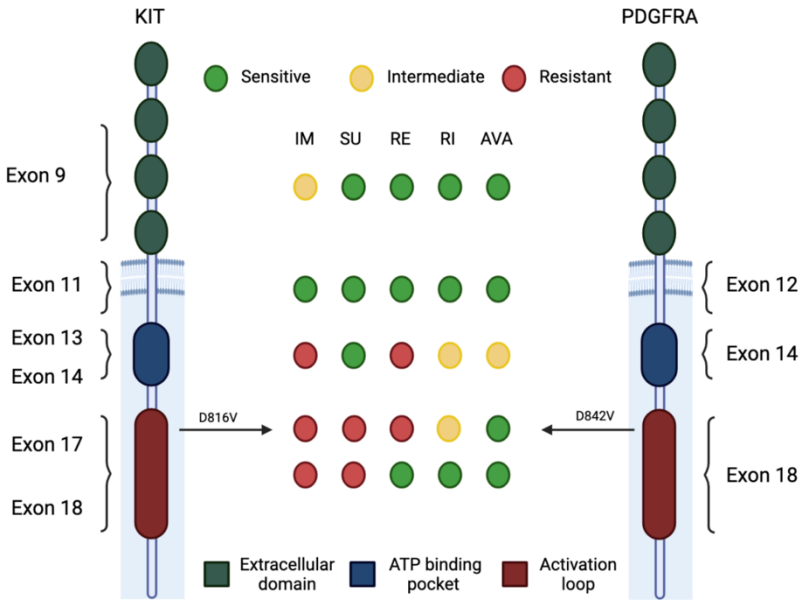

Figure 1. Oncogenic primary and secondary mutations in KIT and PDGFRA, and their specific sensitivity against approved drugs for the treatment of GIST. Drug sensitivity: sensitive (green), intermediate (yellow), resistant (red). Domains: extracellular domain (green), ATP binding pocket (blue), and activation loop (red).

1.5. Biological features

1.5.1. Oncogenic mutations in KIT

KIT is transmembrane receptor that belongs to the type III RTK family, which also includes other members such as PDGFRA, PDGFRB, macrophage colony-stimulating-factor receptor (CSF1R) and Fl cytokine receptor (FLT3). Binding of KIT ligand, the stem cell factor (SCF), to KIT results in receptor homodimerization and kinase activation. The activated kinase then cross-phosphorylate the intracellular tyrosine residues, enhancing the activation and triggering downstream signaling pathways that control main cellular functions (32,73).

Oncogenic gain-of-function mutations are present in 80-85% of GISTs. These mutations lead to ligand-independent kinase constitutive activation, which constitute a central event in GIST tumorigenesis. The most common mutations are located in the exon 11 of the gene, which encodes for the juxtamembrane domain (67%). These mutations disrupt the physiological secondary structure of this domain, which normally exerts an autoinhibitory function impeding the activation loop to switch to the active conformation of the kinase (74). Mutations in exon 11 include in-frame deletions, insertions, and substitutions (75). Some deletions are associated with shorter PFS, particularly those involving codons 557 and 558 (76,77). Beyond exon 11, and less frequently, primary mutations can also occur in exon 9, which encodes for the extracellular domain of the receptor (10%). These mutations elicit a conformational change in the extracellular domain similar to the change resulting from the SCF binding (78). Interestingly, mutations in exon 9 are mostly found in tumors arising in small and large intestine, and their transcriptomic profile differs from that of exon 11-mutant tumors (79). Rarely, primary mutations can also be found affecting exons 13 or 17, which encode for the ATP-binding pocket and the activation loop, respectively. Mutations in the ATP-binding pocket are thought to interfere with the normal autoinhibitory function of the juxtamembrane domain. Mutations in exon 17, on the other hand, enable the stabilization of the active conformation of the receptor (32,80).

1.5.2. Oncogenic mutations in PDGFRA

Oncogenic mutations in PDGFRA resulting in constitutive activation of the receptor can be found in 5-7% of GISTs (27,81). However, this proportion varies among localized and metastatic disease. Whereas PDGFRA mutant GISTs account for up to 15% of in

localized tumors, they represent only the 2% among the metastatic GISTs (82). Mutations in *PDGFRA* are mutually exclusive from those in *KIT* and predominantly occur in exon 18, encoding the activation loop domain of the receptor. In particular, D842V mutation accounts for 60% of all PDGFRA mutations. As previously explained, this substitution confers biochemical resistance to most TKI approved. Less frequently, mutations can affect juxtamembrane domain (encoded by exon 12) and the tyrosine kinase domain (encoded by exon 14). Regions affected by these mutations are homologous in KIT, and thereby they are highly sensitive to imatinib (54,83).

PDGFRA-driven GISTs show distinctive pathological features from those of KIT-mutants GISTs. These features include a predilection for the stomach, variable expression of KIT, differences in the expression profile, and generally lower malignancy potential, including smaller size and lower mitotic rate. Decreased malignant potential might explain the differences in proportion among localized and metastatic GISTs (32).

1.5.3. GIST wild-type

GISTs lacking KIT or PDGFRA mutations account for approximately 10% of all GISTs, and they are grouped as WT GISTs. WT GISTs are clinically indistinguishable from KIT/PDGFRA mutants GISTs, as they have an identical morphology and occur anywhere in the gastrointestinal tract (84). Moreover, WT GISTs may also display KIT expression and activation despite not harboring KIT mutations. However, the molecular mechanisms underlying this activation remains unclear. WT GISTs can be biologically divided in two groups depending on the expression of succinate dehydrogenase (SDH) enzyme.

1.5.3.1. SDH-Deficient GIST

SDH-ubiquinone complex II is a component of the Krebs cycle and the mitochondrial respiratory chain formed by four subunits: A, B, C and D. It is responsible for the oxidation of succinate to fumarate. Inactivation of any of the components encompasses the destabilization and loss of function of the complex. SDH mutations trigger a recurrent DNA hypermethylation phenotype, which may represent the molecular mechanisms underlaying the oncogenic signaling (85,86). Accordingly, unlike KIT mutant GISTs, WT GISTs progress to malignancy without acquiring large-scale chromosomal aberrations (87). Hypoxia-inducible factor (HIF) and insulin growth factor receptor (IGFR) pathways have been found commonly hyperactivated in SDH-deficient GISTs (32). Most commonly

altered subunits are SDHA and SDHB. SDHB-deficient tumors usually present in younger patients as gastric tumor, with epithelioid morphology, multifocal and predominantly in women (88). On the other hand, SDHA-negative WT GISTs affect predominantly to male in the fourth decade and they follow a slower course (89).

1.5.3.2. SDH-intact GIST

WT GISTs that are not SDH deficient usually harbor genetic events leading to RAS/MEK/ERK pathway activation. Almost 10% of neurofibromatosis type I patients, which involve the germinal inactivation of *NF1* gene (negative regulator of RAS/MAPK pathway) eventually develop a GIST during their lifetime (90). Furthermore, mutations in *RAS* gene, although rarely, have been found in GIST patients (91). Finally, oncogenic BRAF mutations are found in up to 2% of all GISTs and between 5 to 15% of SHD-positive WT GISTs (92).

This thesis exclusively explores the biology of KIT-driven GISTs and deepens into the oncogenic program initiated by this receptor.

1.5.4. Cytogenetic progression

Oncogenic activation of KIT/PDGFRA is an early and necessary event in most GISTs. Moreover, KIT/PDGFRA oncogenic signaling continues to be fundamental throughout the entire course of the disease. Nonetheless, KIT/PDGFRA mutations are not sufficient to prompt a malignant behavior, and thereby other genetic events are required for the transformation of a micro-GIST into a malignant tumor. Monosomy of chromosome 14, or partial loss 14q is found in up 70% of GISTs irrespective of mutation in KIT or PDGFRA (32,93,94). Additionally, loss of the long arm of chromosome 22 is also observed in 50% of GISTs (32,94–96). Interestingly, these alterations are found regardless the histological grade of the tumor, suggesting that both are early events during the oncogenesis. On the other hand, losses on chromosomes 1p, 9p, 11p and 17p, although less common, also occur, and they are associated with malignancy. Furthermore, gains on chromosomes 8q, 3q and 17q are relatively common among metastatic GISTs (32,93,96,97). Some of the genes within the regions affected by these gains and losses have been identified during the past years. Located in the chromosome 14q is *MYC associated factor X* (*MAX*), a transcription factor involved in cell-cycle regulation. MAX

inactivation is present in approximately 50% of all GISTs, including low risk and micro-GISTs, emerging as an early event in the development of the tumor. *MAX* genomic inactivation was associated to *Cyclin Dependent Kinase Inhibitor 2A* (CDNK2A*)* silencing even in the absence of coding sequence deletion. Surprisingly, MAX restauration was not associated with a significant enrichment of MYC-related expression signatures or with altered sensitivity to MYC:MAX inhibitors (98). Additionally, inactivating mutations in DEP *Domain Containing 5, GATOR1 Subcomplex Subunit (DEPDC5)*, located in chromosome 22q, has been recently reported to occur in more than 16% of GIST patients. DPEDC5 inactivation promotes GIST tumor growth *in vitro* and *in vivo*, and its inhibition results in cell proliferation impairment through mTORC1 signaling pathway suppression (99). Additionally, loss of *CDKN2A*, located in chromosome 9p, occurs in approximately 50% of metastatic GISTs and it is associated with worse prognosis. *CDKN2A* encodes for INK4A and ARF, which participate in the inhibition of CDK4 and p53 stabilization, respectively (100–103). Finally, the loss dystrophin, encoded by *DMD* gene (located in chromosome Xp), is universally present at late stages in high-risk GISTs. Dystrophin has been described to prevent cell migration and invasion, hereby acting as tumor suppressor. Thus, inactivation of dystrophin emerges as a crucial step for a GISTs to undergo metastatic (104).

Further studies are warranted to elucidate new genes comprised within the regions affected by these chromosomal changes, that participate during the malignant transformation of GISTs.

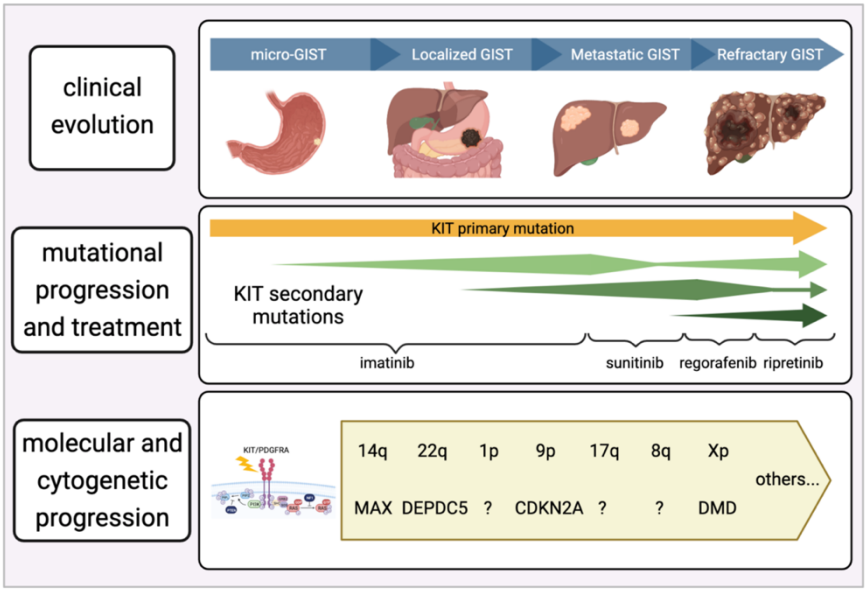

Figure 2. Clinical, mutational and cytogenetic progression of GIST. Modified from (60).

1.5.5. Secondary mutations in KIT

As mentioned above, GISTs display an exquisite addiction to KIT/PDGFRA oncogenic signaling (section 1.5.4). This phenomenon explains that in up to 90% of the cases the mechanism of resistance to imatinib entails the expansion of tumor clones bearing secondary mutations in KIT that render resistance. Resistant mutations occur in two regions of the kinase domain: the ATP-binding pocket (encoded by exons 13 and 14) and the activation loop (encoded by exons 17 and 18) (21,59). Therapeutic strategies for the treatment of GIST patients after progression of imatinib seek to inhibit new KIT mutants. Unfortunately, there is a substantial heterogeneity of secondary mutations across different patients, and within single patients and single lesions. This heterogeneity represents a clinical challenge, as approved drugs in second and third lines are not effective against the entire spectrum of mutations, and they only achieve a modest clinical benefit (57,60). The recent approval of ripretinib in fourth line of treatment provides an additional therapeutic opportunity due to its broader activity, but patients eventually progress with no further options.

1.5.6. Oncogenic signaling pathways in GIST

GIST exhibits a unique core of transcription factors that rely on a well-preserved KIT/PDGFRA-driven program throughout all the stages of the disease. A wealth of evidence support that this oncogenic program is essentially transduced through RAS/MAPK and PI3K/AKT/mTOR pathways, which are the ultimate responsible for the proliferation and survival of tumor cells. First evidence regarding the reliance of GIST upon these two pathways come from tumor extracts from GIST tumors, in which both pathways were found systematically activated (32,84,105–107). Other pathways have been proposed to play an oncogenic function in GIST, such as STAT3, Src kinase or AXL (108,109). However, their specific biological role is yet to be understood. Importantly, RAS/MAPK and PI3K/AKT/mTOR activation occurs irrespective of whether KIT/PDGFRA mutations are imatinib sensitive or imatinib resistant. The prominent role of both pathways was further validated in several *in vitro* and *in vivo* studies over the years, in which their potential as therapeutic target has been also explored.

RAS/MAPK. KIT autophosphorylation enables the assembly of SHC, GRB2 and SOS scaffold proteins, which in turn, prompts the switch of RAS-GDP to RAS-GTP, herby triggering pathway activation. MAPK pathway governs the expression of the ETS-family

transcription factor ETV1, a linage-specific master regulator in GIST. ETV1 is critical for the development and maintenance of ICCs, and also for GIST oncogenesis, by regulating KIT expression (110,111). Moreover, transcriptomic studies unveiled that several sprouty and dual-specific phosphatase (DUSP) family members – known to act as a negative regulators of the MAPK pathway – are among the most transcriptionally downregulated genes upon KIT inhibition (112). Furthermore, different studies have ascertained that genomic events leading to RAS/MAPK pathway dysregulation (i.e., RAS and RAF mutations, or NF1 inactivation) are able to supplant the oncogenic program initiated by KIT, either acting as tumor drivers, or participating in the resistance to KIT-targeted inhibition (90–92). Based on *in vivo* promising results of MAPK inhibition combined with imatinib, a clinical phase I clinical trial was conducted testing this combination in metastatic GIST patients (111). Herein, all patients harboring imatinib-resistant mutations progressed withing 16 weeks (113). However, results in previously untreated GISTs led to a phase II trial evaluating the combination in front-line in advanced GISTs. Promising results were recently reported, in which the combination appears to be highly effective in treatment-naïve GIST, with expected and manageable long-term treatment-associated toxicities (114). Hence, this strategy warrants further evaluation in a direct comparison with imatinib in front-line treatment. According to this principle, it has been recently reported the enhanced proapoptotic activity *in vitro* and *in vivo* of the combination of ripretinib and MEK1/2 inhibitors in a panel of imatinib-sensitive and imatinib-resistant GIST models. Moreover, the combination prevented the emergence of resistant population, even after long-term drug removal buttressing the potential of this therapeutic approach (115).

PI3K/AKT/mTOR. Similar to MAPK pathway, KIT autophosphorylation enables PI3K recruitment and activation, thus triggering pathway activation. PI3K pathway has been shown to be crucial in GIST for tumor initiation and survival (116). Additionally, several preclinical studies underlined the relevance of this pathway for cell proliferation and apoptosis evasion in GIST cells (117–119). In these studies, PI3K inhibition showed strong anti-proliferative and proapoptotic effect - both *in vitro* and *in vivo* – either in monotherapy or in combination with imatinib, thereby emerging as an appealing therapeutic strategy. These observations established the preclinical rationale that encouraged the clinical development of several PI3K/mTOR pathway inhibitors that were eventually tested in metastatic GIST patients as single-agent or in combination with imatinib. Results of these trials published so far showed scarce clinical benefit of the

combination in imatinib-resistant patients (120–122). However, most results are yet to be reported. In this regard, our group undertook a study evaluating copanlisib (a pan-PI3K inhibitor approved for the treatment of relapsed follicular lymphoma) in combination with imatinib in imatinib-sensitive and imatinib-resistant GIST models both *in vitro* and *in vivo.* Consistently to that observed in patients, the combination was highly effective in imatinib-sensitive, but not in imatinib resistant models (123).

Overall, single-pathway inhibition is unlikely to effectively suppress GIST proliferation since KIT remains active and its oncogenic signaling is funneled through the non-suppressed pathway. In this context, combined KIT and KIT-downstream pathways effective inhibition with either PI3K/mTOR or RAS/MPAK inhibitors arises as an attractive therapeutic strategy in advanced or metastatic GIST patients. Nonetheless, based on preclinical and clinical data, the use of imatinib circumscribe the clinical benefit to patients lacking secondary resistant mutations in KIT. In this regard, the use of an agent with a broad activity against most of KIT secondary mutations would extend this benefit to those imatinib-resistant patients.

Concomitant inhibition of the two critical KIT downstream pathways poses as another appealing approach because it would be potentially effective against all tumor cell subpopulations regardless the mutational status of KIT. It would even be effective in those subpopulations in which pathway coactivating mutations act as an oncogenic driver or as a resistance mechanism (21,91,124,125). However, clinical development of this strategy is challenging because the clinical dose of most of TKIs is defined based on toxicity, rather than on target inhibition. Thus, combination of TKIs at their effective doses will most likely result in enhanced overlapping adverse events, or decreased dose intensity with the risk of combining ineffective doses of active compounds. Hence, preclinical modeling of more creative dosing schedules will be required for its safe and effective implementation into clinic (126).

FOXO transcription factors. The FOXO family is a subclass of Forkhead transcription factors (TFs) characterized by a winged helix DNA binding domain known as Forkhead box (127). In humans, the family entails four different members: FOXO1, FOXO3, FOXO4 and FOXO6. The expression of the different members is tissue-specific, and they commonly function as transcriptional activators. They are predominantly regulated by growth factors, of which insulin and insulin-like growth factor (IGF) are the most

extensively studied. In the presence of insulin, or IGF, the PI3K/AKT/mTOR pathway gets activated and AKT phosphorylates FOXO TFs at specific conserved residues, preventing their translocation into the nucleus, and leading to their subsequent degradation via ubiquitin-proteosome system. During a starving situation, PI3K/AKT/mTOR pathway remains inactive due to the absence of insulin or IGF. Thus, lack of phosphorylation allows FOXO TFs to translocate to the nucleus, where they trigger a specific transcriptional program (128–130). Beyond AKT, FOXO TFs can be also post-translationally modified at different residues by many other proteins that become activated upon different stimuli and in different cell contexts, including AMPK, JNK, p38, and more remarkably ERK (131–137). Hence, FOXO TFs can initiate different transcriptional responses depending on the protein responsible of their post-translational modification. Accordingly, genes specifically regulated by FOXO TFs are involved in a wide variety of biological processes, such as autophagy, metabolic homeostasis, cell cycle and apoptosis.

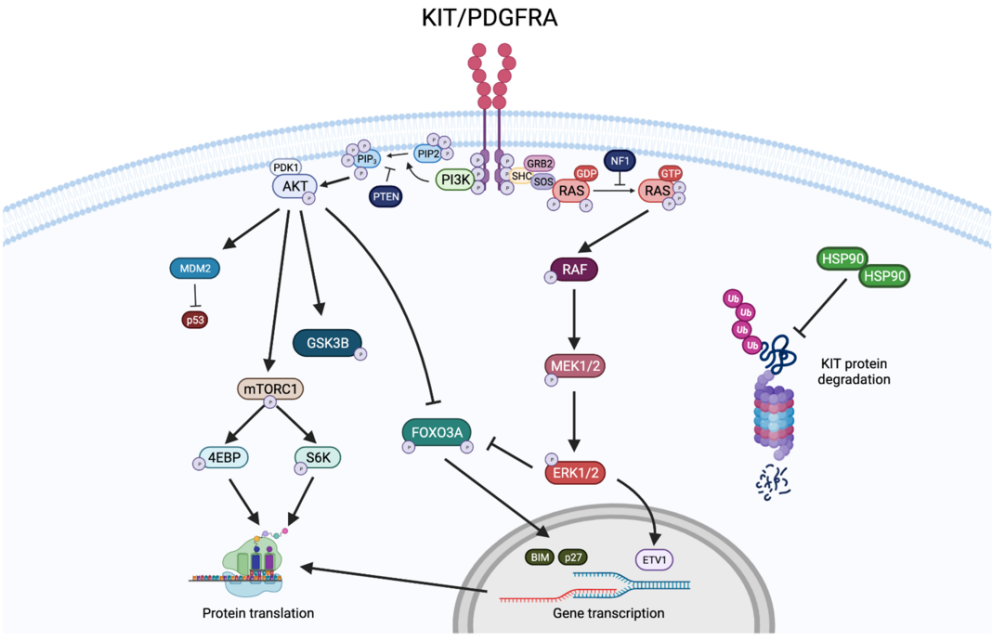

Figure 3. KIT-downstream signaling pathways. Crucial effectors in the oncogenic signaling and the main mediators within each pathways are depicted.

Despite the prominent role that play FOXO TFs in several types of cancers, their role in GIST remains widely unknown. In this regard, it has only been reported the role of FOXO3 as regulator of the expression of the proapoptotic factor BIM, which participates in the apoptotic program triggered by the specific inhibition of KIT (138). Therefore, further studies exploring the different functions of this family of transcription factors are needed to improve our understanding of their role in GIST.

1.6. Mechanisms of treatment adaptation

As previously mentioned, most GIST patients experience a clinical benefit derived from KIT targeted inhibition. Nonetheless, TKIs rarely achieve complete responses, and viable residual GIST cells are invariably present even in responding patients, eventually leading to the emergence of TKI-resistance. Several mechanisms have been described to participate in the attenuation of anti-tumor activity of imatinib, such as RTK cross-activation, or cell quiescence induction.

1.6.1. RTK cross-activation

Several studies have suggested that KIT oncogenic signaling results in an inhibition or functional attenuation feedback of other RTKs, such as fibroblast growth factor receptor 1 (FGFR1), MET proto-oncogene, receptor tyrosine kinase (MET) or AXL Receptor Tyrosine Kinase (AXL). FGFR1 was found to be commonly expressed in GISTs compared to other tumors in transcriptomics studies that included tumors from 42 different histological subtypes. Additionally, it was also expressed in a panel of primary GIST cell lines. Under basal conditions, KIT signaling prevents FGFR1 activation through KIT-MAPK axis. However, KIT inhibition with imatinib releases the negative feedback, allowing FGFR1 activation via FGF2 ligand paracrine secretion. Activated FGFR1 restores MAPK signaling, mitigating the effect of imatinib. In this context, combined inhibition of KIT and FGFR1 resulted in increased apoptosis induction in GIST cells both *in vitro* and *in vivo* (112). This encouraging result led to the clinical evaluation of the combination of imatinib with the pan-FGFR inhibitor BGJ398 on heavily pre-treated GIST patients in a phase Ib trial. Results were recently published showing >32 weeks of stable disease in 25% of patients. Unfortunately, the trial was concluded due to sponsor support withdrawal before dosing schedule was identified (139). On the other hand, MET has been also reported to be expressed and activated in GIST cell lines and patient samples. In this study the authors found increased MET phosphorylation upon KIT targeted inhibition. Moreover, combined MET and KIT inhibition resulted in enhanced anti-tumor activity *in vitro* and *in vivo* (140). Preclinical evidence supported further clinical evaluation of the MET inhibitor cabozantinib in a phase II trial. Results showed 24/41 patients being progression-free after 12 weeks of treatment. Moreover, the objective response was 14% with an encouraging disease control of 82% (141). Besides FGFR1 and MET, AXL has been also proposed to play a role in the adaptation of GIST cells to TKI therapy. Specifically, AXL was found overexpressed and phosphorylated in preclinical imatinib-

resistant models displaying low expression of KIT. The same overexpression pattern was observed in two imatinib-resistant GIST patients showing low expression of KIT. Overall, these findings suggest a role of AXL in the adaptation of GISTs cells to KIT targeted inhibition (109,142).

Cross-activation of RTKs has been also reported in several other kinase-driven cancers as a mechanism of adaptation to the treatment. Interestingly, proteolytic shedding has been demonstrated to mediate RTK activation in several MAPK-driven tumors, such as BRAF mutated melanoma or triple-negative breast cancer (TNBC) (143,144). Specifically, activated MAPK signaling drives proteolytic processing of RTK that are then secreted and exert a paracrine inhibition of different RTKs. TKI-mediated pathway inhibition impedes proteases activation, hereby decreasing RTK proteolytic processing and shedding. The absence of circulating RTK facilitates the eventual cross-activation of different RTKs that restore oncogenic signaling, which enables tumor cells to evade the apoptosis and to adapt to the treatment.

Collectively, RTK cross-activation has been shown to be responsible of oncogenic signaling restoring in different tumor types. Thus, it emerges as a mechanism of tumor cell adaptation that attenuates anti-tumor responses in cancer patients, including GIST.

1.6.2. Induction of cell quiescence

The induction of cell quiescence as a mechanism of adaptation to targeted therapies has been widely reported across several cancer subtypes. In GIST, several studies have underpinned a major role of this mechanism in the adaptation to KIT targeted inhibition. Cell quiescence is a reversible state in which cells cease to proliferate but retain the ability to resume cell cycle progression. The process entails a halt of cell cycle machinery, and the accumulation of tumor cells at G0 phase. It is common among some adult stem cells, which are maintained in a quiescent state but can be rapidly activated upon certain stimuli. Aforementioned studies demonstrated that there is a small group of cells in GIST tumors that do not undergo apoptosis upon imatinib treatment. These cells are not proliferative, and they display high levels of protein $p27^{kip1}$ (a well-known quiescence marker) and low levels of the E3 ligase SKP2 (negative regulator of $p27^{kip1}$) (145). Subsequent studies also revealed the contribution of the so-called DREAM complex (comprised by several proteins). DREAM complex mediates the inhibition of

E2F transcription factor, which plays an important role promoting cell cycle progression (146). Furthermore, autophagy induction has been shown to be pivotal for survival of imatinib-induced quiescence cells. In a study performed in GIST patient samples, imatinib treatment resulted in increased autophagosome formation, which inversely correlated with apoptosis induction. Additional *in vitro* experiments demonstrated that quiescent cells that had escaped from apoptosis displayed higher rates of autophagosome formation, confirming the critical role of autophagy within this subset of cells. Hence, cell cycle arrest represents a protective state that prevents apoptosis induction on GIST cells upon KIT inhibition (147).

1.6.3. Pro-mutagenic state

As mentioned earlier, viable residual tumor cells are invariably found even in responding GIST patients and they are thought to be the niche responsible of the emergence of resistant populations. However, the molecular mechanism underlying the acquisition of this resistance remains controversial. The conventional view is that tumor recurrence occurs because resistant clones are already present before treatment initiation (148). Accordingly, the time to relapse is merely the time needed for these resistant clones to expand. Conversely, there is a different view that considers that resistant clones emerge due to the selective pressure exerted by a certain drug over tumor cells. Interestingly, several studies have recently delved into this latter view. In this regard, EGFR/BRAF inhibition was found to down-regulate mismatch-repair (MMR) genes and homologous repair genes (HR), while upregulate error-prone polymerases, in colorectal cancer persister cells, both *in vitro* and *in vivo*. This mechanism would create a propitious context for the appearance of resistant mutations that foster tumor recurrence (149). A later study identified mTOR as one of the main drivers of the so called “stress-induced mutagenesis”, which consists on cell cycle slowing to generate a permissive mutagenic state defined by an up-regulation of the error-prone polymerase, and a down-regulation of DNA-repair pathways (150). Hence, these studies provide strong evidence of the feasibility that the emergence of drug-resistant populations can occur due to a transient mutagenic state in tumor persister cells, that enables the acquisition of resistant mutations.

This thesis deepens into the process of persister cell generation in GIST. Specifically, it uncovers a new effector involved in cell quiescence induction in GIST cells, as a

mechanism to evade apoptosis after KIT targeted inhibition. Particularly, this mediator belongs to the ubiquitin proteosome system, highlighting the essential role of this system.

1.7. Ubiquitin Proteosome System

The ubiquitin-proteosome system (UPS) comprises a network of enzymes that is responsible for protein homeostasis. UPS mediates the degradation of 80-90% of intracellular proteins, while the remainder proteins are degraded by the lysosome. The UPS consists of ubiquitin (Ub), Ub-activating enzymes (E1), Ub-conjugating enzymes (E2), Ub ligases (E3), deubiquitinases enzymes (DUB) and the proteosome. Protein substrates are modified with ubiquitin, which serves as a tag for the recognition by 26s proteosome, which is, ultimately, the responsible of substrate proteolysis. Ubiquitin is conjugated to the substrate through a multistep cascade involving E1, E2 and E3 enzymes. Specifically, E1 enzymes activate Ub through an ATP-dependent thioester bond between the C-terminal of Ub and a cysteine (Cys) residue in the catalytic site of the E1 enzyme. Ub is then transferred to an E2 enzyme, also forming a thioester bond between them, after which, through cooperation between an E2 and an E3 enzyme, the activated Ub is transferred to a lysine within the target substrate (151) (**Figure 4**).

As aforementioned, 26S proteosome is responsible for the degradation of most intracellular protein. 26S proteosome is a multiprotein complex constituted by a 20S tube-like proteolytic core particle and two 19S regulatory particles at both ends (152). Ubiquitin contains seven lysine (Lys) residues, all of which can covalently attach to other ubiquitins and form linear or branched Ub chains. The lysine involved in the poly-Ub chain formation define the consequence of the ubiquitination. Lys48-linked-poly-Ub chains tag proteins for proteasomal degradation, while Lys63-linked-poly-Ub chains are related with non-proteasomal signaling like endocytic trafficking, DNA replication, and signal transduction (153).

In the human proteome there are 2 E1 enzymes, the ubiquitin activating enzyme (UAE, also known as UBE1), which is responsible of >99% of cellular ubiquitin, and UBA61, which is responsible for charging <1% of ubiquitin. E2 enzymes comprise 40 different proteins, while there are more than 600 E3 enzymes. Lasts are three different groups according to their Ub transfer mechanism from E2 enzyme to the substrate: 1) the really interesting new gene (RING), 2) the homologous to E6-AP carboxil terminus (HECT),

and 3) the RING-between-RING (RBR) (154). RING E3 ligases entail the largest family, and they mediate the transfer of Ub from the E2 enzyme to the substrate without establishing bonds with the Ub (155). They can be subdivided into single subunit or multi-subunit. One example of the latest is the cullin-RING-Ub ligases (CRLs), which allow one core scaffold to regulate the ubiquitylation of diverse substrates through variable substrate recognition (156).

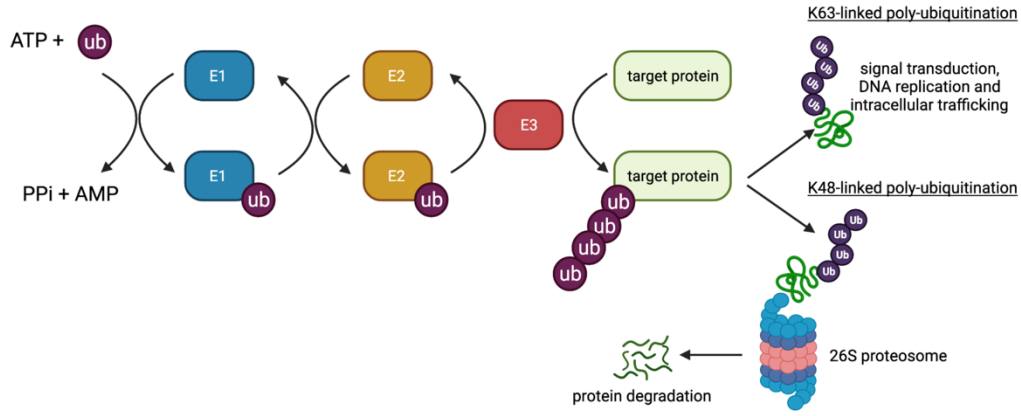

Figure 4. Representation of the ubiquitin-proteosome system cascade.

1.7.1. UPS in cancer

The UPS plays an important role in different diseases, including cancer. Deregulation of the UPS can contribute to onco-pathogenesis through several mechanisms. Among the different members of the UPS, E3 ligases have been revealed to conduct important functions in various cancer by regulating the degradation of tumor promoters, tumor suppressors, or by modulating cell-cycle progression, such as the case of Mdm2, SKP2 or FBXW7, among others (157). Hence, there is an increasing interest in the study and characterization of the oncogenic function of this family of proteins. Furthermore, cancer cells are more dependent on the UPS due to their increased metabolism and protein turnover. Their higher proliferation rate is intrinsically associated with an increased rate of misfolded or unfolded protein production. Therefore, the UPS emerges as an appealing therapeutic target for cancer treatment.

1.7.2. UPS in GIST

Different studies have underpinned the prominent role of UPS in GIST over the years. Heat shock protein 90 (HSP90) is a protein that belongs to chaperone family of proteins,

and plays an essential role in cancer homeostasis by regulating conformational maturation and stability of many oncoproteins, including KIT and PDGFRA, while preventing proteosome degradation (158). *In vitro* and *in vivo* experiments showed that HSP90 inhibition results in KIT destabilization and degradation, and subsequent downstream signaling suppression regardless KIT primary or secondary mutation (159–162). These robust preclinical studies prompted several clinical trials (phase I, II and III) testing different HSP90 inhibitors. Results from these trials evidenced generally acceptable toxicities, but limited anti-tumor activity, restricted to some partial response and a few disease stabilizations (163–168). Nonetheless, more selective inhibitors development and dosage optimization might improve the response rate and limit the potential toxicities.

Additional evidence supporting the relevance of the UPS for GIST cells come from the prominent role of the histone protein H2AX in apoptosis induction upon imatinib treatment. In untreated GIST cells, H2AX is maintained at low levels through KIT-PI3K/mTOR axis, which stimulates H2AX poly-ubiquitination and subsequent proteosome degradation. KIT inhibition after imatinib treatment suppresses KIT-PI3K/mTOR axis, impairing UPS-mediated H2AX degradation, and causing H2AX accumulation, which enhance cell apoptosis (169). This finding paved the way for subsequent preclinical studies evaluating proteosome inhibition as a therapeutic strategy for GIST patients (170). In these studies, proteosome inhibition resulted in potent apoptosis induction, accompanied by H2AX accumulation, and unexpectedly, with a transcriptional downregulation of KIT. Of note, the same results and mechanism of action were obtained using different proteosome inhibitors. Nevertheless, despite the promising results observed *in vitro*, the scarce clinical activity displayed by the proteosome inhibitor bortezomib in solid tumors, together with the marked associated toxicities, such as irreversible neuropathy, have limited the clinical development of such strategy in GIST (171–174). Further work evaluating the activity of second-generation proteosome inhibitors with a better safety profile, such as carfilzomib or ixazomib is required to warrant the value of these agents for GIST treatment (175).

Collectively, these studies highlight the fundamental role of the UPS in GIST cell biology, and hereby demonstrate its potential as a therapeutic target. Importantly, this strategy would not be affected by KIT mutational status, thus overcoming resistance associated with mutational heterogeneity.

This thesis is particularly focused on the role undertaken by the E3 ligase Atrogin-1 in the process of therapeutic adaptation of GIST cells to KIT-targeted inhibition.

1.8. Atrogin-1

Atrogin-1 was originally identified as a muscle-specific gene, and it was shown to be the main driver of muscle atrophy (176). Atrogin-1 is a Cullin-RING E3 ubiquitin ligase. It contains an F-box domain that is commonly found in a specific family of proteins, most of which operate as a component of the SCF (Skip1, Cullin, F-box protein) family of ubiquitin ligases. The F-box domain serves as an adaptor that binds to the Skp1 protein, which in turn binds to cullin (157,177). Atrogin-1 lacks the common motifs present in other F-box proteins that are known to interact to their substrate, such as leucine-rich WD40 repeats. However, it contains a class-II PDZ domain, which is thought to interact with specific sequences at carboxyl terminus of the target protein. Additionally, Atrogin-1 also contains two nuclear localization signals and one nuclear exporting sequence, which enable the interaction with nuclear proteins, such as transcription factors (176).

Atrogin-1 was originally identified for being the most highly expressed gene during muscle atrophy (176). Subsequent studies corroborated its critical participation during muscle atrophy under different conditions, including cancer (178–182). Accordingly, the Eukaryotic Translation Initiation Factor 3 Subunit F (EI3F-f) and myogenic regulatory factor D, myoD have been revealed to be two important targets of Atrogin-1 in skeletal muscle (183–186). In muscle cells, Atogin-1 is under the transcriptional regulation of a member of the Forkhead box O class of transcription factors. Specifically, Atrogin-1 is transcriptionally regulated by FOXO3A, which in turn is negatively regulated by PI3K/AKT pathway. Under basal conditions AKT phosphorylates FOXO3A in specific residues, preventing its translocation to the nucleus and causing its subsequent degradation. During muscle atrophy, PI3K/AKT pathway activity decreases, which enables unphosphorylated FOXO3A to translocate into the nucleus, where it promotes Atrogin-1 transcription (129,187–189).

Beyond muscle atrophy, few studies have explored the role of Atrogin-1 in cancer. Its precise contribution to tumorigenesis appears to be cell context-dependent and remains poorly understood. Atrogin-1 expression is impaired by promoter methylation in ovarian,

esophageal and gastric carcinoma, and it is associated with shorter PFS (188,190). Namely, in ovarian carcinoma cell lines, Atrogin-1 expression restoring prevented colony formation and cell proliferation *in vitro*, and tumor growth *in vivo* (188). Likewise, c-MYC was identified as a target of Atrogin-1 in ovarian and colorectal cancer cell lines. In this study, the expression of Atrogin-1 specifically tagged c-MYC for proteasomal degradation, which resulted in cell proliferation impairment (191). Moreover, Atrogin-1 was demonstrated to suppress tumorigenesis in breast cancer cell lines by targeting the Krüppel-like factor 4 (KLF4) for proteasomal degradation. Finally, Atrogin-1 expression has been found to be repressed by Enhancer of Zeste 2 Polycomb Repressive Complex 2 (EZH2) in alveolar rhabdomyosarcoma, lung and breast cancer cell lines (192–194). In these studies, Atrogin-1 expression turned out to be essential to generate apoptotic cell-death after the inhibition of EZH2 (192,193).

Collectively, Atrogin-1 seems to act as tumor suppressor in different tumor contexts, although its specific role remains poorly understood. This thesis dissects the role of Atrogin-1 in a different tumor subtype, such as GIST, and deepens on its specific regulation within this specific cell context. Of note, GIST features myogenic differentiation and muscle-related genes, such as Dystrophin, are known to be involved in GIST progression (104,195).

2. HYPOTHESIS

Mutational heterogeneity and treatment adaptation currently represent two major challenges for the treatment of GIST. Therefore, there is a compelling need to identify novel molecular targets that can provide new treatment opportunities for these patients. In this context, an in-depth characterization of the two main KIT-downstream pathways, PI3K/AKT/mTOR and RAS/MAPK, will allow to identify key oncogenic signaling effectors that might serve as new therapeutic targets. Indeed, it is conceivable that certain molecules are critically regulated by both pathways regardless the type of KIT primary or secondary mutations, potentially playing essential functions related to GIST cell survival. Therefore, I hypothesize that the identification and functional characterization of these GIST-specific molecules co-regulated by both pathways through targeted inhibition will contribute to improve our understanding of the process of tumor cell adaptation to KIT driver blockage and may also result in new therapeutic targets to enhance the response of GIST patients to current treatments.

3. OBJECTIVES

In GIST, oncogenic signaling initiated by KIT is mainly driven by PI3K/AKT/mTOR and RAS/MAPK pathways. However, the critical effectors within these two pathways are still unknown. Likewise, elements co-regulated by both pathways and their specific role in GIST cell biology are yet to be explored. In this context, the objectives of this Thesis are:

3.1. Dissection of KIT-downstream pathways.

3.1.1. Ascertainment of critical effectors within PI3K/AKT/mTOR and RAS/MAPK pathways through pharmacological screenings.

3.1.2. Characterization of the signaling compensatory mechanism between these two pathways.

3.1.3. Design and validation of a feasible therapeutic strategy based on the concomitant inhibition of both pathways.

3.2. Identification and characterization of common elements co-regulated by PI3K/AKT/mTOR and RAS/MAPK pathways.

3.2.1. Identification of the elements specifically co-regulated by KIT-downstream pathways by RNAseq.

3.2.2. Determination of the mechanism by which these elements are regulated by both pathways.

3.2.3. Functional validation of the elements found in objective 3.2.1, Identification of the elements specifically co-regulated by KIT-downstream pathways.

3.3. Validation of the expression of the co-regulated elements in GIST patients.

3.4. Validation of these elements as potential therapeutic targets in GIST.

4. METHODS

4.1. Cell culture studies

Human GIST cell lines used in these studies derive from GIST patients and have been published previously (196). GIST882 is a patient-derived cell line bearing a KIT primary mutation in exon 13 (K642E) (36). GIST-T1 is a patient-derived cell line bearing a mutation in exon 11 (p.Val560-Tyr578del) (197). GIST430/654 is an imatinib-resistant cell line derived from a GIST patients bearing a KIT primary mutation in exon 11 (p.Val560-Leu576del), and a KIT secondary mutation in exon 13 (V654A) (159). GIST-T1/670 and GIST-T1/816 are sub-cell lines derived from GIST-T1 bearing KIT secondary mutations in exons 14 and 17, respectively (T670I and D816E) (198). HMC-1.1 human mast cell line, a variant subline derived from HMC-1 harboring a mutation in KIT G560V (donated by Prof. Margarita Martín-Andorra, Barcelona University, Spain), was cultured in Iscove's modified Dulbecco's medium supplemented with 10% iron-supplemented fetal calf serum (Sigma, Darmstadt, Germany), 2 mM L-Glutamine, and 1.2 mM α-thioglycerol (Sigma, Darmstadt, Germany). MaMel-144a, a human melanoma cell line bearing a mutation in KIT S476I, was cultured under the same conditions as GISTs cell lines (donated by Prof. Dirk Schadendorf, Essen University, Germany). A673 Ewing sarcoma cell line was grown as GIST cell lines and was shared by Prof. Enrique de Álava. All lines shown to be Mycoplasma free and were periodically credentialed by Sanger sequencing of known mutations.

4.2. GIST xenograft studies

Heterotopic GIST-T1, GIST-T1/670 and GIST882 xenografts were generated and maintained as follow: Six- to 8-week-old female athymic nude mice (NMRI Foxn1/nu-Fosn1/nu) were obtained from Janvier Laboratories and housed under specific pathogen-free conditions. Heterotopic GIST xenografts were generated by subcutaneous injection of $5x10^6$ cells (GIST-T1 and GIST-T1/670) and $10x10^6$ cells (GIST882) in culture medium and Matrigel (Cultek SL) at 1:1 ratio] in anesthetized animals (ketamine 100 mg/kg i.p. and xylacine 10 mg/kg i.p.). Animals were maintained at 22 $\pm$ 2ºC and 35% humidity, on a 12-hour light-dark cycle. An individually positive pressure ventilated cage system was used to house a maximum of 5 mice per cage. Food and water were provided ad libitum. All animal studies were performed in accordance with ARRIVE guidelines and the three Rs rule of replacement, reduction,

and refinement principles. All in vivo work was conducted under appropriate Institutional Animal Care and Use Committee approved protocols.

Unless indicated, randomization, based on balanced tumor volumes, and treatments were initiated when median tumor volume reached 200 mm3 across the following experiments involving xenografts. The treatments were not blind to the investigator. Sample size was not calculated using any statistical method. All animal studies were performed in accordance with ARRIVE guidelines and the three Rs rule of replacement, reduction, and refinement principles. All in vivo work was conducted under appropriate Institutional Animal Care and Use Committee approved protocols.

4.2.1. Combination limiting-toxicity

Mice were treated in the following treatment arms: control group, and combination of continuous trametinib (1 mg/kg orally/every day, q.d) and GDC-0980 (5 mg/kg orally/every day). Body weight was assessed daily, and mice were euthanized when body weight lost exceed 20% and/or mice showed signs of stress.

4.2.2. Intermittent drug-schedule modelling

Treatment consisted of three days of the combination of trametinib and GDC-0980, and then treatment was withdrawn. Mice were euthanized at days 0, 1 and 3 during treatment and at days 1, 2, 3, 5 and 7 after treatment withdrawal.

4.2.3. Intermittent drug-schedule validation

Mice were treated into the following treatments arms: control, trametinib (1mg/kg, q.d), GDC-0980 (5 mg/kg/q.d) and the combination. Tumor volumes and body weights were assessed 3 times per week. Mice were euthanized at day 20 or when tumor volume reached 1200 mm^3.

4.2.4. Atrogin-1 overexpression in vivo.

Doxycycline 1 mg/kg (Sigma, Darmstadt, Germany) was added to water when tumor reached 100 mm3. Tumor volume was assessed every 2 days. Mice were euthanized at day 12.

4.2.5. Combined inhibition of KIT and the UPS

Mice were treated in the following groups: control, imatinib (100 mg/kg, q.d, p.o.), TAK-243 (18.75 mg/Kg, twice a week, i.v.p) and the combination of both. Tumor volume and body weight were assessed 3 times per week. Mice were euthanized at day 21 or when tumor volume reached 1200 mm^3.

4.3. Reagents

Imatinib, sunitinib, regorafenib, BYL-719, GDC-0941, GDC-0980, RAD001, MK-2206, vemurafenib and trametinib were purchased from LC Laboratories (Woburn, MA, USA). TGX-221, CAL-101, SCH722984, Doxorubicin and TAK-243 were from Selleck Chemicals (Houston, TX, USA), and 4-OHT from Sigma-Aldrich (Darmstadt, Germany).

4.4. Plasmids

4.4.1. Atrogin-1 shRNA knock-down

pLKO.1 constructs against Atrogin-1 (shFBXO32 00: TRCN0000433900, targeting CCGGGTTCACAAAGGAAGTACTAAACTCGAGTTTAGTACTTCCTTTGTGAACTTTT TTG and shFBXO32 80: TRCN0000443480, targeting CCGGGATGAGAAGAGCGGCAGTTTCCTCGAGGAAACTGCCGCTCTTCTCATCTTT TTTG were purchased from Sigma-Aldrich (Merck KGaA, Darmstadt, Germany). pLKO.1 shControl (targeting CCTAAGGTTAAGTCGCCCTCG) was purchased from Addgene. Lentiviruses were generated by co-transfecting shFBXO32 hairpin constructs or pLKO.1 shControl with psPax2 and psMDG2 (Addgene) into 293T cells using Polyethyenimine (PEI) MW40000 (Polyscience, Warrington, PA, USA). GIST-T1 and GIST-T1/670 cell lines were transduced with shFBXO32 or shControl and selected with puromycin (1 µg/mL). All the experiments were performed within the first 5 passages post-infection.

4.4.2. pINDUCER-Atrogin-1 lentiviral over-expression

pINDUCER vector was produced by recombination of pINDUCER-20 (Addgene) and pENTR223-FBXO32 (DNAsu). Lentiviruses were generated as described above. Atrogin-1 expression was induced by adding 0.25 µl/mL doxycycline monohydrate (Sigma, Darmstadt, Germany).

4.4.3. Episomal FOXO3a expression

pEGFP-C3 episomal expression vector containing FOXO3a was kindly provided by Prof. Pablo J. Fernández, IMDEA, Madrid, and was transfected using Lipofectamine 3000 (Thermo Fisher Scientific, Waltham, MA, USA).

4.4.4. Retroviral FOXO3aER expression

pLHCX-HA retroviral vector containing FOXO3a gene bound to estrogen receptor gene was kindly provided by Dr. Héctor G. Palmer group, VHIO. Retroviruses were generated by cotransfecting the vector with pUMVC and VSV-G (Addgene) into 293T cells, and GIST cell lines were infected and selected with hygromycin (200 ug/mL). All the experiments were performed within the first 5 passages post-infection.

4.4.5. Atrogin-1 and Atrogin-1-ΔF-box constitutive expression

pLV-EGFP-EF1A lentiviral vector containing Atrogin-1 gene and Atrogin-1 lacking F-box domain (deletion from 667 to 813 of the coding sequence) was obtained from VectorBuilder (Chicago, IL, USA). Lentiviruses were generated as described above. Atrogin-1, Atrogin-1-ΔF-box, or empty vector were constitutively expressed in GIST-T1 cells were transduced and selected with puromycin (1 µg/mL).

4.5. Drug-response assays

4.5.1. Cell viability

Cell viability studies were carried out using Cell Titer-Glo (CTG) luminescent assay (Promega, Madison, WI, USA), in which the luciferase catalyzed luciferin/ATP reaction provides an indicator of cell number. For these studies, cell lines were plated in triplicates at 5,000 (GIST-T1, GIST-T1/670 and GIST-T1/816) and 10,000 (GIST882, GIST430, GIST430/654 and GIST48) cells per well in a 96-well flat-bottomed plate (Falcon), and then incubated for 3 (GIST-T1, GIST-T1/670, GIST-T1/816 and GIST430) or 6 days (GIST882, GIST430/654 and GIST48) with imatinib and copanlisib at different concentrations or DMSO. The Cell Titer-Glo assay luminescence was measured with Infinite 200 Pro Microplate Luminometer (Tecan Trading AG) and the data were normalized to the DMSO control group. All experiments were performed in triplicates.

4.5.2. Cell proliferation – BrdU incorporation

Cell proliferation studies were carried out using BrdU Cell Proliferation ELISA Assay (Roche, Basel, Switzerland) according to the manufacturer's protocol. For these studies, cell lines at 10,000 (GIST-T1, GIST-T1/670 and GIST-T1/816) and 15,000 (GIST882, GIST430, GIST430/654 and GIST48) cells per well in a 96-well tissue culture plate and were incubated in media containing drugs and DMSO for 48 hours. 5-bromodeoxyuridine (BrdU) was added and incubation was continued for 24 hours. Assay plates were measured with Infinite 200 Pro Microplate Luminometer (Tecan Trading AG). All experiments were performed in triplicates.

4.5.3. Apoptosis induction

Apoptosis induction studies were performed by measuring caspase-3 and caspase-7 activity with the Caspase-Glo 3/7 Assay Kit (Promega, Madison, WI, USA) according to the manufacturer's protocol. Cells were plated in triplicates in 96-well flat-bottomed plates at 5,000 (GIST-T1, GIST-T1/670 and GIST-T1/816) and 10,000 (GIST882, GIST430, GIST430/654 and GIST48) cells per well. After 24-hour culture, medium was replaced with fresh medium (with or without respective drugs) and apoptosis was measured according to the manufacturer's instructions at 24 (GIST-T1, GIST-T1/670 and GIST-T1/816) and at 48 hours (GIST882, GIST430, GIST430/654 and GIST48) with Infinite 200 Pro Microplate Luminometer (Tecan Trading AG). All experiments were performed in triplicates.

4.6. Immunoblotting

Preparation of whole-cell lysates, electrophoresis and band detection was performed as follows: cultured cells were scraped in lysis buffer (1% NP40, 50 mmol/l Tris (pH 8.0), 100 mmol/l sodium fluoride, 30 mmol/l sodium PP_i, 2 mmol/l sodium molybdate, 5 mmol/l EDTA, 2 mmol/l sodium vanadate, and 10 μg/ml phenylmethylsulfonyl fluoride) and harvested in eppendorfs. The lysates were rocked overnight at 4°C and then centrifuged to remove insoluble material. Protein concentration was determined using DC Protein Assay (BIO-RAD Laboratories, Hercules, CA, USA). 30 μg of protein was used as standard. Electrophoresis was carried out in 8 to 12% polyacrylamide gels and transferred to polyvinilydene (PVDF) nitrocellulose membranes. Bands were detected by incubating with Immobilon Forte Western HRP Substrate (Millipore MERK KgaA) and captured by chemiluminescence with Amer- sham Imager 600 (GE Healthcare Life

Science) Treatment conditions are detailed in specific experiments. Information regarding clones, vendors and catalog identifications for antibodies used in western blot studies are summarized in **table 2**.

Table 2. List of antibodies used for western blot analysis.

Antibody	Source	Catalog Number
pKIT Y703	Cell Signaling Tech	#3073
pAKT S473	Cell Signaling Tech	#9271
pERK Thr202/Tyr204	Cell Signaling Tech	#9101
pS6 S235/6	Cell Signaling Tech	#2211
pFOXO3a Ser425	Cell Signaling Tech	#64616
pFOXO3a Thr32	Cell Signaling Tech	#9464
pGSK3b Ser9	Cell Signaling Tech	#9336
total AKT	Cell Signaling Tech	#9272
total ERK	Cell Signaling Tech	#9102
total FOXO3a	Cell Signaling Tech	#2497
S6RP1	Cell Signaling Tech	#2317
Clvd. PARP Asp214	Cell Signaling Tech	#9541
Clvd. Caspase 3 Asp175	Cell Signaling Tech	#9664
BIM	Cell Signaling Tech	#2923
Cyclin A	Santa Cruz Tech	sc-751
p27	Santa Cruz Tech	sc-11641
GSK3b	Santa Cruz Tech	sc-729
poly-ubiquination (PD41)	Santa Cruz Tech	sc-8017
SPRY4	RD Systems	AF5070
cKIT	DAKO	A4502
Atrogin-1	Abcam	ab168372
Actin	Sigma	A4700

4.7. Immunofluorescence

$7x10^5$ GIST-T1 cells were seeded upon cover glasses (Ref.: 0111560, Marienfeld-Superior, Lauda-Königshofen Germany) in 12-well cell culture plates and incubated for 24h before specific treatments were added. After indicated treatment times, cells were fixed in 4% paraforlmaldehyde for 30 min, followed by 15 min permeabilization in PBS 0.1% Triton X-100 (Sigma-Aldrich, Darmstadt, Germany) at room temperature (RT). Cells were blocked for 1 hour at RT with PBS 3% BSA (Sigma-Aldrich). Primary antibodies specific for FOXO3a (#2497), or p27 (#3686S), both from Cell Signaling Technology (Leiden, Netherlands), were incubated (1:200) overnight at 4ºC on a dark-wet chamber. An Alexa-Fluor-488-conjugated goat anti-rabbit-IgG (#A-11008, Invitrogen; 1:500) was used as the secondary antibody and incubated for 1h at RT.

For BrdU immunofluorescence, BrdU labeling, and detection was performed with 5-Bromo-2′-deoxy-uridine Labeling and Detection Kit I (Ref.: 11296736001, Sigma-Aldrich), following manufacturer's protocol.

All immunofluorescence images were captured with NIS-Elements AR 4.40.00 (Nikon) and analyzed with ImageJ software analysis using FIJI package version 2.0.0 (199).

4.8. Immunohistochemistry

Tumors excised from the sacrificed mice were immediately formalin-fixed and paraffin-embedded for mitotic count.

Immunohistochemical (IHC) evaluation of Ki-67 in the *in vitro* drug-withdrawal studies was performed as follows: tumor samples were collected immediately fixed in fresh 4% paraformaldehyde at 4ºC overnight. Cells were cultured in and treated in chamber slides (Thermo Fisher Scientific, Waltham, MA, USA). After paraffin embedding, viable areas from single hematoxylin and eosin slides were selected and stained for Ki-67 (Abcam, Cambridge, UK, Ref.: ab15580). Slides were digitalized at 20X using the NanoZoomer 2.0HT (Hamamatsu Photonics). Digitalized images were uploaded into VISIOPHARM (VIS) Image Analysis Software (Visiopharm Integrator System version 2019.02.1.6005, Visiopharm) for the analysis. Evaluation of IHC Atrogin-1 expression was performed in a tissue micro-array (TMA) containing pre-imatinib and/or post-imatinib tumor samples from 92 GIST patients (200). Clinical and molecular data was available as well. Representative sections were incubated with Atrogin-1 primary antibody (ab67866, Abcam, Cambridge, UK) overnight at 4°C (1:100). Peroxidase-labelled secondary antibodies and 3,3′-diaminobenzidine were applied to develop immunoreactivity, according to manufacturer's protocol (EnVision; Dako, Glostrup, Denmark). Atrogin-1 immunostaining was scored from 0 to 3 according to the intensity of expression. At least 1% of the cells should be stained to be considered positive.

All histopathological studies were evaluated independently by two experts.

4.9. Flow cytometry

4.9.1. Annexin V/PI

GIST cells were cultured in 6-well plates. After indicated time-points of drug incubation, $1x10^6$ cells were resuspended in Hank's balanced salts solution (HBSS) from Thermo Fisher Scientific and incubated with annexin V-FITC antibody (Ref.: 550475BD Bioscience, NJ, US) for 15 min in the dark at RT. Then, cells were incubated with propidium iodide (10 ug/mL final concentration) for 5 min RT and immediately analyzed by flow cytometry with BD FACSCelesta™ from BD Bioscience.

4.9.2. Pyronin Y/Hoescht 3332

GIST cells were cultured in 6-well plate. After 48 hours of doxycycline incubation, 1 $x10^6$ cells were resuspended in complete medium and incubated for 45 min with Hoescht 3332 at 7.5 ug/mL. Pyronin Y was added at 3.5 ug/mL and incubated for 15 min and immediately analyzed by flow cytometry with BD FACSCelesta™ from BD Bioscience.

In all conditions, 10,000 cells were recorded, and analysis was performed using Flow Jo V10 software. All experiments were performed in triplicates.

4.10. ChIP-PCR

GIST-T1 cells were cultured and treated as indicated. $3x10^7$ cells were crosslinked in 1% formaldehyde for 10 min at 37ºC. Crosslinking was stopped by adding glycine to a final concentration of 125 mM for 5 min at RT. For nuclear fraction, cells were resuspended and incubated for 15 min in cold soft-lysis buffer (50 mM Tris-HCl, 10 mM EDTA, 0.1% NP-40, and 10% glycerol) supplemented with protease inhibitors. Samples were then centrifuged for 15 min at 800g. Pellets were lysed with SDS-lysis buffer (50 mM Tris pH 8, 1% SDS and 10 mM EDTA) supplemented with protease inhibitors. Extracts were sonicated with Bioruptor® (Diagenode, Belgium) to generate 100–300 bp DNA fragments, incubated on ice for 20 min, centrifuged at 20,000 × g for 10 min, and then diluted 1:10 with dilution buffer (16.7 mM Tris pH 8, 0.01% SDS, 1.1% Triton X-100, 1.2 mM EDTA and 167 mM NaCl). Primary antibody against FOXO3a (Ref.: 16162, Abcam) or an irrelevant antibody (IgG) (Sigma) was added to the sample, and the mixture was incubated overnight with rotation at 4 °C. Chromatin bound to the antibody was immunoprecipitated using protein G magnetic beads (Ref.: 11710353, Fisher

Scientific) for 3 h with rotation at 4 °C. Precipitated samples were washed three times with low-salt buffer (0.1% SDS, 1% Triton X-100, 2 mM EDTA, 20 mM Tris-HCl pH 8.0, 150 mM NaCl), with high-salt buffer (0.1% SDS, 1% Triton X-100, 2 mM EDTA, 20 mM Tris-HCl pH 8.0, 500 mM NaCl), and twice with LiCl buffer (250 mM LiCl, 1% Nonidet P-40, 1% sodium deoxycholate, 1 mM EDTA, 10 mM Tris-HCl pH 8.0). Washed samples were treated with elution buffer (100 mM Na2CO3 and 1% SDS) for 1 h at 37 °C and then incubated at 65 °C overnight with the addition of a final concentration of 200 mM NaCl to reverse the formaldehyde crosslinking. After proteinase K solution (0.4 mg/ml proteinase K (Roche), 50 mM EDTA, 200 mM Tris-HCl pH 6.5) treatment for 1 h at 55 °C, DNA was purified with MinElute PCR purification kit (Qiagen) and eluted in nuclease-free water. Promoter region of Atrogin-1 (primer forward 5'- CAGTCCCTCAGCCAAAGC-3', primer reverse 5'- TAGCCCGTCCACTTCCTC-3') was detected by qPCR. Results were quantified relative to the input and the amount of irrelevant IgG immunoprecipitated in each condition. A heterochromatin region (primer forward 5'- TCAGCCCCTGGAATAGCT-3', primer reverse 5'- TCCACCTGTACAGCCAGC-3') was used as a negative control. All conditions were performed in triplicates.

4.11. FOXO family gene expression in GIST patients

PRJNA521803 dataset (201) was downloaded using SRA Toolkit (V2.10.7) and FASTQ files were rebuilt with fasterq-dump and processed with fastp (v0.20.1). Pair reads were mapped with STAR (v2.7.3a_2020-01-23) against the transcriptome of the GRCh38. A variant calling was performed using freebayes (v1.3.2-40-gcce27fc), which supports RNA sequencing data as input, to characterize the different samples. Variant calls were set up and optimized for tumor-only samples. Samples with primary pathogenic mutations in KIT exon 11 (imatinib-sensitive) and secondary KIT resistance mutations (imatinib-resistant) were selected for the quantification of gene expression using RSEM (v1.3.3).

4.12. GEO data analysis

Public data from experiment GSE15966 (202) with expression arrays was downloaded from the Gene Expression Omnibus using the GEOquery package. Only paired samples with a mutation in KIT were kept for further analysis. A differential expression analysis described by a paired design was conducted with limma (203), testing for differences in gene expression between the conditions pre- and post-administration of imatinib. Prior

to fitting the models, genes showing little variation or consistently low signal were filtered out in order to reduce the number of tests, using the methods implemented in genefilter (R package version 1.72.0), which defaults to filtering 50% of the genes (and fits our assumptions of expressed genes). P-values were adjusted by Benjamini & Hochberg (FDR).

4.13. Statistical Analysis

Statistical significance was calculated by two-way ANOVA followed by a Tukey's multiple comparison test for *in vitro* proliferation studies and by one-way ANOVA followed by a Tukey's multiple comparison test in experiments with more than one condition. Welch's corrected two-tailed unpaired T test was performed to assess statistical significance in experiments comparing two conditions and in *in vivo* studies at final time point. * $\leq$ 0.05, ** $\leq$ 0.005, *** $\leq$ 0.001, **** $\leq$0.0001.

4.14. RNA sequencing

The quality control for quantity and quality of the total RNA was done using the Qubit® RNA HS Assay (Life Technologies) and RNA 6000 Nano Assay on a Bioanalyzer 2100 (Agilent). The RNASeq libraries were prepared using TruSeq®Stranded mRNA LT Sample Prep Kit (Illumina Inc., Rev.E, October 2013) and sequenced on HiSeq 4000 (Illumina) in paired-end mode (2x76bp), following the manufacturer's protocol. Raw reads were pre-processed and the quality was assessed with FastQC. Reads were mapped to the Ensembl GRCh38 human genome reference and the annotation from Gencode version 25 using STAR version 2.5.2a, allowing the default ratio of mismatches in a read pair, keeping only alignments with valid splice junctions, mapping to no more than 20 loci and a minimum overhang of 8 for spliced alignments. Gene quantification was performed with RSEM version 1.2.28, using the same gene model used before to guide the aligner, and handling overlapping reads as suggested in the default options. For the differential expression analysis, we used R version 4.0.2 and limma with voom transformation to normalize, transform, and model RNA-Seq data. A design including one term combining the treatment and timepoint, blocking for the cell line, was used for testing the differences in gene expression between the treatment combining the two drugs at 24 hours and the baseline expression at 0 hours, after subtraction of the specific effects at 24h of the drugs administered alone. Also, analyses for each cell line separate from the others were done in parallel, using the same design (without blocking) and

contrast of interest. P-values were adjusted by Benjamini & Hochberg (FDR), and genes with FDR <0.01 and a fold change in expression of at least 2 were considered differentially expressed. The molecular signatures from MSigDB were used to identify enrichment of known gene sets, namely KEGG, GO biological processes (GOBP), hallmarks gene sets and oncogenic signatures, using a GSEA analysis implemented in the package clusterProfiler.

The data discussed in this Thesis have been deposited in GEO database under accession number GSE156680.

5. RESULTS

5.1. Conjoined signaling from KIT-downstream RAS/MAPK and PI3K/mTOR pathways is critical for GIST cell survival and proliferation

Several pieces of evidence support RAS/MAPK and PI3K/mTOR as the two main pathways downstream KIT. However, the specific and relative contribution of each of the signaling nodes within both pathways to GIST cell survival and proliferation is not fully understood. Critical targetable nodes were pharmacologically screened in a panel of GIST cell lines with clinically-representative KIT primary and secondary mutations (**Fig. 5A; Table 3**). Inhibition of MEK1/2 with trametinib resulted in the deepest impact on cell viability irrespective of the type of KIT mutation. All cell lines also remained sensitive to the inhibition of MEK1/2-target ERK1/2. As expected, no effect on viability was observed upon BRAF blockage. Simultaneous inhibition of all PI3K class IA variants was necessary to impact on cell viability in most, although not in all KIT-mutants. Abrogation of PI3K/mTOR pathway across all GIST models only occurred at low IC50 values with dual blockade of PI3K class IA and mTOR, by using GDC-0980 inhibitor. Surprisingly, little effect was derived from AKT targeting. Proliferation studies with BrdU incorporation largely overlapped cell viability results (**Fig. 5B**), thereby confirming MEK1/2 and PI3K class IA/mTOR as the most critical targetable nodes downstream KIT. Kinase inhibition studies demonstrated on-target effect in four representative imatinib-sensitive (GIST-T1, GIST882) and -resistant (GIST-T1/670, GIST-T1/816) GIST cell lines (**Fig. 6A-D**).

Table 3. List of drugs used in pharmacological screenings, their specific target, company and range of concentrations used.

TARGET	DRUG	COMPANY	RANGE TESTED (nM)
PI3K/AKT/mTOR pathway relevant nodes			
PI3Kα	BYL-719	LC Labs	5 – 5,000
PI3Kβ	TGX-221	Selleck	5 – 5,000
PI3Kδ	CAL-101	Selleck	5 – 5,000
PI3K IA	GDC-0941	LC Labs	5 – 5,000
PI3K IA/mTOR	GDC-0980	LC Labs	5 – 5,000
mTOR	RAD001	LC Labs	5 – 5,000
AKT 1,2,3	MK-2206	LC Labs	5 – 5,000
RAS/MAPK pathway relevant nodes			
BRAF V600E	Vemurafenib	LC Labs	5 – 5,000
MEK 1/2	Trametinib	LC Labs	5 – 5,000
ERK 1/2	SCH722984	Selleck	5 – 5,000

A

Cell line	KIT genotype	Imatinib	PI3K/AKT/mTOR							RAS/MAPK		
			PI3Kα	PI3Kβ	PI3Kδ	PI3K IA	PI3K IA mTOR	mTOR	AKT	BRAF	MEK	ERK
GIST-T1	Ex 11	Sensitive	>5000	>5000	>5000	415	300	393	>5000	>5000	9	141
GIST430	Ex 11	Sensitive	701	>5000	>5000	343	478	1779	>5000	1119	3	219
GIST882	Ex 13	Sensitive	>5000	>5000	>5000	2718	133	2	1788	>5000	2	366
GIST430/654	Ex 11 + Ex 13	Resistant	1419	>5000	>5000	301	163	6	576	>5000	12	683
GIST-T1/670	Ex 11 + Ex 14	Resistant	>5000	>5000	>5000	794	284	>5000	>5000	>5000	39	353
GIST-T1/816	Ex 11 + Ex 17	Resistant	>5000	>5000	>5000	>5000	645	>5000	>5000	>5000	68	401
GIST48/820	Ex 11 + Ex 17	Resistant	2549	>5000	>5000	25	139	1406	703	>5000	4	382

Log10 IC50
Row max
Row min

B

Cell line	KIT genotype	Imatinib	PI3K/AKT/mTOR							RAS/MAPK		
			PI3Kα	PI3Kβ	PI3Kδ	PI3K IA	PI3K IA mTOR	mTOR	AKT	BRAF	MEK	ERK
GIST-T1	Ex 11	Sensitive	>5000	>5000	>5000	856	216	167	>5000	>5000	8	379
GIST430	Ex 11	Sensitive	1227	3766	3198	36	64	3	1935	1395	2	108
GIST882	Ex 13	Sensitive	>5000	>5000	>5000	>5000	1281	26	>5000	>5000	77	>5000
GIST430/654	Ex 11 + Ex 13	Resistant	>5000	4672	>5000	100	98	1	539	>5000	4	475
GIST-T1/670	Ex 11 + Ex 14	Resistant	>5000	>5000	>5000	>5000	832	>5000	>5000	>5000	27	206
GIST-T1/816	Ex 11 + Ex 17	Resistant	>5000	>5000	>5000	>5000	1015	>5000	>5000	>5000	109	760
GIST48/820	Ex 11 + Ex 17	Resistant	657	117	10	78	47	2	82	310	3	46

Log10 IC50
Row max
Row min

Figure 5. KIT-downstream pathways dissection. Heatmap depicting IC50 values from in vitro cell viability assays (A), and in vitro cell proliferation assays (B), performed in 7 imatinib-sensitive and -resistant GIST cell lines against the specified signaling nodes. Specific drugs and targets are detailed in the Table 3. Cell viability was measured by Cell Titer-Glo assay and cell proliferation was measured by BrdU incorporation. Ex, exon.

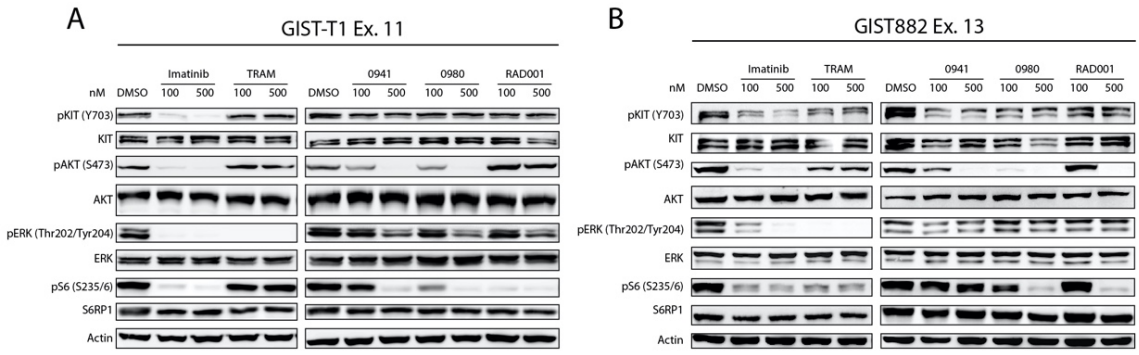

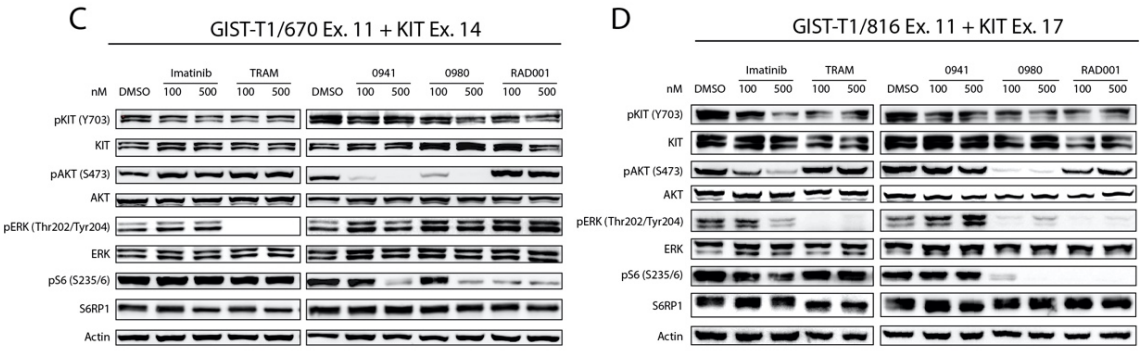

Figure 6. Immunoblots for kinase inhibition studies at 4 hours using imatinib, GDC-0941, GDC-0980, RAD001 and trametinib, at the indicated doses, targeting, respectively, PI3K, PI3K/mTOR, mTOR and MEK1/2. On-target inhibition effect for each drug is observed in imatinib-sensitive GIST-T1 (A) and GIST882 (B), and in imatinib-resistant GIST-T1/670 (C) and GIST-T1/816 (D). Ex, exon; TRAM, trametinib

However, single pathway ablation at MEK1/2 and PI3K/mTOR nodes did not result in sustained antiproliferative effect, nor in substantial apoptosis induction (**Fig. 7A,B**). In the absence of pathway cross-activation or re-activation, it is likely that KIT oncogenic signaling through the non-inhibited pathway sustains cell survival (**Fig. 8A-D**). Accordingly, concurrent blockade of KIT-downstream pathways *in vitro* led to a significant inhibition of cell proliferation and apoptosis induction irrespective of the type of KIT mutation (**Fig. 7A,B, 9**).

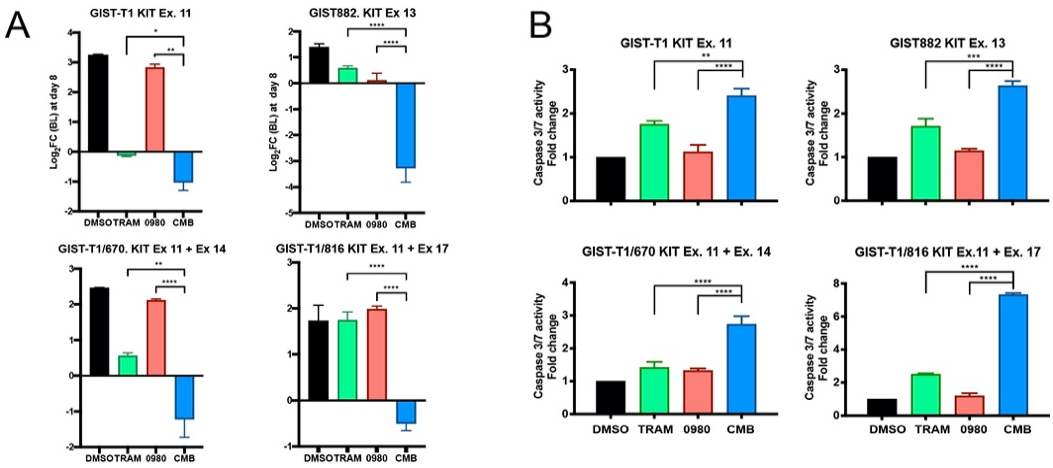

Figure 7. **A**, 8-day cell proliferation studies (raw cell count) in two imatinib-sensitive cell lines, GIST-T1 and GIST882, and two imatinib-resistant cell lines, GIST-T1/670 and GIST-T1/816; drug conditions: DMSO, trametinib (TRAM) 100nM, GDC-0980 500nM, and the combination (CMB). **B**, Apoptosis studies (Caspase-Glo) using the same treatment concentrations as in A.

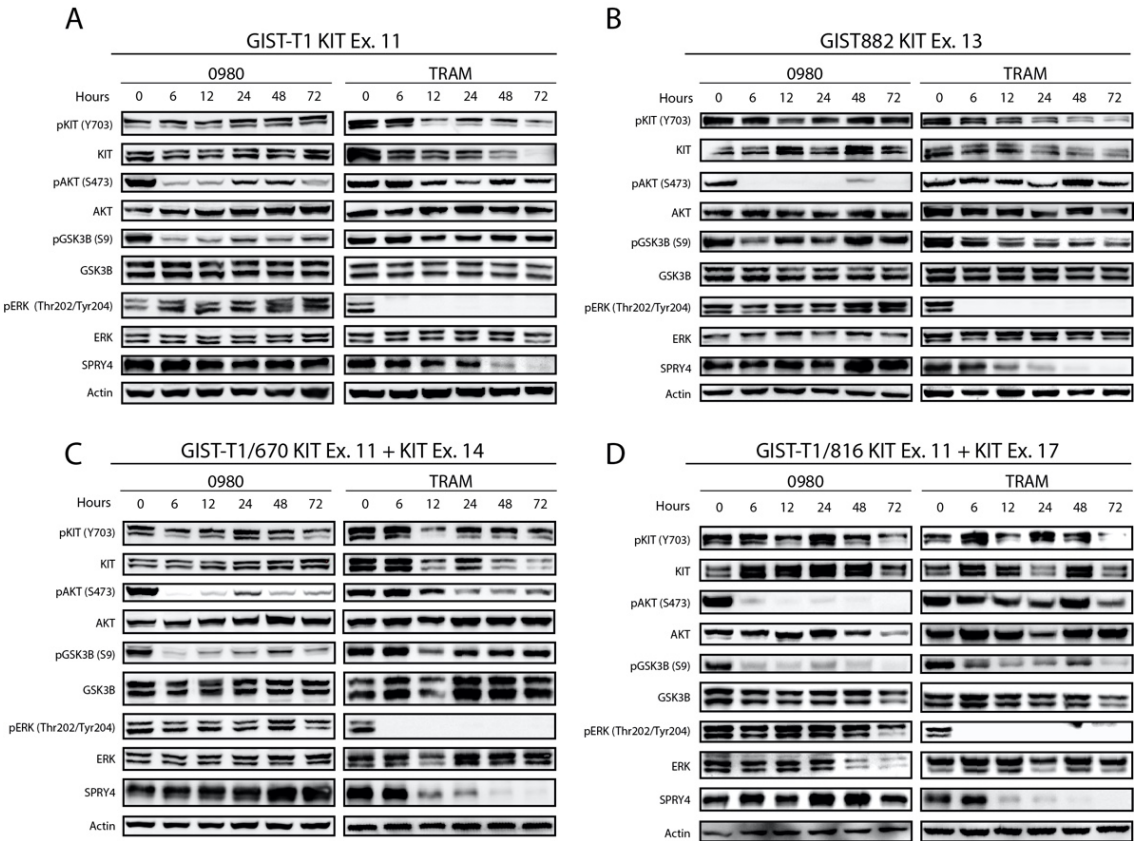

Figure 8. Immunoblots for kinase inhibition studies using trametinib 100 nM or GDC-0980 500 nM at 0, 4, 12, 24, 48 and 72 hours after single dosing in imatinib-sensitive GIST-T1 (**A**) and GIST882 (**B**), and in imatinib-resistant GIST-T1/670 (**C**) and GIST-T1/816 (**D**). Ex, exon; TRAM, trametinib.

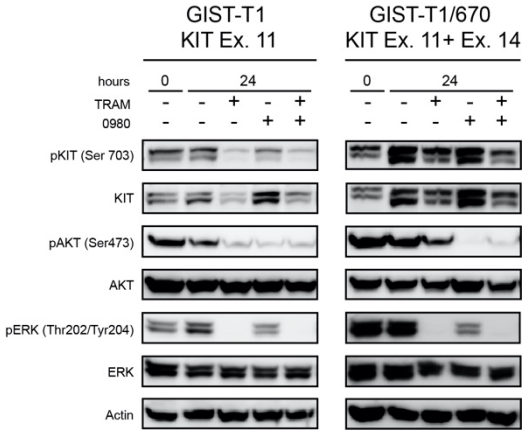

Figure 9. Kinase inhibition studies at 24 hours in GIST-T1 and GIST-T1/670 using the same treatment concentrations as in Figure 3A and B. TRAM, trametinib; Ex, exon.

The relevance of KIT-downstream RAS/MAPK and PI3K/mTOR pathways was further confirmed *in vivo*. First, an intermittent treatment schedule using off-drug periods was modelled aiming to minimize the high toxicity associated with concurrent and continuous

inhibition of both pathways observed in cancer models and patients, which was also confirmed. Namely, 5 days of concomitant pathway inhibition was the maximum time frame tolerated by mice before they had to be scarified due to treatment-related toxicities. Of note, the proliferation rate was significantly lower in tumors from mice undergoing concurrent pathway inhibition compared to vehicle (**Fig. 10A,B**).

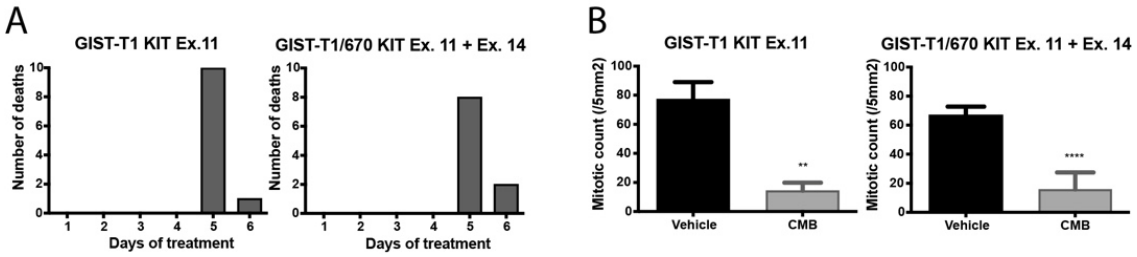

Figure 10. **A**, raw number of GIST-T1 and GIST-T1/670 xenografts sacrificed by day after continuous concurrent administration of trametinib 1mg/kg QD and GDC-0980 5mg/kg QD. **B**, number of mitoses per 5 mm2 (40x) in the vehicles in comparison with treated tumors obtained at the time of sacrifice, (n = 3-10). CMB, combination.

Two to three days of continuous concurrent RAS/MAPK and PI3K/mTOR inhibition was needed to halt GIST cell proliferation both *in vitro* (**Fig. 11A-B**) and *in vivo* (**Fig11C-D**), as assessed by Ki-67 immunostaining and mitotic count. Tumor regrowth after treatment withdrawal also occurred in two to three days (**Fig. 11A-D**), both *in vitro* and *in vivo*. Together, it was defined an intermittent treatment schedule consisting in cycles of three days of continuous concurrent treatment with trametinib and GDC-0980 followed by three or two days off-treatment in imatinib-sensitive and imatinib-resistant GIST cell models, respectively (**Fig. 11E,F**).

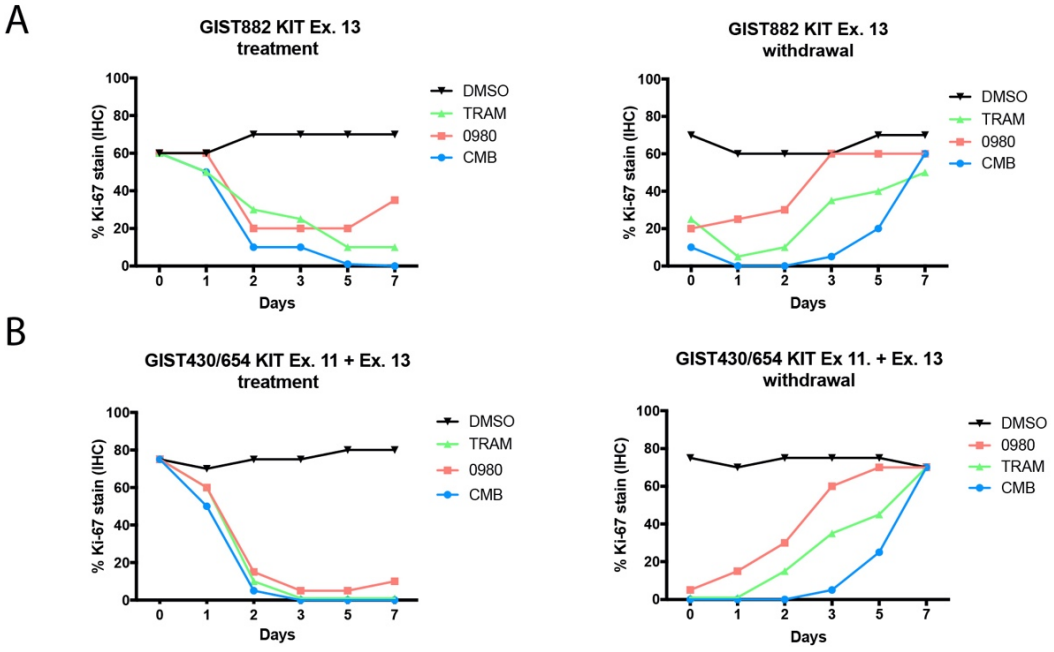

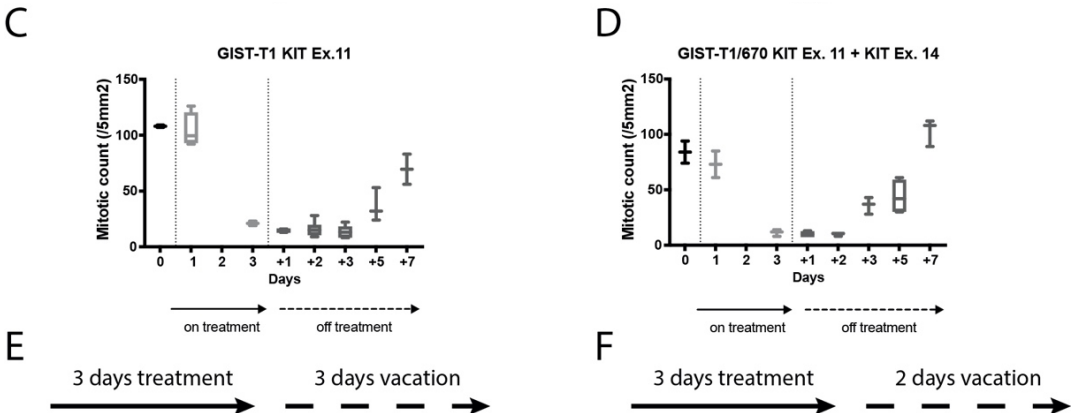

Figure 11. **A**, **B**, Ki-67 immunohistochemistry readouts for GIST882 (**A**) and GIST430/654 (**B**) cells treated *in vitro* in chamber slides with DMSO, trametinib (TRAM) 100nM, GDC-0980 500nM and the combination (CMB); the length of treatment before drug withdrawal was 3 days. **C**, **D**, GIST-T1 (**C**) and GIST-T1/670 (**D**) were treated for 3 days with the combination of trametinib and GDC-0980 at the previously indicated doses and sacrificed at the indicated time-points (n = 2-4). Proliferation is expressed as mitotic count/5 mm2. **E**, **F**, resulting in vivo intermittent treatment schedules for GIST-T1 (**E**) and GIST-T1/670 (**F**). Ex, exon;

Subsequent intermittent combined inhibition of MEK1/2 and PI3K/mTOR with trametinib and GDC-0980, respectively, significantly reduced tumor proliferation *in vivo* in both imatinib-sensitive and -resistant xenograft models compared to monotherapies (**Fig. 12A,B**), also resulting tolerable throughout (**Fig. 12C,D**). Together, these data support that MEK1/2 and PI3K/mTOR are the most critical targetable nodes downstream KIT, and that their dual inhibition largely phenocopy KIT blockade regardless the heterogeneity of primary and secondary KIT mutations.

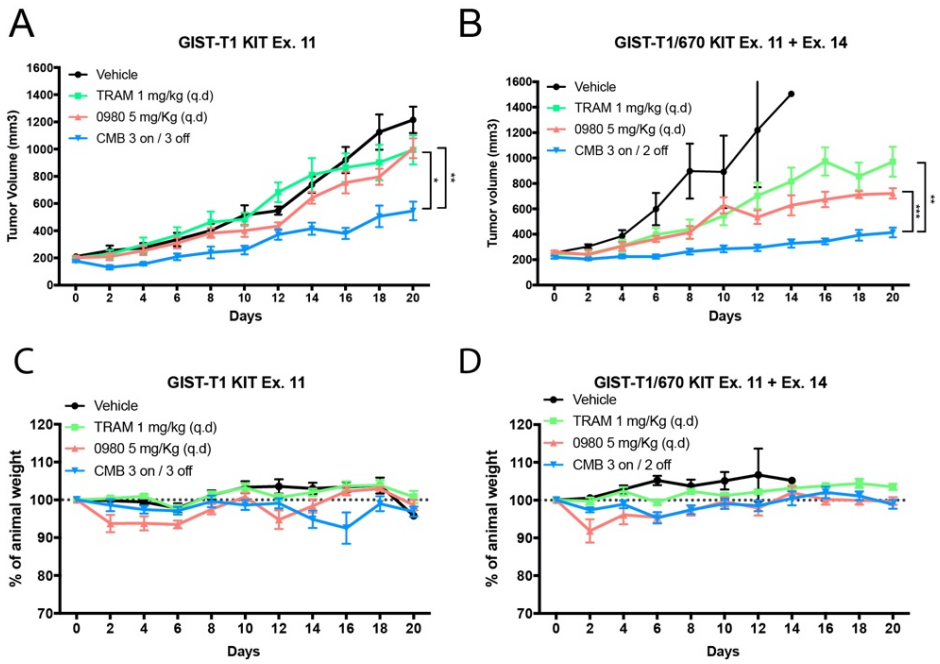

Figure 12. **A**, **B**, treatment response of GIST-T1 (**A**) and GIST-T1/670 (**B**) xenografts in NMRInu/nu mice. The treatment cohorts are as follows: (i) vehicle (black); (ii) trametinib 1mg/kg QD given continuously (green); (iii) GDC-0980 5mg/kg QD given continuously (red); (iv) the combination of trametinib and GDC-0980 at the same doses following the intermittent treatment schedule of 3 days on / 3 days off in GIST-T1 and 3 days on / 2 days off in GIST-T1/670. **C**, **D**, Animal tolerance to drug-induced toxicity was objectivized through animal weight measurements across the experiment and expressed as percentage of weight variation (in grams). n=4-6 per treatment arm, mean ± SEM. Ex, exon; TRAM, trametinib; CMB, combination.

5.2. Atrogin-1 is a KIT-downstream node co-regulated by RAS/MAPK and PI3K/mTOR pathways

Given the relevance of RAS/MAPK and PI3K/mTOR downstream KIT, it is conceivable that KIT transcriptomic program is primarily conducted through the conjoined activity of these two pathways. Thus, to uncover novel molecular targets critically regulated by KIT in GIST, a whole-transcriptome study was conducted with the goal of identifying genes co-regulated by RAS/MAPK and PI3K/mTOR pathways irrespective of the type of KIT primary or secondary mutation, and whose effect could not be explained by one single pathway. Four GIST cell lines were treated with trametinib, GDC-0980 or the combination of both, inhibiting previously validated targetable nodes downstream KIT (**Fig. 13**). Gene expression differences at 24 hours between GIST cell lines and between treatments were evidenced in the principal component analysis (PCA) (**Fig. 14**).

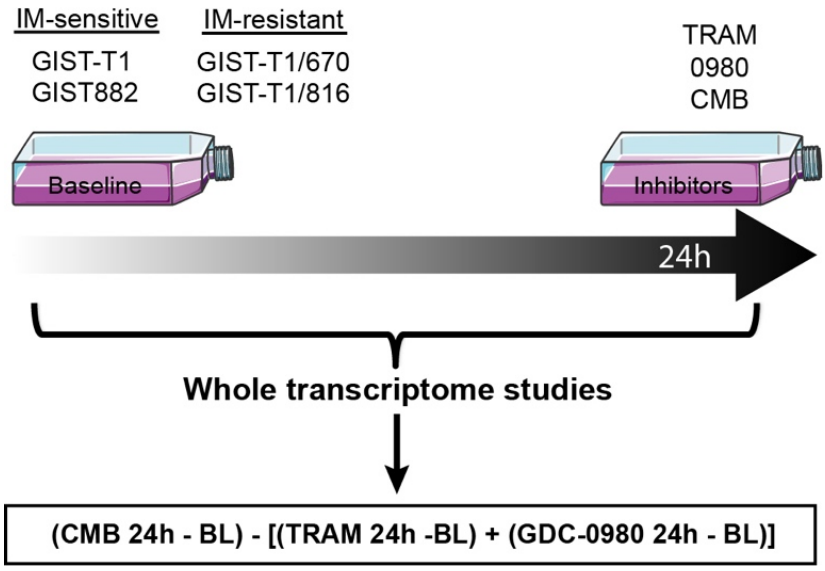

Figure 13. Two imatinib-sensitive (GIST-T1, GIST882) and -resistant (GIST-T1/670, GIST-T1/816) GIST cell lines were treated in biological triplicates for 24 hours with trametinib 100nM, GDC-0980 500nM or the combination and compared with untreated cells at baseline. RNA-seq data analysis focused on the

identification of genes regulated by the conjoined activity of RAS/MAPK and PI3K/mTOR KIT-downstream pathways, and therefore it was subtracted the individual effect of each agent. BL, baseline; TRAM, trametinib; CMB, combination; IM, imatinib.

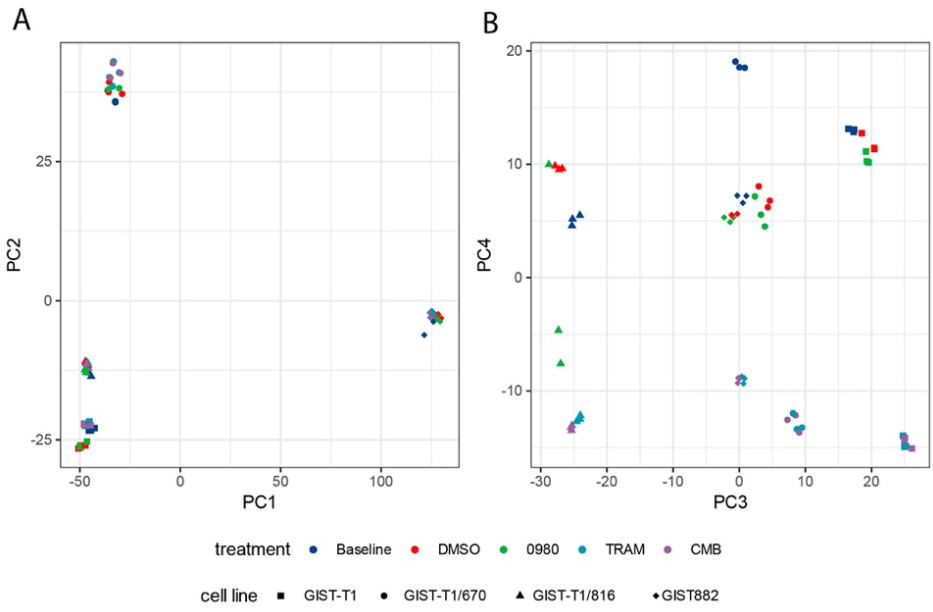

Figure 14. Principal component analysis (PCA) from the whole transcriptome study using the top 500 most variable genes. Cell line peculiarities are very strong (1st to 3rd components, PC1, PC2 and PC3) **(A**), but drug effects are cleanly captured in the 4th component (PC4) (**B**). TRAM, trametinib; CMB, combination; DMSO, dimethyl sulfoxide.

A paired design analysis combining all four cell lines and subtracting single pathway effect yielded a total of 271 genes differentially expressed, 129 upregulated and 142 down-regulated (**Fig. 15; Table 4**). Genes known to be dysregulated upon KIT inhibition with imatinib, such as SPRY4, DUSP6 or ETV5 (112), also reached the highest changes in differential expression with the combined effect of RAS/MAPK and PI3K/mTOR inhibition. From the top 50 differentially expressed genes (adjusted p-value) co-regulated by KIT-downstream pathways, FBXO32 showed the highest fold change increase among those found upregulated (**Fig. 15; Table 4**). As explained in the introduction, FBXO32/Atrogin-1 is a muscle-specific F-box protein regulated by the IGF-1/AKT/FOXO axis, and it is the substrate-recognition subunit of the SCF E3 ubiquitin ligase complex that mediates protein degradation and subsequent muscular atrophy, where it is shown markedly upregulated. Atrogin-1 was of immediate interest giving the myogenic nature of GIST.

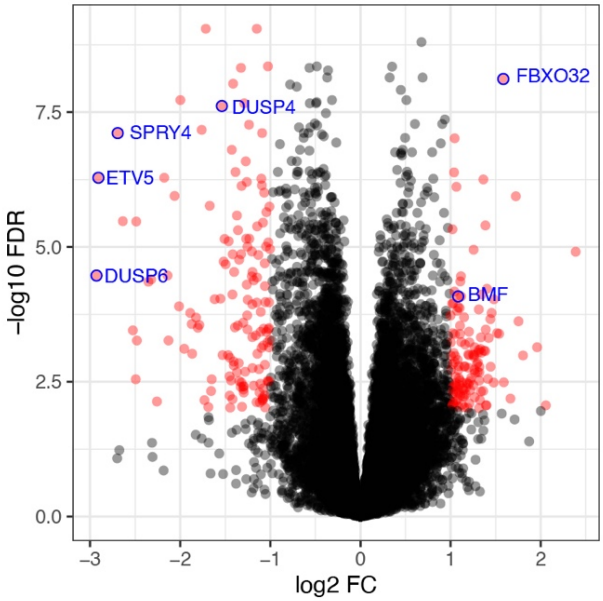

Figure 15. Volcano plot showing 271 genes significantly dysregulated across all 4 GIST cell lines (paired design analysis, significance thresholds: FDR 1% and abs(logFC)>1). FBXO32 together with other known genes are depicted.

Table 4. Top 10 ranked differentially expressed genes yielded from a paired design analysis combining the 4 different cell lines of MEK1/2 and PI3K/mTOR co-inhibition subtracting single-pathway effect.

Gene name	logFC	adj.P.Value
CTPS1	-1,1506471	8,9907E-10
CRHR2	-1,7163319	8,9907E-10
MGAT5	-1,0266155	4,4778E-09
NAV1	-1,325423	4,779E-09
FABP5	-1,4131465	9,3865E-09
FBXO32	1,58494078	7,6775E-09
SPSB4	-1,2902041	2,1696E-08
DUSP4	-1,5376443	2,4335E-08
UBASH3B	-1,9983194	1,8901E-08
HOXA-AS3	-1,236777	5,4081E-08

Individual transcriptomic analyses of each cell line were also undertaken and revealed different subsets of genes differentially expressed (**Fig. 16; Table 5**). However, only four genes were found significantly dysregulated in all four GIST cell lines, showing FBXO32 the strongest enrichment (**Fig. 17A,B**). The highest induction of FBXO32/Atrogin-1 expression upon combined RAS/MAPK and PI3K/mTOR inhibition compared to single pathway ablation was further confirmed at both RNA (**Fig. 18A**) and protein levels (**Fig. 18B**).

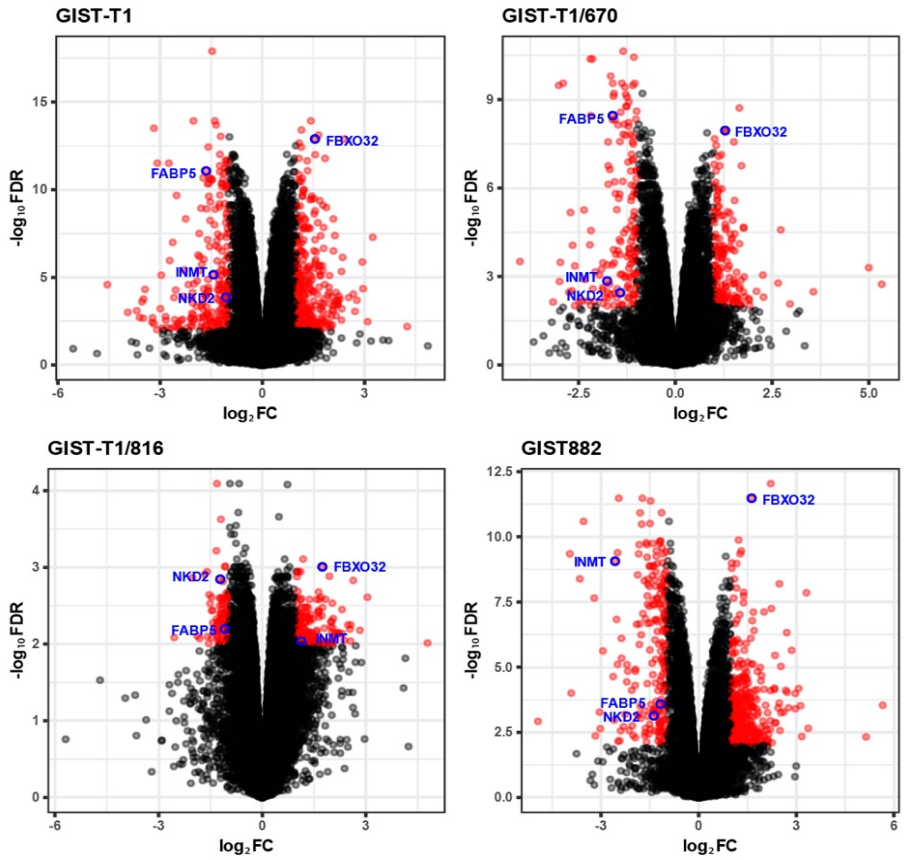

Figure 16. Volcano plots from individual RNA-seq analysis showing differentially expressed genes in each cell line. Significance thresholds: FDR 1% and abs(log2FC)>1. FBXO32 is overexpressed in all cell lines and depicted together with other known genes.

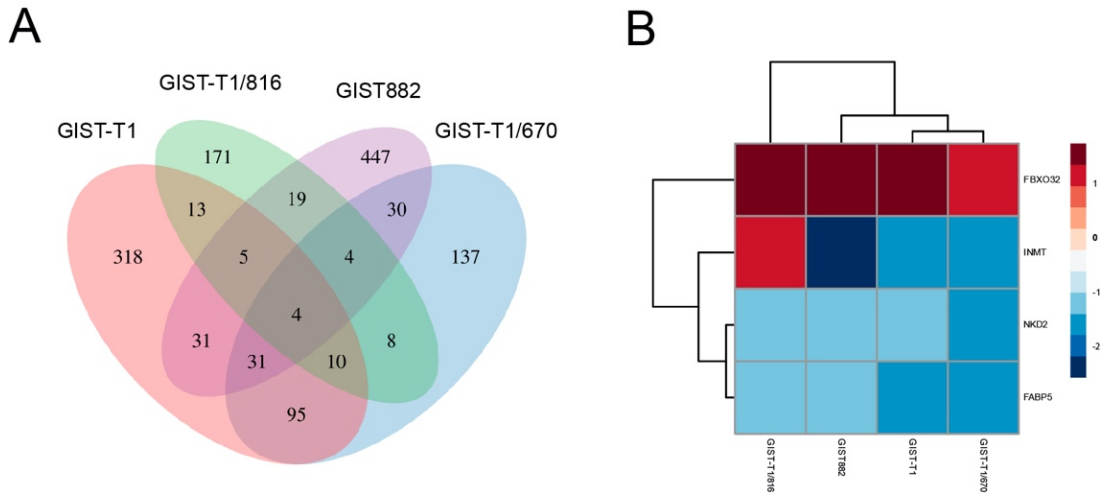

Figure 17. **A**, Venn-diagram showing common differentially expressed genes across the 4 GIST cell lines. **B**, A total of 4 genes, including FBXO32, were found significantly up- or down-regulated in all 4 GIST cell lines.

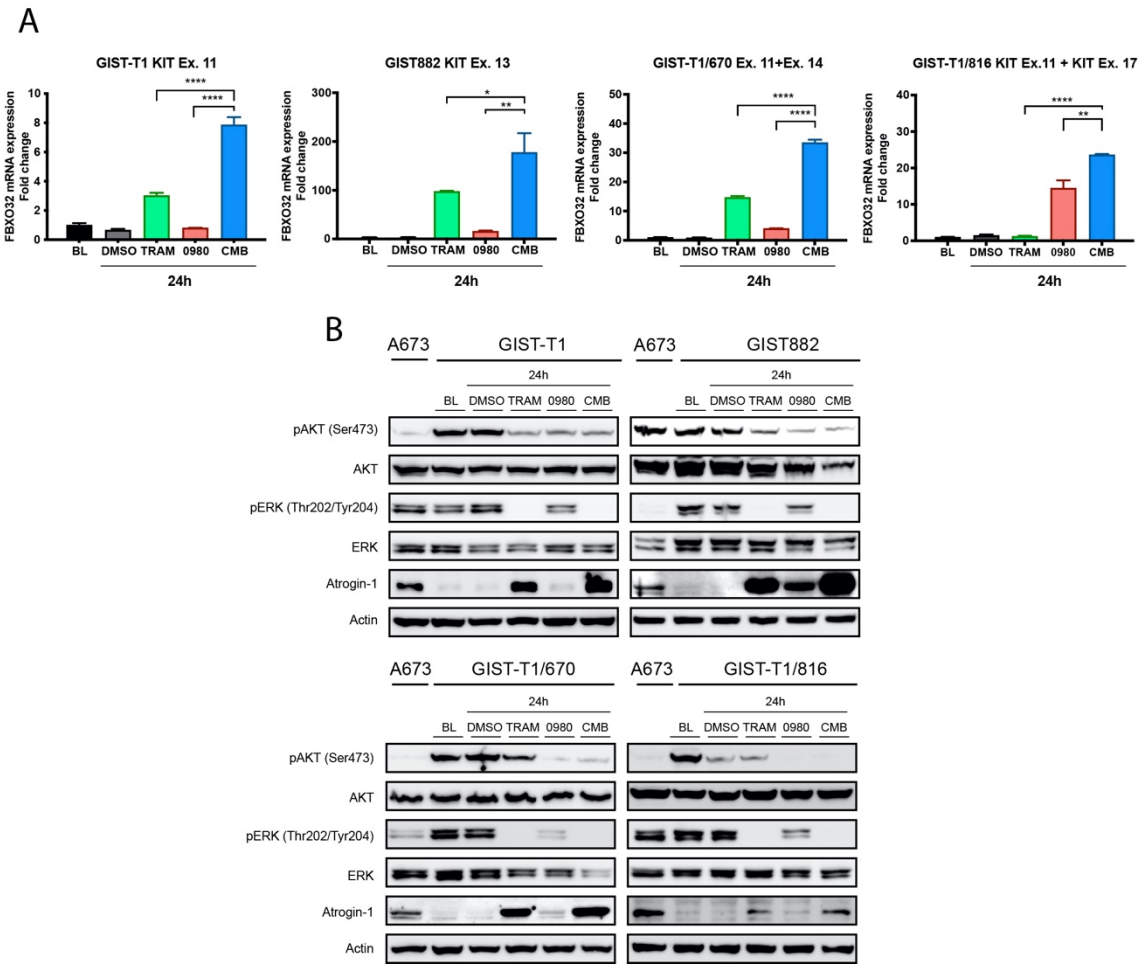

Figure 18. *FBXO32* mRNA (**A**) and protein (**B**) expression is shown significantly upregulated upon combined inhibition of RAS/MAPK and PI3K/mTOR pathways compared to single pathway ablation. A673 cell line expresses constitutively Atrogin-1 and is used as a positive control. TRAM, trametinib; CMB, combination; DMSO, dimethyl sulfoxide**.**

Table 5. FBXO32 depicted from the results of differentially expressed genes after MEK1/2 and PI3K/mTOR concurrent inhibition subtracting single pathway effect in the four GIST cell lines analyzed individually.

Cell line	Gene	logFC	adj. P.Value
GIST-T1	FBXO32	1,54613118	1,2804E-13
GIST882	FBXO32	1,62832534	3,3288E-12
GIST-T1/670	FBXO32	1,28484238	1,1256E-08
GIST-T1/816	FBXO32	1,73791207	9,8352E-04

Previous data support RAS/MAPK and PI3K/mTOR as the two most critical pathways transducing KIT and PDGFRA oncogenic program. In order to further confirm FBXO32 dependency on KIT oncogenic signaling, RNA-seq analysis was performed in GIST-T1

cell line treated with imatinib. FBXO32 was among the 50 highest differentially expressed genes (**Fig. 19A,B**), which is in line with previously reported datasets (112,204).

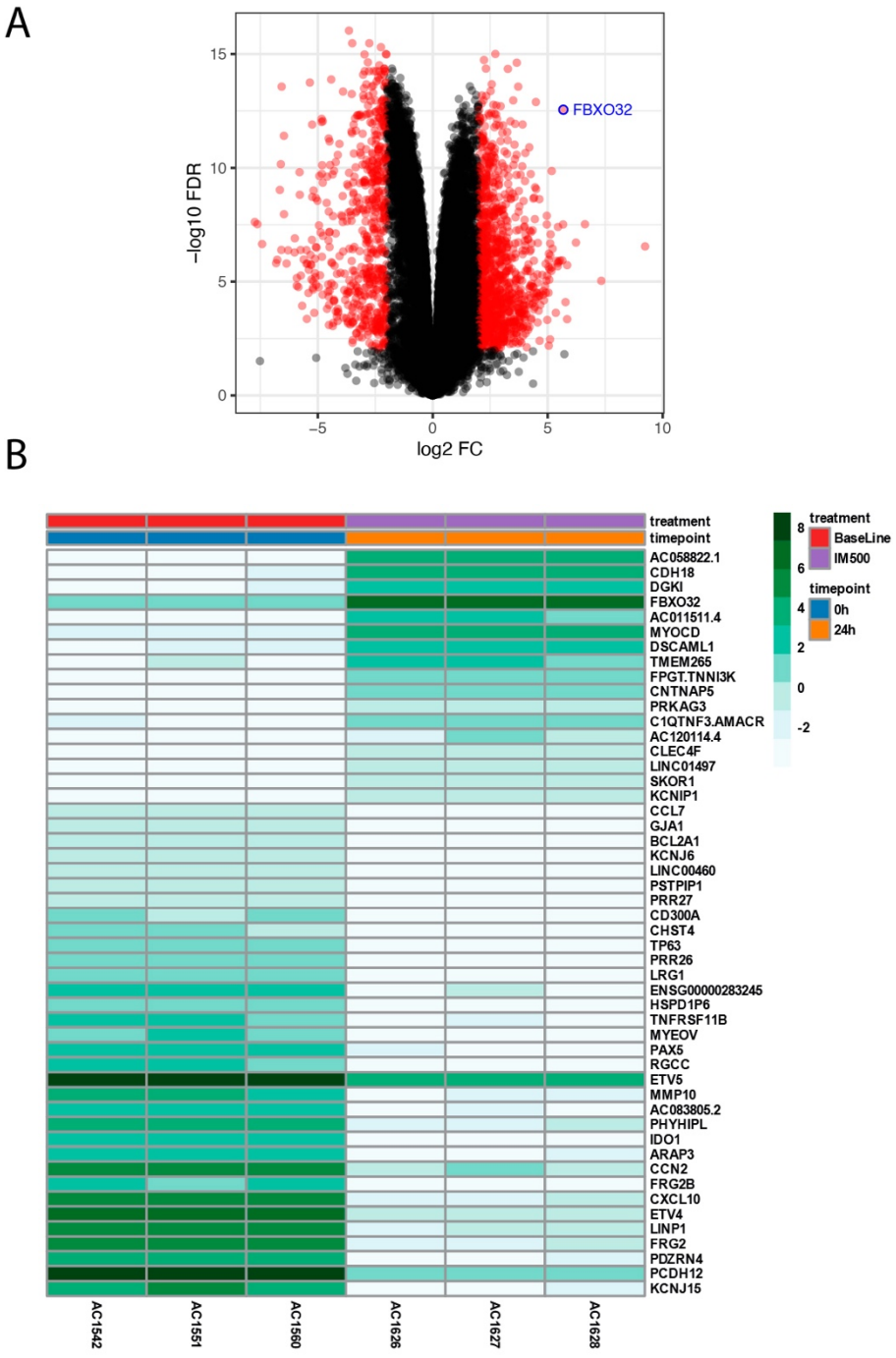

Figure 19. **A**, RNA-seq study and resulting volcano plot depicting genes differentially expressed in biological triplicates of GIST-T1 cell line after 24 hours of imatinib 500nM (significance thresholds: FDR 1% and abs(logFC)>1). **B**, Heatmap showing top 50 genes differentially expressed in GIST-T1 upon treatment with imatinib 500 nM for 24 hours. Triplicates from baseline and treatment conditions are displayed.

KIT and KIT-downstream signaling abrogation with KIT inhibitors active against specific primary or secondary mutations resulted in a significant increase in FBXO32/Atrogin-1 expression (**Fig. 20A-C**), but not in the absence of KIT inhibition when imatinib was used against imatinib-resistant GIST cell lines (**Fig. 20D,E**). Moreover, a significant overlap was observed between genes differentially expressed with KIT inhibition and with combined inhibition of KIT-downstream pathways (**Fig. 21**), thus reinforcing the critical role of these two pathways in GIST oncogenic program.

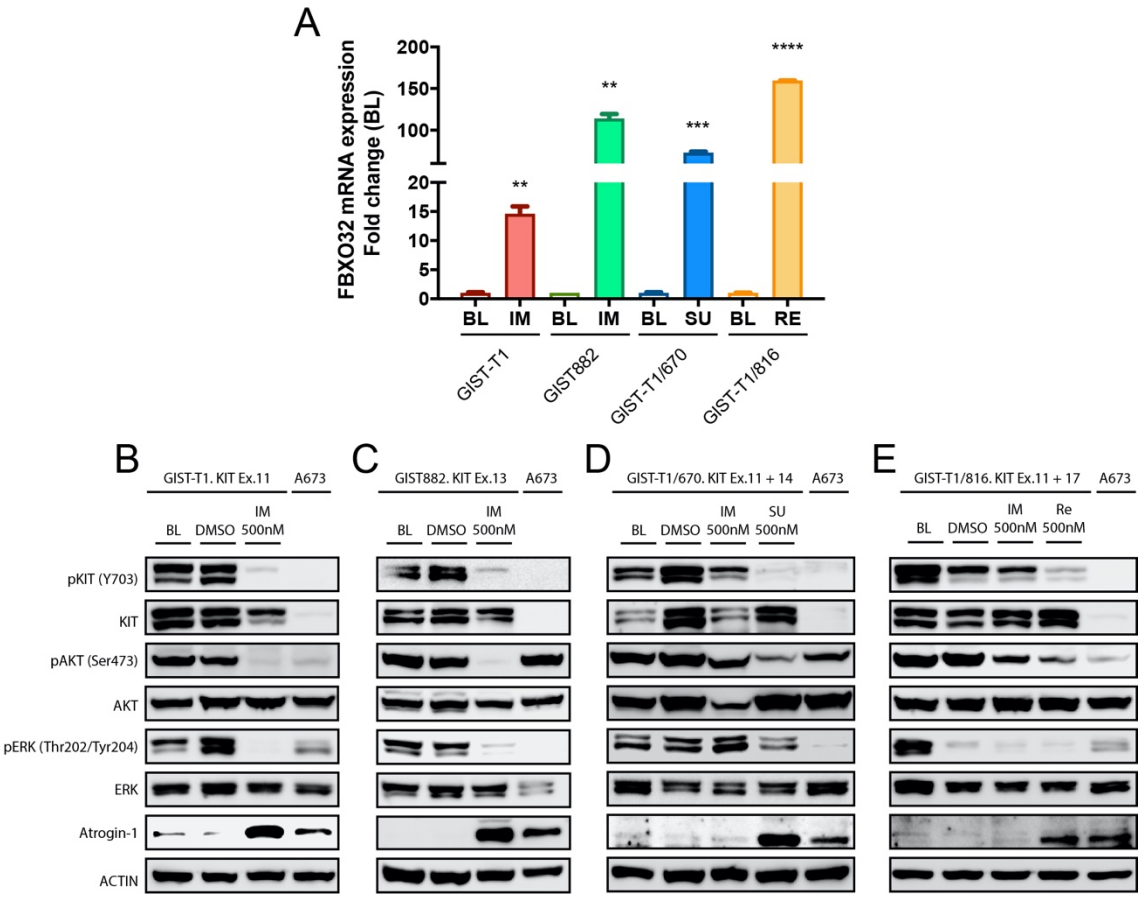

Figure 20. Targeted inhibition of KIT oncogenic signaling with specific KIT inhibitors resulted in increased *FBXO32* mRNA expression (**A**), and protein (**B-E**). Targeted inhibition of KIT oncogenic signaling with specific KIT inhibitors resulted in increased Atrogin-1 expression, while absence of KIT signaling abrogation in imatinib-resistant GIST cell lines did not increase Atrogin-1 expression (B-E). Ewing sarcoma A673 cell line is used as an internal control of constitutive Atrogin-1 expression. Baseline (BL); DMSO, dimethyl sulfoxide; trametinib (TRAM); combination (CMB); imatinib (IM); sunitinib (SU); regorafenib (RE); Ex, exon.

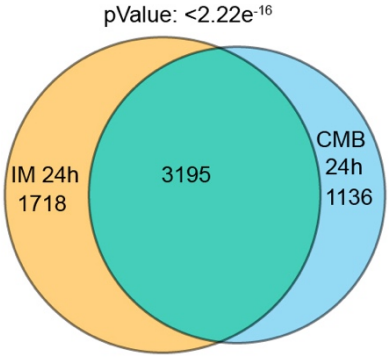

Figure 21. There is a significant overlap between genes differentially expressed in GIST-T1 treated with imatinib and the combination of trametinib and GDC-0980 (hypergeometric test, p-value <2.22e-16).

These results underscore that FBXO32/Atrogin-1 is critically regulated by KIT oncogenic signaling in GIST through the two main KIT-downstream pathways. The potential analogy between muscular atrophy and suppression of KIT activation in a myogenic cancer such as GIST prompted further experiments to decipher Atrogin-1 function in this cellular context.

5.3. Atrogin-1 expression is transcriptionally regulated by FOXO3a in GIST

Regulation of Atrogin-1 in cancer is still poorly understood and diverse mechanisms have been involved across several cancer types. Conversely, Atrogin-1 regulation in skeletal muscle is well characterized (see section 1.5.8): under catabolic conditions, decreased growth factor stimuli leads to AKT dephosphorylation, FOXO3a release and translocation to the nucleus, resulting in transcriptional activation of Atrogin-1. FOXO family of transcription factors have several regulatory phosphorylation sites, including RAS/MAPK and PI3K/mTOR pathways (205,206). Thus, it was certainly interesting to investigate whether Atrogin-1 regulation in muscle was paralleled in GIST.

Notably, FOXO3a demonstrated to be the predominant isoform expressed in GIST cell lines and KIT-mutant GIST patients (**Fig. 22A,B**). On the other hand, GIST-T1 cells transfected with a pEGFP-C3 expression vector containing FOXO3a showed significantly increased FOXO3a nuclear translocation upon combined RAS/MAPK and PI3K/mTOR pathways inhibition, either with trametinib and GDC-0980 treatment or through KIT inhibition with imatinib, compared to single pathway ablation (**Fig. 23A,B**).

Remarkably, this was accompanied with FOXO3a dephosphorylation at both ERK1/2 (Ser425) and AKT (Th32) sites after KIT or conjoined KIT-downstream pathways suppression in GIST-T1 and GIST-T1/670 (**Fig. 24A,B**).

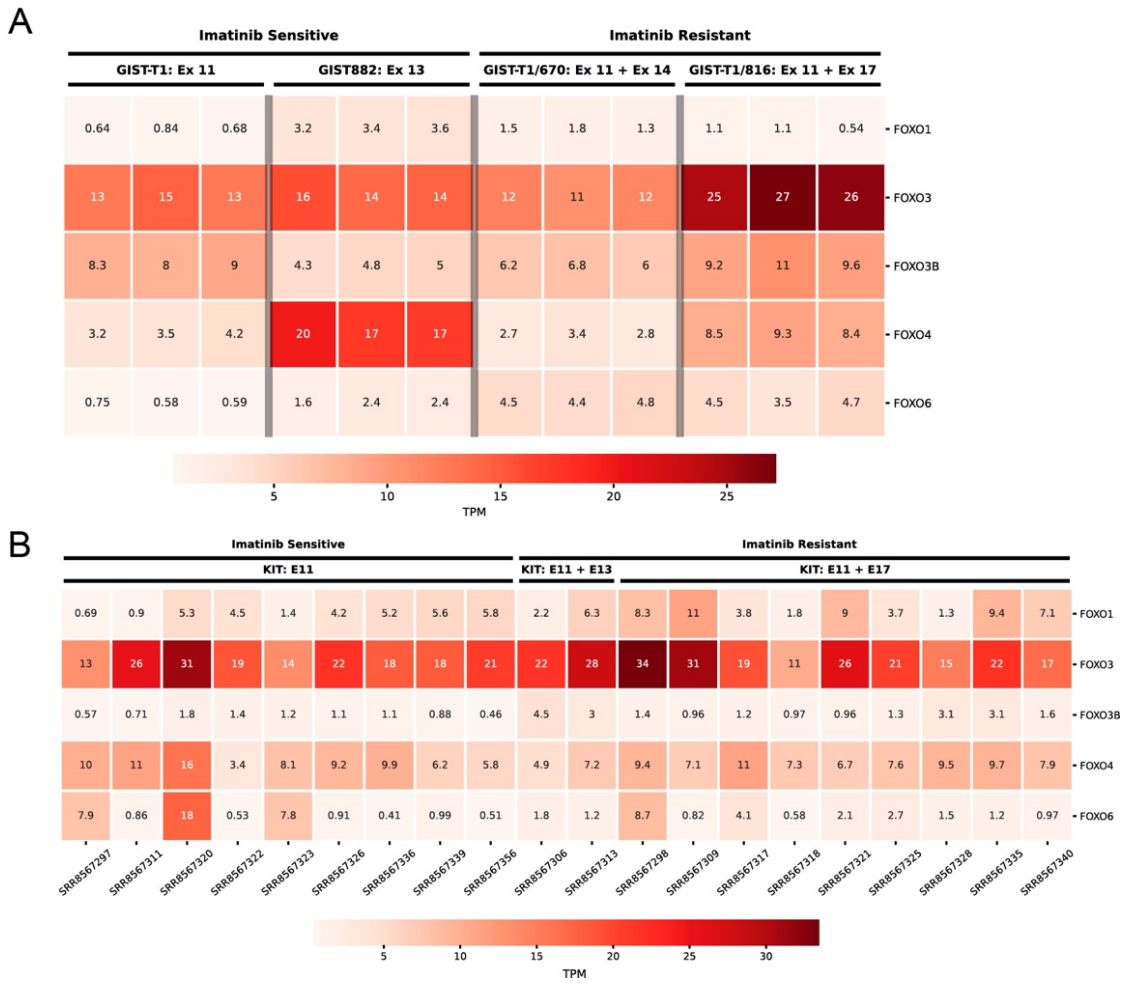

Figure 22. FOXO3a is the main FOXO isoform expressed in GIST regardless KIT mutational status, as shown by transcriptomic analysis performed in GIST cell lines (**A**) and publicly available data from GIST patients' samples (**B**).

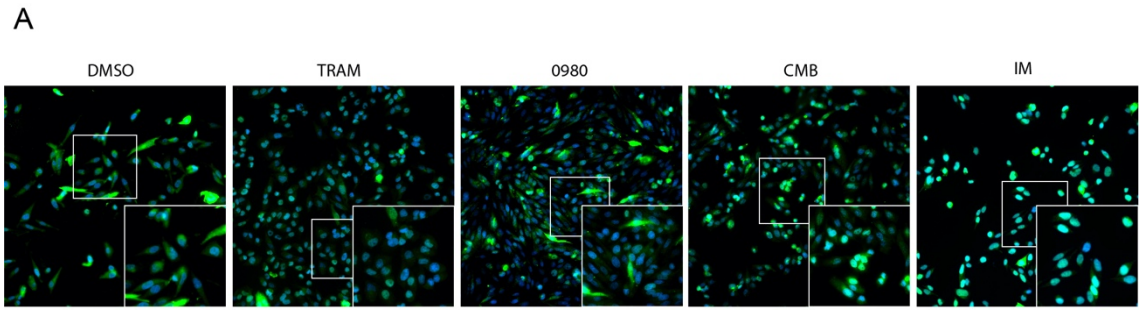

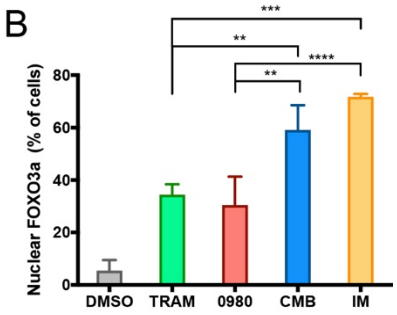

Figure 23. **A**, Representative immunofluorescence images at 20X (insets at 60X). **B**, Percentage of nuclear positive cells, results from 3 observations in 3 different areas. BL, Baseline; TRAM, trametinib; CMB, combination; IM, imatinib; DMSO, dimethyl sulfoxide.

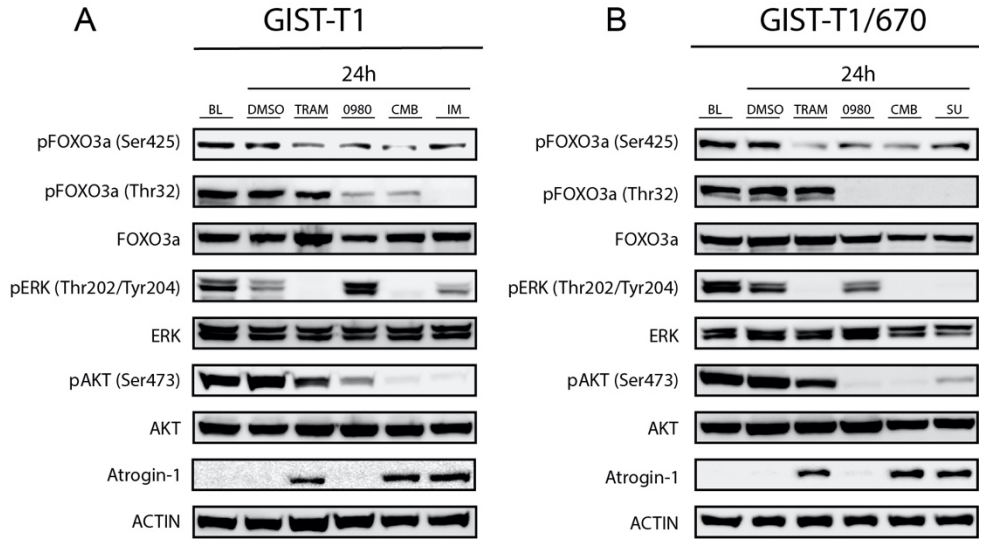

Figure 24. FOXO3a-specific phosphorylation residues for ERK1/2 (Ser425) and AKT1/2 (Thr32) activation were interrogated, along with other key molecules within KIT signaling, in GIST-T1 (**A**) and GIST-T1/670 (**B**). Simultaneous dephosphorylation is predominantly observed with the combination (CMB) and upstream KIT inhibition with imatinib (IM) and sunitinib (SU). TRAM, Trametinib.

A tamoxifen-inducible (4-hydroxy-tamoxifen, 4-OHT), AKT/ERK-insensitive mutant of FOXO3a (FOXO3a3A-ERTM) (207) was expressed in GIST-T1 and GIST-T1/670. Exogenous FOXO3a accumulated in the nucleus after 4-OHT treatment (**Fig. 25A,B**), resulting in increased FBXO32 mRNA and protein expression (**Fig. 25C-F**). p27Kip1, a known FOXO3a target gene, also showed increased expression (**Fig. 25D,F**).

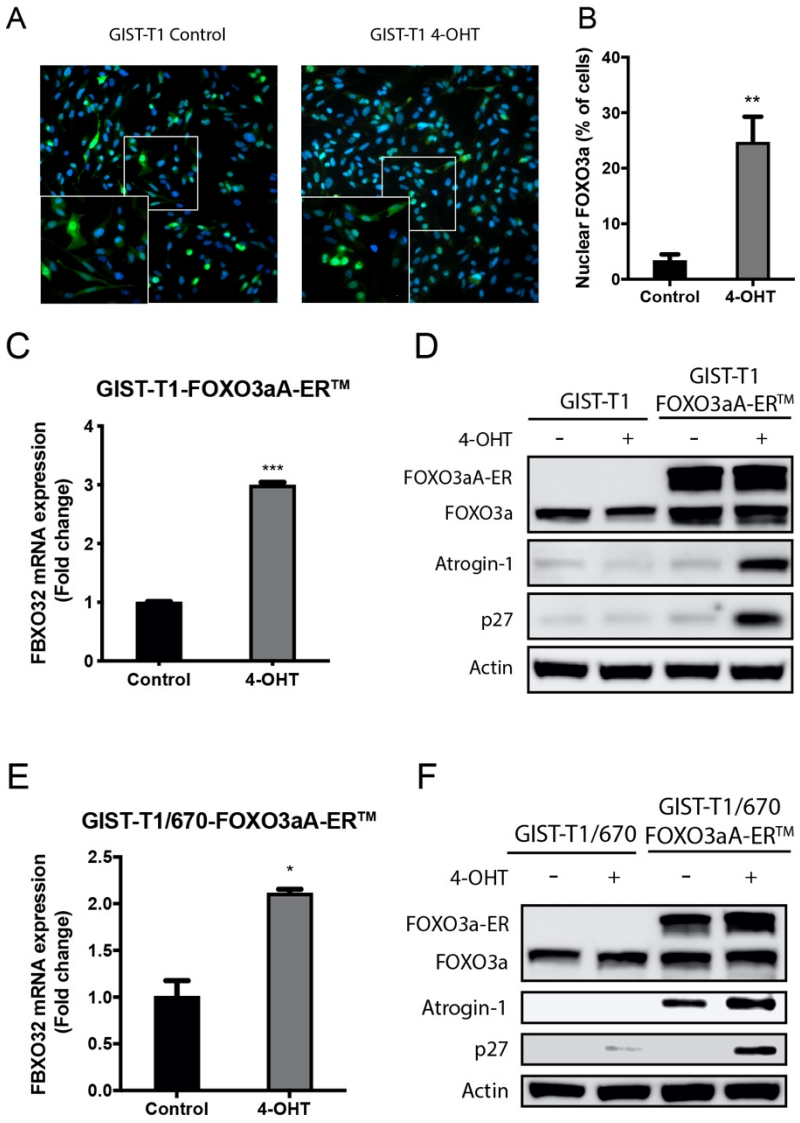

Figure 25. **A**, **B**, GIST-T1 cells expressing the tamoxifen-inducible FOXO3a3A-ERTM vector increased FOXO3a nuclear translocation upon tamoxifen treatment, as shown by immunofluorescence. In GIST-T1 (**C, D)** and GIST-T1/670 (**E, F**), tamoxifen-induced FOXO3a nuclear translocation led to a significant increase of FBXO32 mRNA (**C, E**) and protein (**D, F**) expression. GIST cells transduced with FOXO3a3A-ERTM showed exogenous FOXO3 expression (upper band). However, increased expression of Atrogin-1 and FOXO3a-target gene p27 is only observed after nuclear translocation upon tamoxifen treatment, (n = 3). Baseline (BL); trametinib (TRAM); combination (CMB); imatinib (IM); sunitinib (SU); 4-hydroxy-tamoxifen (4OHT); dimethyl sulfoxide (DMSO).

Finally, it was fundamental to prove that the higher levels of Atrogin-1 shown upon FOXO3a shuttling from the cytoplasm to the nucleus were the result of direct transcriptional regulation. Chromatin immunoprecipitation (ChIP) assay in GIST-T1 demonstrated a significant enrichment of FOXO3a binding to the *FBXO32* promoter after

24 hours of treatment with either the combination of trametinib and GDC-0980, or imatinib. A heterochromatin region was used as a negative control (**Fig. 26**).

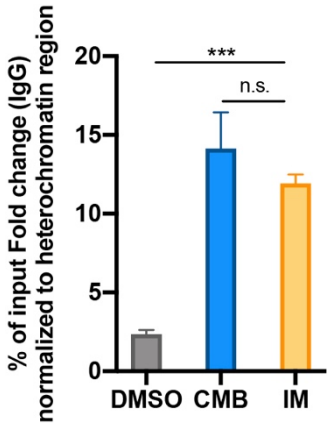

Figure 26. Chromatin immunoprecipitation (ChIP) was performed in GIST-T1 to demonstrate the transcriptional activation of Atrogin-1 by FOXO3a after inhibition of KIT with imatinib or the combined inhibition of KIT-downstream pathways with trametinib and GDC-0980. A heterochromatin region was used as a negative control. Dimethyl sulfoxide (DMSO); combination (CMB); imatinib (IM).

Together, it has been demonstrated that FOXO3a shuttles from the cytoplasm to the nucleus upon KIT and/or conjoined KIT-downstream pathways inhibition, leading to transcriptional activation of Atrogin-1. Therefore, Atrogin-1 regulation shares similar pathways in GIST and muscle cells, namely FOXO3a-dependent upregulation following deprivation of growth factor signaling.

5.4. Atrogin-1 mediates apoptosis evasion to KIT targeted inhibition through induction of cell quiescence

Atrogin-1-induced skeletal and cardiac muscle atrophy results primarily from accelerated protein degradation through the UPS, and it is characterized by a decrease in the size of pre-existing muscle fibers. However, Atrogin-1 function in cancer remains largely unknown. To shed light on its role, Atrogin-1 was knocked down using short hairpin RNAs (shRNAs) in imatinib-sensitive (GIST-T1) and imatinib-resistant (GIST-T1/670) cell models. Blockade of Atrogin-1 upregulation in response to KIT or conjoined PI3K/mTOR and RAS/MAPK pathways inhibition mostly resulted in enhanced apoptotic induction, as shown by cleaved caspase immunostaining (**Fig. 27A,B**) and further confirmed by cell count and Annexin V/PI staining (**Fig. 28A-D**).

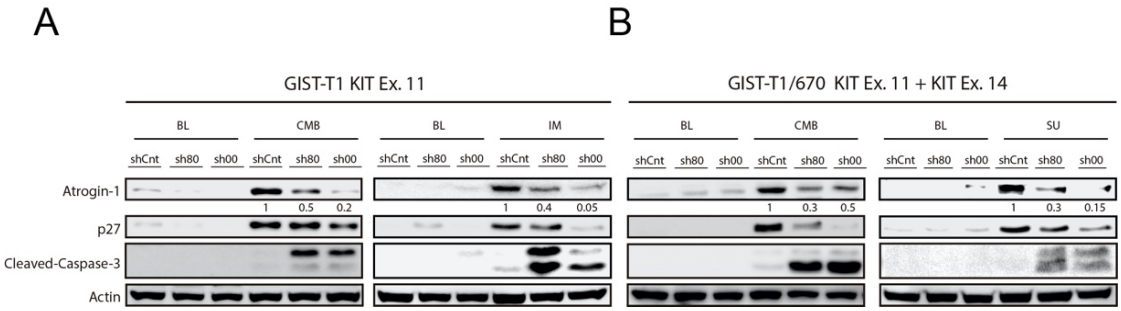

Figure 27. **A**, **B**, Atrogin-1 overexpression was efficiently blocked (~70% average) with two different shRNAs (sh80 and sh00). Imatinib-sensitive GIST-T1 (**A**) and imatinib-resistant GIST-T1/670 (**B**) were treated for 24 hours with the combination of trametinib 100 nM and GDC-0980 500 nM, or specific KIT inhibitors (imatinib and sunitinib). BL, baseline; CMB, combination; IM, imatinib; SU, sunitinib.

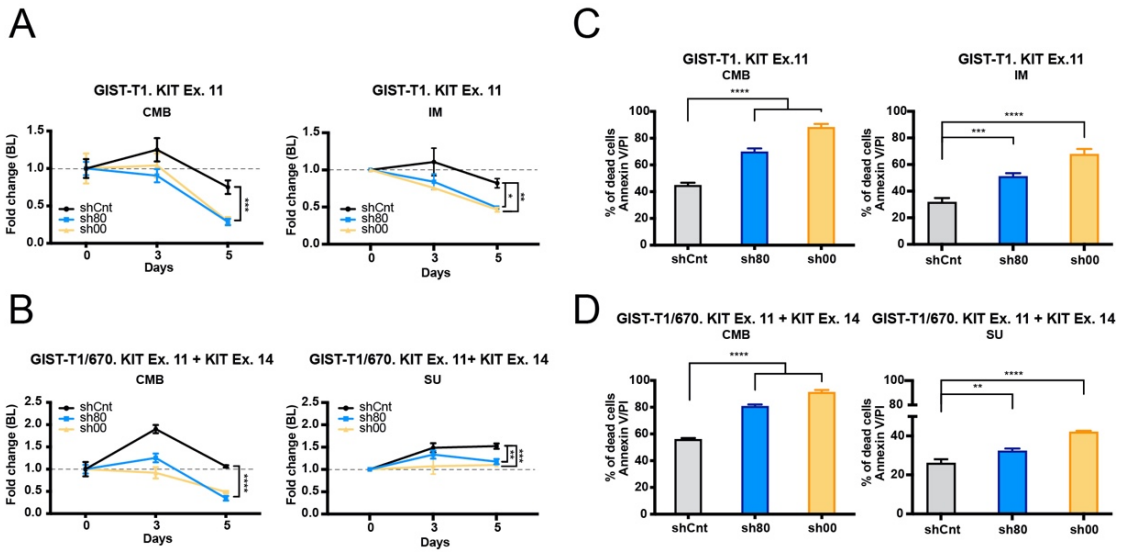

Figure 28. **A**,**B**, 6 days of continuous treatment with the combination of trametinib 100 nM plus GDC-0980 500 nM, or specific KIT inhibitors (imatinib 500 nM or sunitinib 500 nM) resulted in a significantly lower number of cells in GIST-T1 (**A**) and GIST-T1/670 (**B**) transduced with sh80 and sh00 compared to shControl. C, D, Annexin V/PI studies were performed in GIST-T1 (**C**) and GIST-T1/670 (**D**) under the same conditions, also showing a significant apoptosis increase in cells transduced with sh80 and sh00. CMB, combination; IM, imatinib; SU, sunitinib.

Indeed, insufficient Atrogin-1 response sensitized GIST cells to KIT and KIT-downstream pathways targeted inhibition, resulting in IC50 values 5- to 10-fold lower, thus highlighting the pro-survival role of Atrogin-1 (**Fig. 29A,B**). Additionally, a doxycycline-inducible vector was generated for Atrogin-1 overexpression (**Fig. 29C**). Transduced GIST-T1 cells with induced basal Atrogin-1 overexpression had decreased cleaved PARP and caspase-3 levels after KIT or KIT-downstream pathways inhibition (**Fig. 29D**), thus confirming its protective role against TKI-mediated apoptosis.

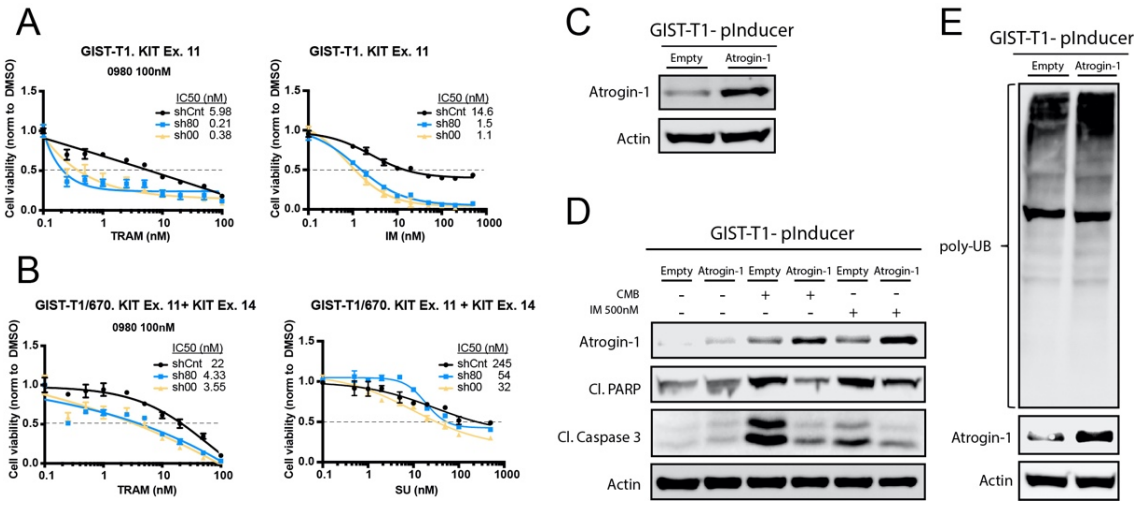

Figure 29. **A**, **B**, Cell viability assays were performed in GIST-T1 (**A**) and GIST-T1/670 (**B**) using either GDC-0980 at 100 nM and increasing concentrations of trametinib, or increasing imatinib or sunitinib concentrations. Lower IC50s were observed across all treatment conditions in GIST cells transduced with sh80 and sh00. **C**, Atrogin-1 overexpression is induced after 24 hours of doxycycline 0.25 ug/mL. **D**, At 48 hours of Atrogin-1 induction with doxycycline, all empty conditions showed higher levels of cleaved PARP and Caspase 3 apoptosis markers. **E**, Global ubiquitination was studied with a polyUb antibody in GIST-T1-Atrogin-1 compared to GIST-T1-empty after 24 hours of doxycycline 0.25 ug/mL and 12 hours of MG132 5 nM for ubiquitin stabilization.

Atrogin-1 is the final effector of the ubiquitin ligase cascade and, as any E3 ligase, regulates the fate of specific substrates through ubiquitination – something that we could observe in GIST upon induced overexpression (**Fig. 29E**). However, although Atrogin-1 substrates for proteasome degradation remain largely unknown, SCF E3 ubiquitin ligases have been widely involved in cell cycle progression (208). Therefore, it was reasonable to explore whether the apoptosis evasion mediated by Atrogin-1 occurred through cell cycle dysregulation. CDK inhibitor p27Kip1 was shown upregulated *in vitro* upon KIT or conjoined KIT-downstream pathways inhibition in shRNA control cells (**Fig. 27A,B**), which is consistent with previous observations indicative of cell cycle stop (11,12). By contrast, abrogation of Atrogin-1 response by shRNA knock-down was associated with maintenance of cell cycle progression, as expressed by low p27Kip1 induction, which paralleled the increased cell death (**Fig. 27A,B**). Accordingly, exogenous Atrogin-1 overexpression halted the cell cycle and prevented proliferation both in vitro (**Fig. 30A,B**) and in vivo (**Fig. 30C**). This effect on the cell cycle was GIST-specific and non-toxic, as Atrogin-1 overexpression in two different receptor tyrosine kinase (RTK)-driven cancer models (HCC827, EGFR-mutant lung cancer; MaMel-144a, KIT-mutant melanoma) did not affect cell proliferation (**Fig. 31A,B**).

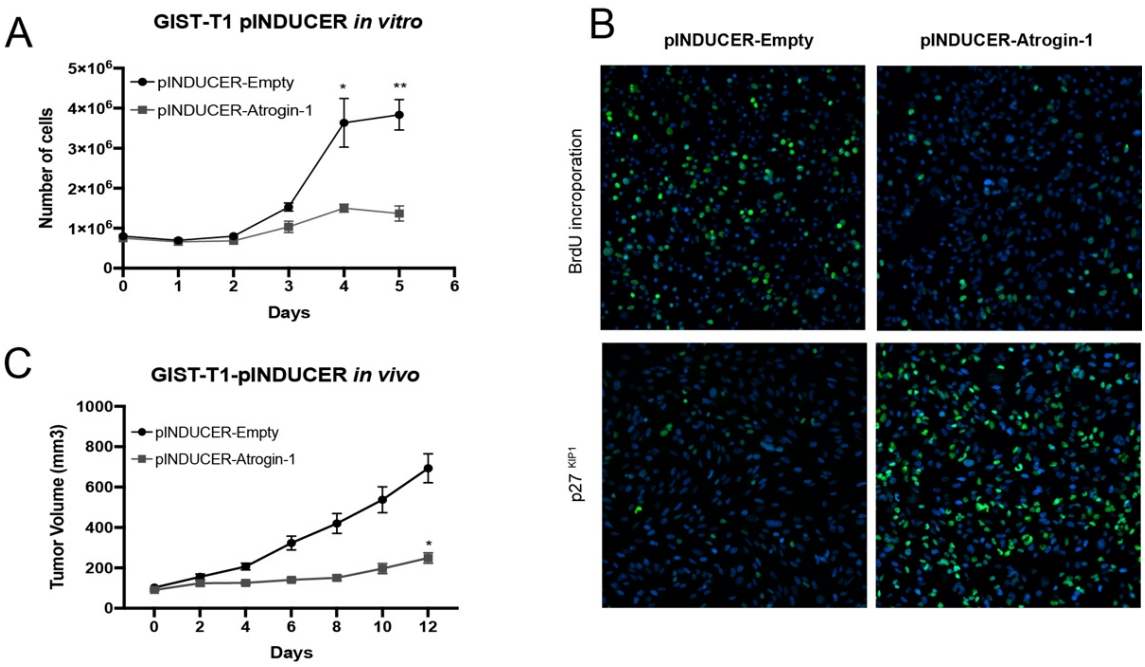

Figure 30. **A**, GIST-T1 cells transduced with either the empty vector or pINDUCER-Atrogin-1 were grown in doxycycline 0.25 ug/ml and assessed for cell proliferation, expressed in raw counts. **B**, Cell quiescence was evaluated through immunofluorescence staining GIST-T1 cells with BrdU and p27 after 48 hours of doxycycline induction. **C**, GIST-T1 cell transfected with empty (n=9) and pINDUCER-Atrogin-1 (n=9) vectors were xenografted and induced in vivo. Proliferation was assessed through tumor volume every 2 days.

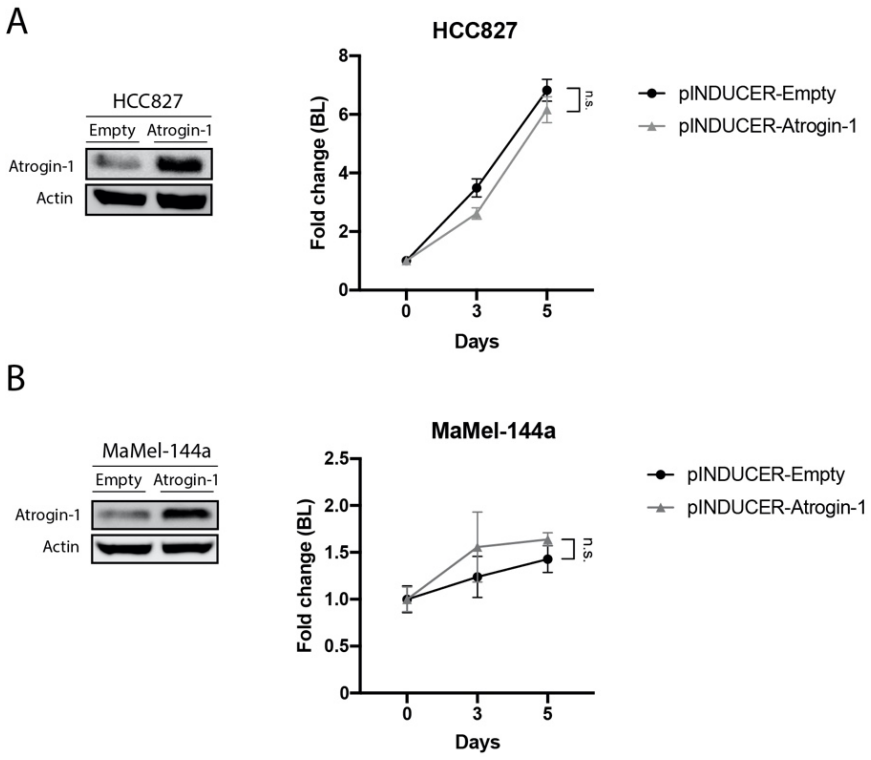

Figure 31. Atrogin-1 overexpression with pINDUCER-Atrogin-1 did not affect proliferation of HCC827 and MaMel-144a cell lines compared to the empty vector, as assessed in vitro through cell count.

The low BrdU incorporation and high p27Kip1 expression pattern observed in Atrogin-1 overexpressing GIST cells is highly indicative of cell quiescence state, but not fully definitory. Thus, flow cytometric detection of G0 live cells was assessed with Hoechst 33342 and Pyronin Y co-staining. A significant increase in G0 cells together with a significant decrease in S and G2/M cells occurred after Atrogin-1 induction (**Fig. 32A,B**). This process was reversible after doxycycline wash out (**Fig. 32C**), further confirming the quiescence nature. Collectively, Atrogin-1 overexpression emerges as a tightly regulated pro-survival mechanism in GIST that leads to adaptation to KIT-targeted inhibition by apoptosis evasion through induction of cell quiescence. This mechanism is shared in both imatinib-sensitive and -resistant GIST.

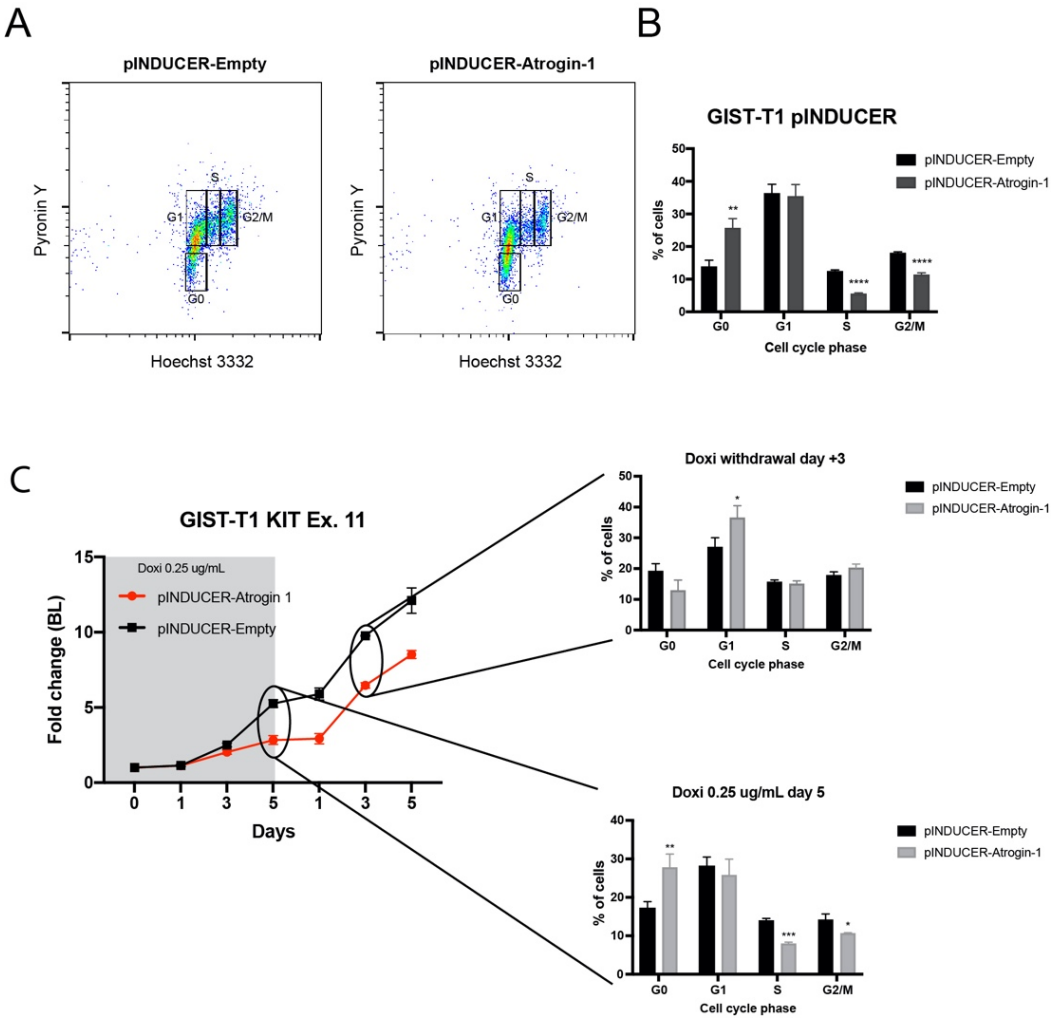

Figure 32. **A**, **B**, Representative flow cytometry charts (**A**) from 3 independent experiments using pINDUCER-Atrogin-1 and pINDUCER-empty vectors grown in doxycycline 0.25 ug/ml for 48 hours. Pyronin

Y/Hoechst 3323 stain allows to define the cell cycle G0 phase showing a significant increase in the percentage of cells with Atrogin-1 overexpression (**B**). **C**, Reversion of the GIST-T1 cell quiescence state induced by exogenous Atrogin-1 overexpression (pINDUCER-Atrogin-1) in vitro, in comparison with the empty vector. Cells were grown in doxycycline 0.25 ug/mL for 5 days and then withdrawn (WD). Cell proliferation and flow cytometry Pyronin Y/Hoechst 3323 evaluation were assessed at the indicated timepoints.

In order to corroborate that the function of Atrogin-1 observed is determined by its capacity of ubiquitinating specific proteins, Atroign-1, or an Atrogin-1 mutant lacking the F-box domain were constitutively expressed in GIST-T1 cells. As expected, higher global ubiquitination was observed in Atrogin-1 expressing cells compared to cells expressing mutant Atrogin-1, or the control (**Fig. 33A**). Furthermore, constitutively expression of full-length Atrogin-1 resulted in a significant increase of cells in G0, and in a decrease in the number of cells in G1 and G2/M, compared to cells expressing the Atrogin-1 lacking F-box domain (**Fig. 33B**). Hence, this confirms that Atrogin-1 function in GIST cells relies on its canonical activity as E3 ubiquitin ligase, and highlights the essential role of the UPS in GIST.

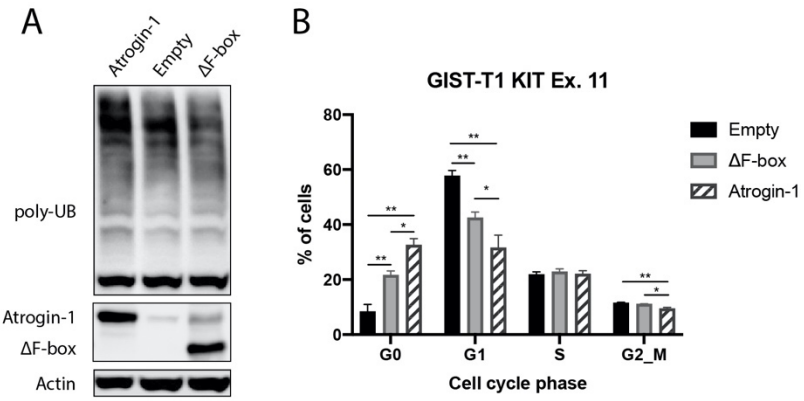

Figure 33. **A,** Kinase blot of GIST-T1 cells constitutively expressing full-length Atrogin-1, Atrogin-1 lacking F-box domain (ΔF-box), or control. Cells were incubated with MG132 5 μM for 8h. **B,** Flow cytometry values from 3 independent experiments using cells than in A. Pyronin Y/Hoechst 3323 stain were used to define the cell cycle G0 phase.

5.5. Increase in Atrogin-1 expression is GIST-cell specific and occurs in response to imatinib treatment in GIST patients

Oncogenic activation of KIT is the crucial driver in little neoplastic conditions besides GIST. Therefore, we explored whether the KIT-FOXO3a-Atrogin-1 axis was also present in other cancer types, such as systemic mastocytosis and a subset of melanomas, represented herein by the HMC-1.1 (KIT G560V) and MaMel-144a (KIT S476I) cell lines,

respectively. Neither the combined inhibition of RAS/MAPK and PI3K/mTOR pathways, nor KIT blockage with imatinib led to a significant increase in Atrogin-1 expression (**Fig. 34A**). External damaging agents (i.e.: doxorubicin) did not induce either an unspecific increase in Atrogin-1 levels (**Fig. 34B**). Therefore, KIT-FOXO3a-Atrogin-1 axis is biologically relevant only in a GIST-cell specific context.

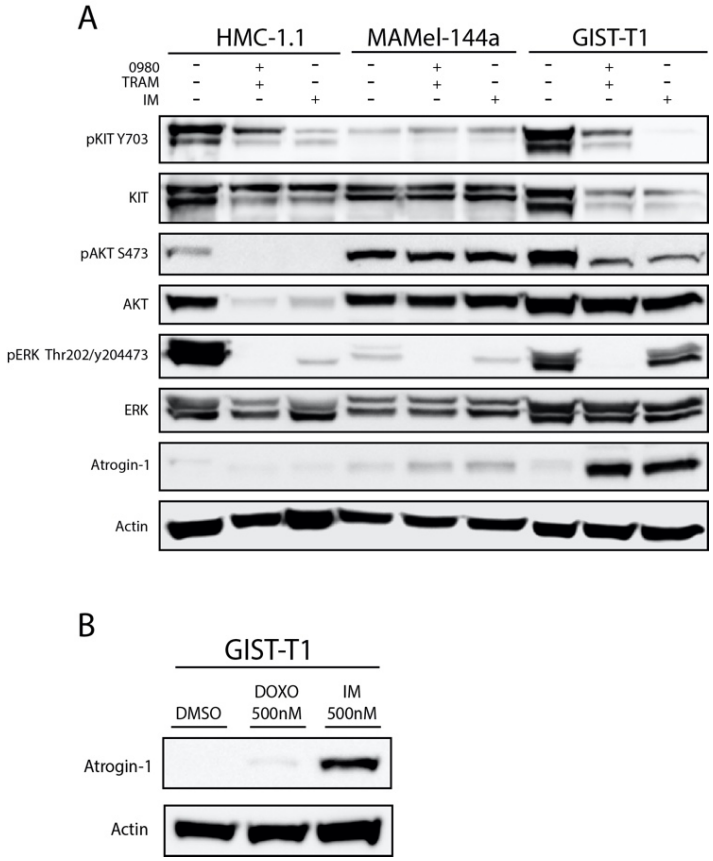

Figure 34. **A**, 24 hours treatment with the combination (CMB) of trametinib 100 nM and GDC-0980 500 nM, or imatinib 500 nM in HMC-1.1, MaMel-144a and GIST-T1 cell lines. **B**, Treatment of GIST-T1 cell line with doxorubicin (DOXO) or imatinib (IM) at the indicated doses for 24 hours.

On the other hand, two cohorts of GIST patients were further evaluated to determine whether Atrogin-1 expression was induced after front-line imatinib treatment. First, pre- and post-imatinib publicly available microarray data was retrieved from KIT-mutant GIST patients treated in a phase II trial investigating neoadjuvant imatinib in locally-advanced GIST (202). A statistically significant increase in FBXO32 mRNA expression was observed in post-imatinib tumor samples, compared to matched tumor samples before the beginning of the treatment. This increase in FBXO32 expression occurred in all but one patient (**Fig. 35A,B**). Additionally, Atrogin-1 immunohistochemistry expression was evaluated in a previously reported tissue-microarray from 92 locally advanced or

metastatic GIST patients that included pre- and/or post-imatinib tumor samples. Accordingly, a significant increase in Atrogin-1 expression was confirmed in post-imatinib tumor samples (**Fig. 35C,D**).

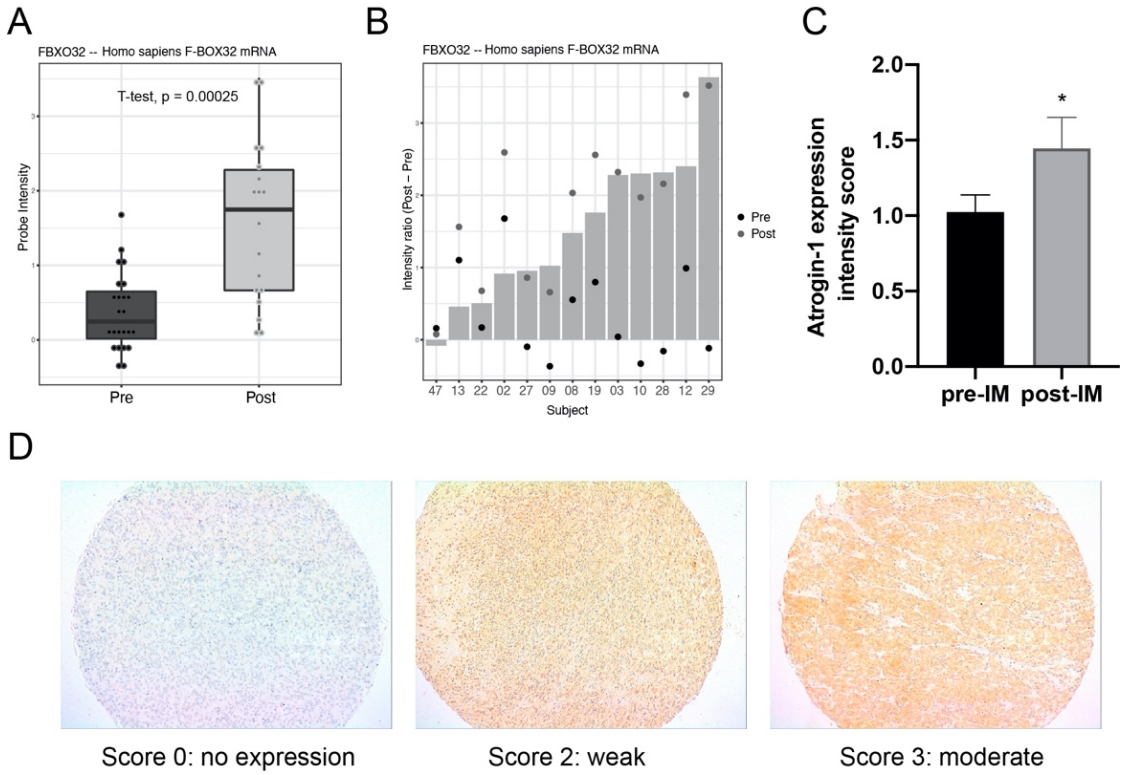

Figure 35. **A**, Publicly available microarray data (GSE 15966) from matched pre- and post-imatinib tumors samples revealed a significantly increase in the probe intensity of FBXO32 in post-imatinib tumor samples (p=0.00025). KIT-mutant patients were selected for this analysis. **B**, Bar graph displaying individual patient data from GSE 15966 analysis. Pre- (black) and post-imatinib (gray) FBXO32 intensities are depicted, together with the intensity ratio of the change in expression. **C**, Atrogin-1 immunohistochemistry expression was assessed in a tissue micro-array containing 82 pre- and 28 post-imatinib tumor samples in duplicates from 92 GIST patients. Atrogin-1 expression was significantly increased in post-imatinib tumor samples (mean ± SEM, 1.446 ± 0.2047) compared to the pre-imatinib counterparts (mean ± SEM, 1.025 ±0.1128), p=0.0326. **D**, Representative immunostains for Atrogin-1 in GIST tumor samples exemplifying different scores for expression intensity (10X): no expression (score 0), weak (score 2), and moderate (score 3).

5.6. GIST reliance on the ubiquitin-proteasome system can be exploited therapeutically to maximize imatinib therapeutic response

Previous results underscore the critical role of Atrogin-1 in the adaptation to the therapeutic inhibition of KIT, and also highlight more broadly the relevance of the UPS in GIST. In the absence of specific Atrogin-1 inhibitors, the aim was to prove the relevance of targeting the ubiquitin-ligase pathway using TAK-243, a first-in-class

inhibitor of the E1 ubiquitin-activating enzyme (UAE) that is currently being investigated in clinical trials (209). As previously mentioned, UAE is the primary enzyme responsible for the initiation of the ubiquitin multistep process, and therefore a key component of the UPS (210).

TAK-243 treatment resulted in IC50s within the nanomolar range *in vitro* (**Fig. 36A**). UAE inhibition induced an expected reduction in the global levels of polyubiquitylated chains (**Fig. 36B**). Combined treatment with imatinib and TAK-243 led to a dose-dependent, 10- to 20-fold decrease in cell viability (**Fig. 36C,D**), together with an increase in apoptosis induction (**Fig. 36E**).

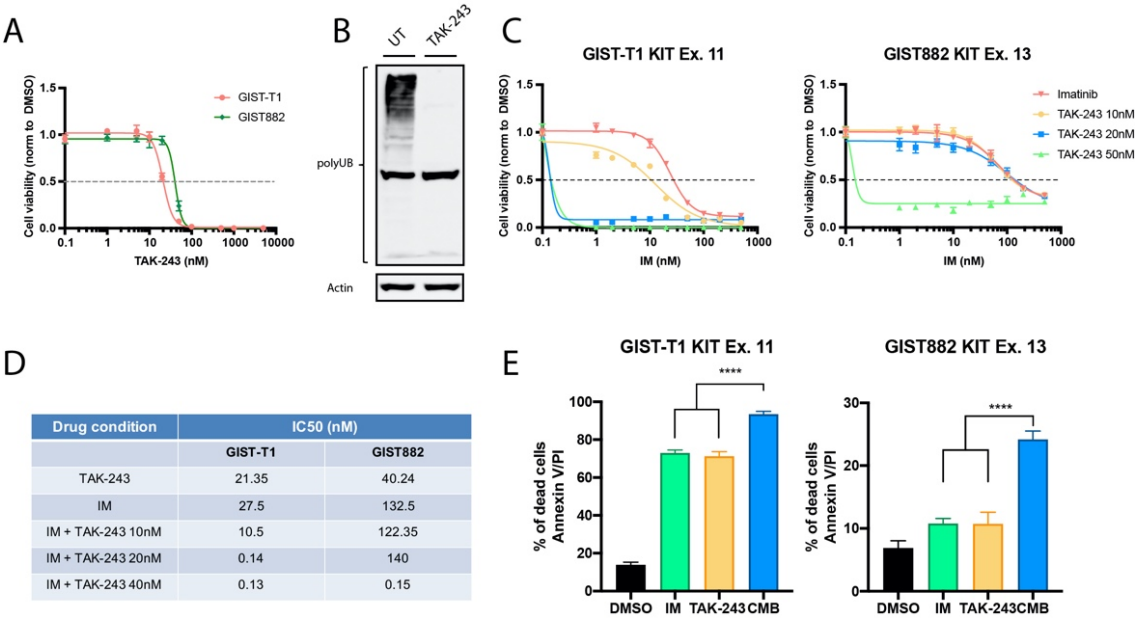

Drug condition	IC50 (nM)	
	GIST-T1	GIST882
TAK-243	21.35	40.24
IM	27.5	132.5
IM + TAK-243 10nM	10.5	122.35
IM + TAK-243 20nM	0.14	140
IM + TAK-243 40nM	0.13	0.15

Figure 36. **A**, Cell viability studies (CTG) with single-agent TAK-243. **B**, Loss of global polyubiquitination (polyUb) after 24 hours of TAK-243 100 nM in GIST-T1. **C**, Cell viability studies (CTG) using 3 different doses of TAK-243 and increasing doses of imatinib in GIST-T1 and GIST882. **D**, Resulting IC50 values from **A** and **C** cell viability studies. **E**, Annexin V/PI studies assessing apoptosis induction after 48 hours of imatinib 100 nM, TAK-243 100 nM or the combination at the same doses. DMSO, dimethyl sulfoxide; UT, untreated; IM, imatinib; Cl, cleaved; CMB, combination.

Next the combination of imatinib and TAK-243 was evaluated *in vivo*. Compared to monotherapies, the addition of TAK-243 to imatinib resulted in sustained reduction in tumor volume (**Fig. 37A,B**), which is consistent with *in vitro* data. The combination also resulted tolerable throughout (**Fig. 37C,D**). Therefore, inhibition of ubiquitination in GIST maximizes the response to imatinib treatment through enhanced apoptosis and impaired tumor cell growth.

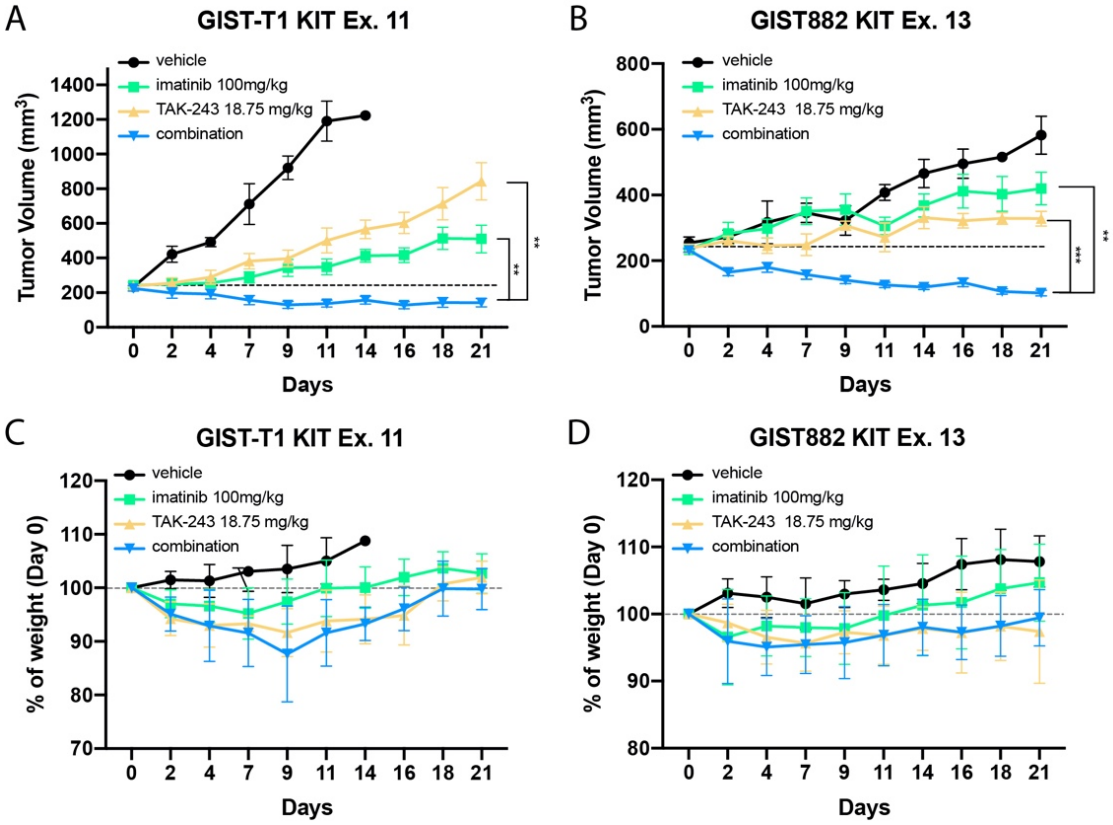

Figure 37. **A**,**B**, *In vivo* evaluation in subcutaneous xenografts of GIST-T1 (**A**) and GIST882 (**B**) at the indicated doses and length of treatment. n=5-7 per treatment arm in GIST-T1 and n=5 in GIST882, except for combination (n=10), mean ± SEM. Animal tolerance to drug-induced toxicity was objectivized through animal weight measurements across the 3 weeks of experiment and expressed as percentage of weight variation (in grams) in GIST-T1 (**C**) and GIST882 (**D**).

6. DISCUSSION

The essential role that oncogenically-active KIT exerts in the transition from the ICCs to clinically aggressive GIST turns this disease into a paradigmatic cancer model to study oncogenic dependencies (60,110,211). This thesis unveils Atrogin-1 as one of the most critical genes differentially dysregulated in GIST upon KIT and/or KIT-downstream pathways inhibition, independently of the type of KIT primary or secondary mutation. Atrogin-1, a muscle-specific SCF E3 ubiquitin ligase, is the crucial effector of muscle atrophy in cachexia of any origin. Interestingly, this Thesis demonstrates that Atrogin-1 regulation is shared by GIST and skeletal muscle. Namely, FOXO3a-mediated transcriptional activation after a decay in growth factor receptors signaling – KIT signaling impairment in the case of GIST. Atrogin-1 overexpression turned out to be a crucial pro-survival mechanism for therapeutic adaptation to targeted inhibition of KIT, driving apoptosis evasion through induction of cell quiescence (**Fig. 38**). Consequently, ubiquitin ligase pathway blockage with TAK-243 maximized the therapeutic activity of imatinib.

6.1. Identification of critical effectors within KIT-downstream pathways

KIT/PDGFRA oncogenic program in GIST is conserved throughout all stages of the disease (56,59,72,110,211,212). Notably, this dependency is maintained after first-line imatinib failure, as polyclonal emergence of KIT secondary mutations remains the main mechanism of resistance in up to 90% of GIST, including heavily pretreated patients (56,212). This is however a clinical challenge, since TKIs in imatinib-resistant disease are active only against a subset of these secondary mutations (53,212). Although all RTKs display variable degrees of pleiotropy, a wealth of evidence supports that KIT/PDGFRA oncogenic program is primary sustained by RAS/MAPK and PI3K/mTOR pathways, regardless the type of KIT primary or secondary mutation (84,108,110,213,214). Herein, pharmacological screenings performed in clinically-representative GIST cell models were performed to dissect these pathways and to ascertain their critical effectors.

6.1.1. PI3K/AKT/mTOR pathway

Remarkably, all PI3K class IA isoforms demonstrated to be equally important for GIST cells. This differs from what occurs in other cancer types, in which depending on the tumor driver, or cell lineage, one specific isoform predominantly funnels the oncogenic

signaling (215,216). On the other hand, AKT signaling has demonstrated to be crucial in different neoplasms, such as PI3KIA-mutant, or HER2-amplified breast tumors (217). Intriguingly, AKT inhibition did not impact on cell viability or proliferation in GIST cells. This phenomenon could be due to the fact that other molecular mediators, besides AKT, might be involved in the transduction of the signaling coming from PI3K, so that inhibition of AKT alone does not have relevant consequences in terms of cell viability or cell proliferation. Conversely, dual inhibition of PI3K and mTOR displayed the strongest impact on GIST cell models both in cell viability and proliferation, being superior to that observed after their individual inhibition. This poses both nodes as pivotal mediators of the oncogenic signaling through the PI3K/AKT/mTOR pathway, and suggests that signaling through these effectors is not redundant, which is consistent to that reported in other studies (213).

6.1.2. RAS/MAPK pathway

Interestingly, B-RAF is not essential for RAS/MAPK pathway signaling in GIST cells since its specific inhibition did not affect cell viability or cell proliferation. This is coherent to what has been observed in other neoplasms, such as colorectal cancer, in which B-RAF inhibition results in scarce anti-tumor activity when there is a simultaneous overactivation of an RTK (218). In these cases, signaling is likely maintained through the other members of the RAF family, A-RAF and C-RAF, attenuating the consequences of B-RAF suppression. Nonetheless, GIST cells are extremely sensitive to the inhibition of other downstream mediators such as MEK1/2 and ERK1/2. Specifically, MEK1/2 turned out to be the most determinant node in RAS/MAPK pathway signaling, even more than ERK1/2. However, results suggest that these two nodes are fundamental and cannot be circumvented by alternative mediators.

6.2. KIT- downstream pathway crosstalk

The inhibition of the critical nodes within KIT-downstream pathways identified in this thesis, such as PI3K IA/mTOR and MEK1/2, completely abrogates the signaling on their respective pathways. Moreover, there is no cross-reactivation between the two pathways, and when one is suppressed, it is not reactivated by the pathway that remains active. However, potential interactions between both pathways were observed. Abrogation of the PI3K/AKT/mTOR pathway causes a transient decrease in the levels of

ERK phosphorylation. This phenomenon has already been described in other tumor types, such as breast cancer, and could be due to an interaction between PI3K and RAS. PI3K can interact with RAS by stabilizing it on its active conformation, RAS-GTP, so that when PI3K is inhibited, this interaction is lost. This would decrease RAS activation leading to a decrease in ERK phosphorylation (215,219). Nevertheless, this is a transient decrease and its specific role in GIST biology has not been elucidated. It is also noteworthy that low levels of AKT phosphorylation are maintained for up to 72 hours. Interestingly, a slight recovery in the phosphorylation is observed at 24-48 hours, which is probably insufficient for a complete pathway reactivation, but that may contribute to the modest proapoptotic effects upon single inhibition of this pathway.

On the other hand, suppression of the RAS/MAPK pathway results in a decrease on AKT phosphorylation levels at 12-24 hours. This can be explained because loss of RAS/MAPK pathway signaling leads to a destabilization of the transcriptional factor ETV1, which ultimately results in a decrease expression of KIT. The consequence is a mild and transient diminution on the activity of KIT, and thereby in diminution on the activation of its downstream pathways. (111).

6.3. Dual pathway suppression recapitulates KIT inhibition

6.3.1. *In vitro* experiments

Despite the fact that RAS/MAPK and PI3K/AKT/mTOR are the pivotal signaling pathways in GIST, their individual suppression does not have substantial effects in terms of cell proliferation, except for GIST-T1, in which RAS/MAPK pathway suppression results in a cytostatic effect, presumably due to a more pronounced reliance of this cell line in this pathway. As mentioned before, this circumstance is not due to cross-reactivation of any of KIT-downstream pathways that would eventually be responsible of sustaining the entire oncogenic program. Conversely, it is most likely due to an "oncogenic compensation" mechanism whereby the non-inhibited pathway is able to convey the oncogenic signaling coming from KIT, while the other pathway remains suppressed. This would explain the fact that solid antiproliferative and cytotoxic effects are only observed after the concomitant abrogation of both pathways, and hereby after the complete ablation of KIT-downstream pathways. Likewise, apoptosis induction was markedly higher upon concurrent inhibition of PI3K/mTOR and RAS/MAPK pathways,

compared to single-pathway suppression. Of note, albeit the experiment was not designed to obtain a synergy index, the results suggest a potential synergistic effect of simultaneous pathway suppression, as the levels of apoptosis upon the combination exceed the sum of the effect obtained after individual pathway inhibition.

Unexpectedly, the apoptosis studies suggest that the apoptotic process in GIST cells is more dependent on RAS/MAPK. This is in disagreement with first works exploring KIT-oncogenic signaling in GIST cells, in which PI3K/mTOR was thought to govern the apoptotic process. Indeed, AKT has been shown to directly interact with proteins and factors involved in cell death such as BIM, BAD or MDM2 (220). However, the experiments presented in this thesis show that the inhibition of PI3K/mTOR pathway generates lower levels of apoptosis than those observed upon the abrogation of RAS/MAPK pathway. As previously explained, inhibition of RAS/MAPK is accompanied by an early diminution of KIT expression due to KIT-ETV1 axis disruption, which ultimately results in a transient decrease of PI3K signaling. This phenomenon could contribute to the differences observed in short-term apoptosis induction after single-pathway suppression. However, there are probably other factors yet to be uncover that determine in this process.

6.3.2. *In vivo* experiments

The results presented in this thesis evidence that concurrent inhibition of PI3K/mTOR and RAS/MAPK pathways recapitulates the effects observed upon KIT-targeted inhibition in GIST cells. Furthermore, concomitant pathway inhibition demonstrated to have cytotoxic and pro-apoptotic effects *in vitro* regardless primary, or secondary mutation in KIT. The clinical efficacy of this strategy had already been evaluated on clinical trials in advanced solid tumors using a continuous administration schedule (126). In these, the toxicity resulting from the combination led to the use of suboptimal doses of each drug, hereby limiting the antitumor activity of the strategy. Herein, a creative intermittent schedule of PI3K/mTOR and MEK1/2 inhibition was designed and validated in imatinib-sensitive and imatinib-resistant GIST models. A safety window of 2-3 days is established in which tumor cells remain non-proliferative in the absence of drug. This time frame allows non-transformed cells to recover, thus attenuating the treatment-associated toxicity, and enabling the use of optimal doses of each pathway inhibitor. Accordingly, this therapeutic strategy was effective delaying tumor growth *in vivo* in mice

GIST xenografts, independently of KIT mutation. Strikingly, little toxicity associated to the combination was observed. Hence, the *in vitro* and *in vivo* studies presented in this thesis serve as a proof-of-concept regarding the feasibility of this type of strategy, which doubtlessly merit to be further explored in the clinical setting due to its therapeutic potential independently of the primary or secondary mutations in KIT.

6.4. Atrogin-1 is the most up-regulated gene upon KIT or KIT - downstream pathways inhibition

The oncogenic compensatory signaling observed between KIT-downstream pathways is at least partially due to common genes co-regulated by both pathways. In this regard, transcriptomic studies performed in clinically-representative GIST cell models unveiled *FBXO32* among the most differentially expressed genes after concurrent inhibition of RAS/MAPK and PI3K/mTOR pathways, thus emerging as one of the main genes conjointly regulated by these two pathways in GIST cells. Likewise, upstream KIT suppression also resulted in a prominent upregulation of *FBXO32*. Indeed, additional transcriptomic analysis in GIST-T1 showed *FBXO32* as a top-ranked dysregulated gene after KIT targeted inhibition with imatinib, which agrees with previously reported data (112,204). Notably, there exists a significant overlap between genes dysregulated by both imatinib and KIT-downstream pathways inhibition, which emphasizes the major role of these two pathways funneling KIT oncogenic signaling.

6.4.1. Atrogin-1 regulation in GIST cells shares similarities with its regulation in muscle cells upon atrophy induction.

Atrogin-1 function, and regulation has been extensively studied in muscle cells, in which it exerts a critical role during muscle atrophy of any origin, including cancer. Of note, the mechanism by which the expression of Atrogin-1 is regulated in GIST cells shares striking similarities with the mechanism of regulation in muscle cells, since its expression mainly relies on the transcription factor FOXO3a in both cell contexts. However, there are some particularities. In GIST cells FOXO3a function is tightly regulated by KIT through RAS/MAPK and PI3K/mTOR pathways, in which ERK and AKT phosphorylate the transcription factor at specific residues (Ser425 and Thr32, respectively), controlling its subcellular location. Instead, in muscle cells this regulation exclusively relies on PI3K pathway, and ultimately, on AKT phosphorylation. The fact that one protein that exerts a prominent role in muscle cells is one of the main genes expressed upon KIT inhibition in

GIST cells, together with the similarities on the mechanism of regulation shared by both cell-contexts result extremely interesting and could be explained by the embryogenic origin of GIST cells. As explained in the introduction of this Thesis (1.2. Origin), GIST cells are thought to originate from ICCs, which share a common progenitor with smooth muscle cells of the longitudinal muscular layer of the gastrointestinal tract. Accordingly, GIST tumors display myogenic traits and they are usually grouped among tumors of muscular origin (104,195). Therefore, this is a very intriguing example in which tumor cells express, or recover the expression, of genes or transcriptional programs that are relevant in other cellular contexts, with which share embryonic origin. Herein, it is the case of Atrogin-1, but also of the transcription factor FOXO3a, which is the predominant isoform of FOXO TFs family in GIST, and has been shown to play a prominent role in a muscular cell context. It would certainly be interesting to explore whether both, Atrogin-1 and FOXO3a, have a function in differentiated ICCs, and also, whether Atrogin-1 plays a role in tumors of muscular origin, such as rhabdosarcoma or leiomyosarcoma.

6.4.2. Minor differences observed in Atrogin-1 expression upon single-pathway inhibition

As aforementioned, Atrogin-1 is tightly regulated in GIST by both, RAS/MAPK and PI3K/mTOR pathways. Nevertheless, single-pathway abrogation does not result in a strong induction of Atrogin-1 expression. This is because FOXO3a is still phosphorylated by the non-suppressed pathway, which limits the presence of the transcription factor inside the nucleus. Interestingly, RAS/MAPK inhibition consistently results in higher levels of Atrogin-1 expression, compared to PI3K/mTOR blockade. This could be explained by the fact that, as previously explained (6.3.1), RAS/MAPK suppression entails the disruption of KT-ETV1 axis, which leads to a mild, and transient decrease of KIT expression, and thereby a transient decrease of PI3K/mTOR pathway. This phenomenon could resemble to the effect obtained after concomitant inhibition of both pathways and could explain the differences in Atrogin-1 expression observed upon single-pathway suppression. However, there were no differences regarding nuclear presence of FOXO3a after individual inhibition of each pathway. Therefore, it is possible that the difference in Atrogin-1 expression after single-pathway suppression is determined by the transcriptional activity of FOXO3a, that may differ depending on which residues are phosphorylated, rather than by its nuclear translocation. Thus, phosphorylation of FOXO3a in Ser425 by ERK1/2 could hamper at higher extent its

transcriptional activity over Atrogin-1 than phosphorylation at Thr32 undertaken by AKT. Nonetheless, only concurrent inhibition of both pathways yields strong and consistent expression of Atrogin-1 among the different GIST-cell line models.

6.4.3. KIT-induced Atrogin-1 expression is restricted to a GIST specific context

Noteworthy, KIT regulation of Atrogin-1 expression is exclusive of a GIST-cell specific context. Accordingly, KIT or KIT-downstream pathway inhibition in other KIT-driven diseases did not result in Atrogin-1 expression. Hence, Atrogin-1 belongs to a subset of essential genes for GIST-cell biology that are integrated within an oncogenic program initiated by KIT, and that is restricted to GIST cells (110,211,221).

6.4.4. The pivotal role of Atrogin-1 in cell quiescence induction

Atrogin-1, as an E3 ubiquitin ligase, acts at the last step of the ubiquitin transfer cascade and its overexpression in skeletal muscle results in accelerated proteasome-mediated degradation of key specific proteins (176,183,184,187). Conversely, data regarding the function of Atrogin-1 in cancer is limited and its specific role is still poorly understood (176,222). In this thesis, it has been thoroughly demonstrated through several *in vitro* and *in vivo* experiments that Atrogin-1 is a critical mediator for the adaptation of GIST cells to KIT-targeted inhibition. Accordingly, Atrogin-1 overexpression drives GIST cells into a cell-quiescent state, in which cells remain arrested in G0 phase as a protective mechanism to prevent cell death upon KIT inhibition.

Cell quiescence is a well-known mechanism of cancer cells to evade drug-induced apoptosis, hereby creating a niche favorable for the emergence of drug-resistant subpopulations. Previous studies in GIST showed that imatinib induces cell quiescence in those tumor cells that do not undergo apoptosis. In this regard, different mechanisms have been revealed to be involved in this process, such as APC/CDH1-SKP-p27^{kip1}, the DREAM complex, and autophagy (1.6.2). Thus, it is conceivable that such an important process for GIST cells is the result of the interaction of several players. Nonetheless, the main findings presented in this Thesis demonstrate that Atrogin-1 plays a pivotal role in cell-quiescence induction: first, *FBXO32*/Atrogin-1 is the top-ranked gene derepressed upon suppression of KIT, and emerges at a very early timepoint; second, Atrogin-1 expression is tightly regulated within the KIT-FOXO3a axis in the unique GIST-cell

context; third, microarray and immunohistochemistry results from GIST patients treated with imatinib evidence that Atrogin-1 overexpression is sustained over time; and fourth, ubiquitin pathway inhibition hinders the adaptation to KIT suppression with imatinib and enhances the apoptosis response. Together, we can speculate that Atrogin-1 is likely the first and more persistent mediator of cell quiescence induction for TKI-mediated apoptosis evasion in GIST, while several other known and unknown mechanisms buttress the quiescence state shortly thereafter (112,145,146,204).

6.4.5. Atrogin-1, tumor suppressor or oncogene?

As discussed above, only few studies have explored the role of Atrogin-1 in tumorigenesis, and thus it remains poorly understood. Intriguingly, Atrogin-1 promoter is hypermethylated in several cancers cell lines, such as rhabdomyosarcoma, breast, ovarian, esophageal, and colorectal carcinoma (190,194,222,223). In these, Atroign-1 overexpression hampers cell proliferation *in vitro* and prevents tumor growth *in vivo*. Indeed, Atrogin-1 was shown to hinder cell proliferation in an ovarian and breast cancer cell line by catalyzing the ubiquitination of the oncogenic transcription factor c-MYC, and KLF4, respectively, prompting their proteosome-mediated degradation (191,224). On the other hand, Atrogin-1 was found to participate in cell apoptosis induced by EZH2 inhibition in colorectal carcinoma cell lines. Surprisingly, in this study Atrogin-1 overexpression did not have any consequence for cancer cells by itself, and its role was contingent upon the inhibition of EZH2 protein (192,193). Collectively, these studies suggest that Atrogin-1 may play a tumor suppressor role in cancer, although it might be cell-context dependent.

The results presented in this Thesis are consistent with those previously mentioned, regarding the consequences of Atrogin-1 expression in cancer cells. Namely, Atrogin-1 overexpression in GIST cells leads to cell-quiescence induction, characterized by an accumulation of cells in phase G0. Nonetheless, in GIST cells, this cell cycle arrest serves as a protective mechanism that prevents tumor cells from drug-induced cell-death and favors their adaptation. Hence, although Atrogin-1 expression impairs cell proliferation *in vitro*, and prevents tumor growth *in vivo*, which would suggest a tumor suppressor role, this entails a treatment-adaptation mechanisms that protect tumors cells from apoptosis induced by KIT inhibition. Accordingly, unlike other tumors, Atrogin-1 plays an oncogenic role in GIST cells.

A major difference between other tumors and GIST, which might explain the different role of Atrogin-1, is that in most of those tumors Atrogin-1 expression is repressed by promoter hypermethylation. Specifically, EZH2 protein has been reported to epigenetically regulate Atrogin-1 expression in several tumor types, such as rhabdomyosarcoma, esophageal, ovarian, and colorectal carcinoma. EZH2 protein is a methyltransferase commonly overexpressed in several types of cancer, in which is responsible of the repression of many tumor suppressors. Thus, while in other tumors Atrogin-1 expression is controlled by a generic mechanism of gene expression regulation, in GIST its expression is specifically governed by the oncogenic driver, and hereby is part of a particular oncogenic transcriptional program. This could explain why the expression of the same protein in two different cellular contexts, despite having the same consequences, plays very different, even opposite, roles.

6.4.6. Atrogin-1 targets

Several different targets of Atrogin-1 have been identified in different cellular contexts. As previously explained, Atrogin-1 was first identified as critical effector in the induction of muscular atrophy of any origin. In this cell context, myoD and EI3F were identified as the main targets of Atrogin-1, both being degraded after Atrogin-1-mediated K48-linked poly-ubiquitination during muscle atrophy (183,184). Of note, FOXO3a was also identified as a target of Atrogin-1 in murine cardiomyocytes. In these, Atrogin-1-mediated K63-linked ubiquitination of FOXO3a prompted its nuclear retention, boosting its transcriptional activity (189). This is extremely interesting in the context of this Thesis for three different reasons: first, it is an example of the K63-linked ubiquitination signaling activity of Atrogin-1; second, the consequences of the enhancement of FOXO3a transcriptional activity would be consistent with the phenotype observed upon Atrogin-1 overexpression in GIST cells, as many of the transcriptional targets of FOXO3a are involved in cell cycle arrest, such as $p27^{kip}$; and third, it is a muscular cell context and it has been shown herein, that Atrogin-1 regulation in GIST cells share strong similarities with its regulation in muscle cells, particularly regarding FOXO3a participation. Hence, the possibility that FOXO3a is a target of Atrogin-1 in GIST cells merits to be further explored in the future.

Beyond muscular cells, several targets of Atrogin-1 have been uncovered in ovarian, and especially in breast cancer cell models. In ovarian carcinoma cell lines, Atrogin-1 was

shown to specifically target c-MYC for proteosome-mediated degradation, leading to cell proliferation impairment (191). Likewise, Atrogin-1 was shown to target the transcription factor KLF4 for proteosome-mediated degradation in breast cancer cells, hindering their tumorigenic potential (224). Also in breast cancer cell models, IKBα was identified to be specifically targeted by Atrogin-1 for proteosome-mediated degradation upon a genotoxic stress, which triggers NFKB pathway activation, contributing to the activation of cell cycle checkpoints and DNA repair pathways (225). Finally, Atrogin-1 was shown to stabilize the transcriptional co-regulator factor CtBP1 through K63-linked ubiquitination during epithelial to mesenchymal transition in a murine breast cancer model (226).

Based on the results presented in this thesis, it is likely that the targets of Atrogin-1 in GIST cells are involved in cell cycle. Accordingly, different F-box E3 ubiquitin ligases have been shown to regulate many of the main mediators of cell cycle progression, such as Cyclin D1, Cyclin E, Cyclin A, Cyclin B, p27, or p21 among others (227). Therefore, it is conceivable that Atrogin-1 elicits a reversible cell cycle arrest by mediating the proteosome-degradation of a specific protein involved in cell cycle progression. As previously mentioned, other non-excluding possibility that merits to be further explored is that in GIST, as it has been already shown in cardiomyocytes, Atrogin-1 enhances FOXO3a transcriptional activity by prompting its nuclear retention by mediating its K63-linked ubiquitination. This would lead to a stabilization of the expression of specific genes regulated by FOXO3a, such as p27, which is a well-known negative regulator of cyclin-dependent kinases 4 and 6 (CDK4 and CDK6, respectively).

Collectively, several targets, of Atrogin-1 have been identified in different cellular and pathological context. Further studies looking for specific Atrogin-1 targets in GIST are warranted to expand the understanding of the role of this E3 ubiquitin ligase in GIST cells.

6.4.7. Targeting Atrogin-1 and the UPS in GIST

Due to its pivotal role as a mediator in the adaptation of GIST cells to targeted KIT inhibition, Atrogin-1 raises as a very appealing therapeutic target to enhance the anti-tumor action exerted by imatinib, or any other KIT inhibitor. Accordingly, the combination of a specific Atrogin-1 inhibitor with imatinib would hinder the adaptation mechanisms of

GIST cells to KIT inhibition, and consequently, the potential emergence of drug-resistant subpopulations.

Atrogin-1 is the F-box component of SCF E3 ligases that recognizes degron domains with the highest specify, and there is an increasing interest in targeting specific components of the ubiquitin ligase cascade, given their higher substrate specificity over the proteasome, and their involvement on several critical human biological processes, such as cancer (208). Therefore, the use of specific Atrogin-1 inhibitors in combination with imatinib would be clinically more feasible than using agents with broader activity such as proteasome inhibitors. Regrettably, Atrogin-1 crystallographic structure has not been yet resolved and specific inhibitors are not available. However, the critical role of Atrogin-1 in GIST cell survival emphasizes the fundamental role of UPS in GIST cells, and the therapeutic potential of co-targeting this pathway and KIT to render GIST cells to TKI-mediated cell apoptosis and thus overcome adaptive resistance. Herein, the combination of imatinib and TAK-243 yield striking results *in vitro* and *in vivo* in terms of anti-tumor activity, and thus, may serve as a solid proof-of-concept of the therapeutic potential of this strategy. Nonetheless, it should be considered that TAK-243 causes a broad inhibition of cellular ubiquitination, and hereby toxicity- associated problems may emerge, similar to other UPS inhibitors (209).

6.4.8. UPS as a weapon, rather than a target

Over the last few years, there has been an increasing interest of controlling the UPS to specifically degrade proteins. In this regard, the development of the proteolysis targeting chimeras (PROTACS) represents the onset of a new class of drugs. PROTACS are heterobifunctional molecules that consist of two moieties, one binding to the target protein and the other to an E3 ligase, both connected by a linker. The proximity with the E3 ligase enables the ubiquitylation of the target and its subsequent degradation (228). Based on this rationale, other agents are being developed, such as lysosome-targeting chimeras (LYTACS), which prompts lysosome degradation of a specific membrane protein, such as KIT receptor. These strategy results extremely appealing for the treatment of GIST, since it brings the opportunity to target essential proteins for GIST cell biology, that have been historically considered undruggable, such in the case of ETV1. Likewise, this strategy would enable to specifically target Atrogin-1, hampering

adaptive resistance to KIT-targeted inhibition. Hence, this approach is one of the most promising strategies in the coming years for the treatment of GIST patients.

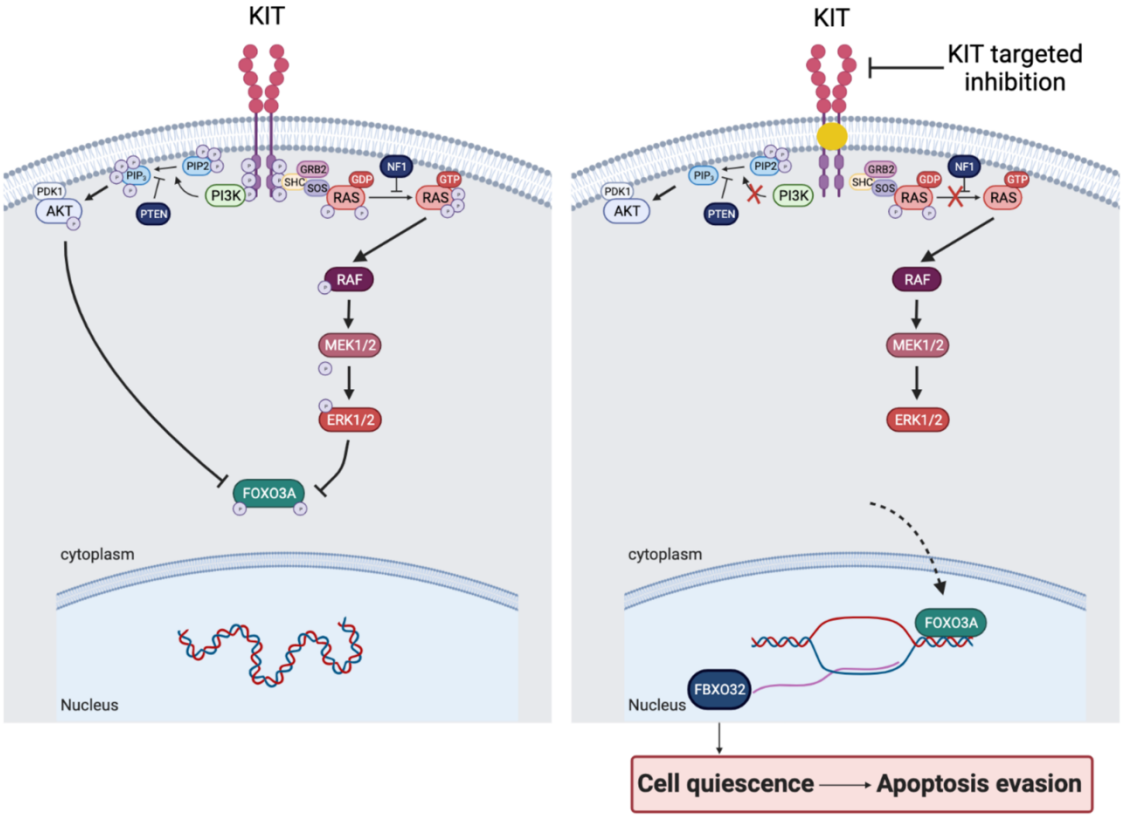

Figure 38. Model of the role of Atrogin-1 in GIST. Left, under KIT constitutive activation, KIT-downstream pathways phosphorylate and retain FOXO3a in the cytoplasm. Right, KIT and KIT-downstream pathways inactivation upon KIT-targeted inhibition results in FOXO3a dephosphorylation, which in turn shuttles to the nucleus and activates the transcription of Atrogin-1, eventually resulting in cell quiescence and apoptosis evasion. Created with BioRender.

7. CONCLUSIONS

7.1. PI3KIA/mTOR and MEK1/2 are the most critical signaling nodes within KIT-downstream PI3K/AKT/mTOR and RAS/MAPK pathways, respectively.

7.2. Intermittent concurrent inhibition of PI3KIA/mTOR and MEK1/2 is an effective and well tolerated therapeutic strategy to overcome the heterogeneity of resistant KIT secondary mutations.

7.3. FBXO32/Atrogin-1 is the most differentially up-regulated gene after KIT, or KIT-downstream pathways suppression.

7.4. Atrogin-1 is tightly regulated in GIST cells through the KIT-ERK/AKT-FOXO3a axis and emerge as a crucial mediator of adaptive resistance to KIT-targeted inhibition.

7.5. Atrogin-1 drives the induction of cell-quiescence in GIST cells as a pro-survival mechanism to evade apoptosis immediately after KIT inhibition.

7.6. Combined inhibition of KIT and the ubiquitination cascade is an extraordinarily effective anti-tumor strategy that also hinders therapeutic adaptation of tumor cells. However, the specific inhibition of critical mediators within the system, such as Atrogin-1, would decrease potentially associated toxicities, while maintaining the anti-tumor activity.

8. REFERENCES

1. Hirota S, Isozaki K, Moriyama Y, Hashimoto K, Nishida T, Ishiguro S, et al. Gain-of-function mutations of c-kit in human gastrointestinal stromal tumors. Science (80-). 1998;279(5350):577–80.
2. Tran T, Davila JA, El-Serag HB. The epidemiology of malignant gastrointestinal stromal tumors: An analysis of 1,458 cases from 1992 to 2000. Am J Gastroenterol [Internet]. 2005 Jan [cited 2022 Jan 13];100(1):162–8. Available from: https://pubmed.ncbi.nlm.nih.gov/15654796/
3. Thomas RM, Sobin LH. Gastrointestinal cancer. Cancer. 1995;75(1 S):154–70.
4. Miettinen M, Lasota J. Gastrointestinal stromal tumors - Definition, clinical, histological, immunohistochemical, and molecular genetic features and differential diagnosis [Internet]. Vol. 438, Virchows Archiv. Virchows Arch; 2001 [cited 2022 Jan 13]. p. 1–12. Available from: https://pubmed.ncbi.nlm.nih.gov/11213830/
5. Nilsson B, Bümming P, Meis-Kindblom JM, Odén A, Dortok A, Gustavsson B, et al. Gastrointestinal stromal tumors: The incidence, prevalence, clinical course, and prognostication in the preimatinib mesylate era - A population-based study in western Sweden [Internet]. Vol. 103, Cancer. Cancer; 2005 [cited 2020 Nov 1]. p. 821–9. Available from: https://pubmed.ncbi.nlm.nih.gov/15648083/
6. Ducimetière F, Lurkin A, Ranchère-Vince D, Decouvelaere AV, Péoc'h M, Istier L, et al. Incidence of sarcoma histotypes and molecular subtypes in a prospective epidemiological study with central pathology review and molecular testing. PLoS One. 2011;6(8).
7. Kawanowa K, Sakuma Y, Sakurai S, Hishima T, Iwasaki Y, Saito K, et al. High incidence of microscopic gastrointestinal stromal tumors in the stomach. Hum Pathol. 2006 Dec 1;37(12):1527–35.
8. Agaimy A, Wünsch PH, Hofstaedter F, Blaszyk H, Rümmele P, Gaumann A, et al. Minute Gastric Sclerosing Stromal Tumors (GIST Tumorlets) are common in adults and frequently show c-KIT mutations. Am J Surg Pathol [Internet]. 2007 Jan [cited 2022 Jan 13];31(1):113–20. Available from: https://pubmed.ncbi.nlm.nih.gov/17197927/
9. Cassier PA, Ducimetière F, Lurkin A, Ranchère-Vince D, Scoazec JY, Bringuier PP, et al. A prospective epidemiological study of new incident GISTs during two consecutive years in Rhne Alpes region: Incidence and molecular distribution of GIST in a European region. Br J Cancer [Internet]. 2010 Jul 13 [cited 2022 Jan 13];103(2):165–70. Available from: https://pubmed.ncbi.nlm.nih.gov/20588273/
10. Hulzinga JD, Thuneberg L, Klüppel M, Malysz J, Mikkelsen HB, Bernstein A. W/kit gene required for interstitial cells of cajal and for intestinal pacemaker activity. Nature. 1995;373(6512):347–9.
11. Sircar K, Hewlett BR, Huizinga JD, Chorneyko K, Berezin I, Riddell RH. Interstitial cells of cajal as precursors of gastrointestinal stromal tumors. Am J Surg Pathol. 1999;
12. Klüppel M, Huizinga JD, Malysz J, Bernstein A. Developmental origin and Kit-dependent development of the interstitial cells of Cajal in the mammalian small intestine. Dev Dyn. 1998;211(1):60–71.
13. Sommer G, Agosti V, Ehlers I, Rossi F, Corbacioglu S, Farkas J, et al. Gastrointestinal stromal tumors in a mouse model by targeted mutation of the Kit receptor tyrosine kinase. Proc Natl Acad Sci U S A [Internet]. 2003 May 27 [cited 2020 Nov 1];100(11):6706–11. Available from:

www.pnas.orgcgidoi10.1073pnas.1037763100

14. Chi P, Chen Y, Zhang L, Guo X, Wongvipat J, Shamu T, et al. ETV1 is a lineage survival factor that cooperates with KIT in gastrointestinal stromal tumours. Nature [Internet]. 2010;467(7317):849–53. Available from: http://dx.doi.org/10.1038/nature09409
15. Scarpa M, Bertin M, Ruffolo C, Polese L, D'Amico DF, Angriman I. A systematic review on the clinical diagnosis of gastrointestinal stromal tumors [Internet]. Vol. 98, Journal of Surgical Oncology. J Surg Oncol; 2008 [cited 2022 Jan 13]. p. 384–92. Available from: https://pubmed.ncbi.nlm.nih.gov/18668671/
16. Chou FF, Eng HL, Sheen-Chen SM. Smooth muscle tumors of the gastrointestinal tract: Analysis of prognostic factors. Surgery [Internet]. 1996 [cited 2022 Jan 13];119(2):171–7. Available from: https://pubmed.ncbi.nlm.nih.gov/8571202/
17. Demetri GD, von Mehren M, Blanke CD, Van den Abbeele AD, Eisenberg B, Roberts PJ, et al. Efficacy and Safety of Imatinib Mesylate in Advanced Gastrointestinal Stromal Tumors. N Engl J Med [Internet]. 2002 Aug 15 [cited 2019 Jul 24];347(7):472–80. Available from: http://www.ncbi.nlm.nih.gov/pubmed/12181401
18. Von Mehren M, Randall RL, Benjamin RS, Boles S, Bui MM, Casper ES, et al. Gastrointestinal stromal tumors, version 2.2014: Featured updates to the NCCN Guidelines. JNCCN J Natl Compr Cancer Netw [Internet]. 2014 Jun 1 [cited 2022 Jan 13];12(6):853–62. Available from: https://pubmed.ncbi.nlm.nih.gov/24925196/
19. Gastrointestinal stromal tumours: ESMO Clinical Practice Guidelines for diagnosis, treatment and follow-up. Ann Oncol [Internet]. 2014 Sep 1 [cited 2022 Jan 13];25:iii21–6. Available from: https://pubmed.ncbi.nlm.nih.gov/25210085/
20. Fletcher, C.D.M.; Gronchi A. WHO Classification of Tumours of Soft Tissue and Bone. Vol. 14, WHO Classification of Tumours of Soft Tissue and Bone. 2013. 14–18 p.
21. Serrano C, George S, Valverde C, Olivares D, García-Valverde A, Suárez C, et al. Novel Insights into the Treatment of Imatinib-Resistant Gastrointestinal Stromal Tumors. Target Oncol. 2017;12(3):277–88.
22. Fletcher CDM, Berman JJ, Corless C, Gorstein F, Lasota J, Longley BJ, et al. Diagnosis of gastrointestinal stromal tumors: A consensus approach. Hum Pathol. 2002 May 1;33(5):459–65.
23. Liegl B, Hornick JL, Corless CL, Fletcher CDM. Monoclonal antibody DOG1.1 Shows higher sensitivity than KIT in the diagnosis of gastrointestinal stromal tumors, including unusual subtypes. Am J Surg Pathol [Internet]. 2009 Mar [cited 2021 Sep 21];33(3):437–46. Available from: https://pubmed.ncbi.nlm.nih.gov/19011564/
24. Miettinen M, Makhlouf H, Sobin LH, Lasota J. Gastrointestinal stromal tumors of the jejunum and ileum: A clinicopathologic, immunohistochemical, and molecular genetic study of 906 cases before imatinib with long-term follow-up. Am J Surg Pathol. 2006;30(4):477–89.
25. Robinson TL, Sircar K, Hewlett BR, Chorneyko K, Riddell RH, Huizinga JD. Gastrointestinal stromal tumors may originate from a subset of CD34-positive interstitial cells of Cajal. Am J Pathol. 2000;156(4):1157–63.
26. Heinrich MC, Maki RG, Corless CL, Antonescu CR, Harlow A, Griffith D, et al. Primary and secondary kinase genotypes correlate with the biological and clinical activity of sunitinib in imatinib-resistant gastrointestinal stromal tumor. J Clin Oncol. 2008 Nov 20;26(33):5352–9.
27. Hirota S, Ohashi A, Nishida T, Isozaki K, Kinoshita K, Shinomura Y, et al. Gain-of-function

mutations of platelet-derived growth factor receptor α gene in gastrointestinal stromal tumors. Gastroenterology [Internet]. 2003 Sep 1 [cited 2020 Nov 1];125(3):660–7. Available from: http://www.gastrojournal.org/article/S0016508503010461/fulltext

28. Heinrich MC, Corless CL, Demetri GD, Blanke CD, Von Mehren M, Joensuu H, et al. Kinase mutations and imatinib response in patients with metastatic gastrointestinal stromal tumor. J Clin Oncol [Internet]. 2003 Dec 1 [cited 2022 Jan 13];21(23):4342–9. Available from: https://pubmed.ncbi.nlm.nih.gov/14645423/
29. McCarter MD, Antonescu CR, Ballman K V., Maki RG, Pisters PWT, Demetri GD, et al. Microscopically positive margins for primary gastrointestinal stromal tumors: Analysis of risk factors and tumor recurrence. J Am Coll Surg [Internet]. 2012 Jul [cited 2022 Jan 13];215(1):53–9. Available from: https://pubmed.ncbi.nlm.nih.gov/22726733/
30. Joensuu H, Wardelmann E, Sihto H, Eriksson M, Sundby Hall K, Reichardt A, et al. Effect of KIT and PDGFRA mutations on survival in patients with gastrointestinal stromal tumors treated with adjuvant imatinib: An exploratory analysis of a randomized clinical trial. JAMA Oncol. 2017;3(5):602–9.
31. Dematteo RP, Heinrich MC, El-Rifai WM, Demetri G. Clinical management of gastrointestinal stromal tumors: Before and after STI-571. Hum Pathol [Internet]. 2002 [cited 2022 Jan 13];33(5):466–77. Available from: https://pubmed.ncbi.nlm.nih.gov/12094371/
32. Corless CL, Barnett CM, Heinrich MC. Gastrointestinal stromal tumours: Origin and molecular oncology. Vol. 11, Nature Reviews Cancer. 2011. p. 865–78.
33. Druker BJ, Tamura S, Buchdunger E, Ohno S, Segal GM, Fanning S, et al. Effects of a selective inhibitor of the Ab1 tyrosine kinase on the growth of Bcr-Ab1 positive cells. Nat Med [Internet]. 1996 [cited 2022 Jan 13];2(5):561–6. Available from: https://pubmed.ncbi.nlm.nih.gov/8616716/
34. Druker BJ, Talpaz M, Resta DJ, Peng B, Buchdunger E, Ford JM, et al. Efficacy and Safety of a Specific Inhibitor of the BCR-ABL Tyrosine Kinase in Chronic Myeloid Leukemia. N Engl J Med [Internet]. 2001 Aug 20 [cited 2021 Sep 1];344(14):1031–7. Available from: https://www.nejm.org/doi/10.1056/NEJM200104053441401
35. Heinrich MC, Griffith DJ, Druker BJ, Wait CL, Ott KA, Zigler AJ. Inhibition of c-kit receptor tyrosine kinase activity by STI 571, a selective tyrosine kinase inhibitor. Blood. 2000 Aug 1;96(3):925–32.
36. Tuveson DA, Willis NA, Jacks T, Griffin JD, Singer S, Fletcher CDM, et al. STI571 inactivation of the gastrointestinal stromal tumor c-KIT oncoprotein: Biological and clinical implications. Oncogene [Internet]. 2001 Aug 28 [cited 2021 Sep 1];20(36):5054–8. Available from: https://www.nature.com/articles/1204704
37. Gajiwaia KS, Wu JC, Christensen J, Deshmukh GD, Diehl W, Dinitto JP, et al. KIT kinase mutants show unique mechanisms of drug resistance to imatinib and sunitinib in gastrointestinal stromal tumor patients. Proc Natl Acad Sci U S A [Internet]. 2009 Feb 3 [cited 2022 Jan 13];106(5):1542–7. Available from: https://pubmed.ncbi.nlm.nih.gov/19164557/
38. Verweij J, Casali PG, Zalcberg J, LeCesne A, Reichardt P, Blay JY, et al. Progression-free survival in gastrointestinal stromal tumours with high-dose imatinib: Randomised trial. Lancet [Internet]. 2004 Sep 25 [cited 2022 Jan 13];364(9440):1127–34. Available from: https://pubmed.ncbi.nlm.nih.gov/15451219/
39. Blanke CD, Rankin C, Demetri GD, Ryan CW, Von Mehren M, Benjamin RS, et al. Phase III randomized, intergroup trial assessing imatinib mesylate at two dose levels in patients with

unresectable or metastatic gastrointestinal stromal tumors expressing the kit receptor tyrosine kinase: S0033. J Clin Oncol [Internet]. 2008 Feb 1 [cited 2022 Jan 14];26(4):626–32. Available from: https://pubmed.ncbi.nlm.nih.gov/18235122/

40. Joensuu H, Roberts PJ, Sarlomo-Rikala M, Andersson LC, Tervahartiala P, Tuveson D, et al. Effect of the Tyrosine Kinase Inhibitor STI571 in a Patient with a Metastatic Gastrointestinal Stromal Tumor. N Engl J Med [Internet]. 2001 Apr 5 [cited 2022 Jan 13];344(14):1052–6. Available from: https://pubmed.ncbi.nlm.nih.gov/11287975/
41. von Mehren M, Heinrich MC, Joensuu H, Blanke CD, Wehrle E, Demetri GD. Follow-up results after 9 years (yrs) of the ongoing, phase II B2222 trial of imatinib mesylate (IM) in patients (pts) with metastatic or unresectable KIT+ gastrointestinal stromal tumors (GIST). J Clin Oncol. 2011 May 20;29(15_suppl):10016–10016.
42. Demetri GD, Rankin CJ, Benjamin RS, Borden EC, Ryan CW, Priebat DA, et al. Long-term disease control of advanced gastrointestinal stromal tumors (GIST) with imatinib (IM): 10-year outcomes from SWOG phase III intergroup trial S0033. J Clin Oncol. 2014 May 20;32(15_suppl):10508–10508.
43. Van Glabbeke M. Comparison of two doses of imatinib for the treatment of unresectable or metastatic gastrointestinal stromal tumors: A meta-analysis of 1,640 patients. J Clin Oncol [Internet]. 2010 Mar 1 [cited 2022 Jan 13];28(7):1247–53. Available from: https://pubmed.ncbi.nlm.nih.gov/20124181/
44. DeMatteo RP, Ballman K V., Antonescu CR, Maki RG, Pisters PW, Demetri GD, et al. Adjuvant imatinib mesylate after resection of localised, primary gastrointestinal stromal tumour: a randomised, double-blind, placebo-controlled trial. Lancet [Internet]. 2009 [cited 2022 Jan 14];373(9669):1097–104. Available from: https://pubmed.ncbi.nlm.nih.gov/19303137/
45. Joensuu H, Eriksson M, Hall KS, Hartmann JT, Pink D, Schütte J, et al. One vs three years of adjuvant imatinib for operable gastrointestinal stromal tumor: A randomized trial. JAMA - J Am Med Assoc [Internet]. 2012 Mar 21 [cited 2022 Jan 14];307(12):1265–72. Available from: https://pubmed.ncbi.nlm.nih.gov/22453568/
46. Tirumani SH, Shinagare AB, Jagannathan JP, Krajewski KM, Ramaiya NH, Raut CP. Radiologic assessment of earliest, best, and plateau response of gastrointestinal stromal tumors to neoadjuvant imatinib prior to successful surgical resection. Eur J Surg Oncol. 2014 Apr 1;40(4):420–8.
47. McAuliffe JC, Hunt KK, Lazar AJF, Choi H, Qiao W, Thall P, et al. A randomized, phase II study of preoperative plus postoperative Imatinib in GIST: Evidence of rapid radiographic response and temporal induction of tumor cell apoptosis. Ann Surg Oncol [Internet]. 2009 Apr [cited 2022 Jan 14];16(4):910–9. Available from: https://pubmed.ncbi.nlm.nih.gov/18953611/
48. Eisenberg BL, Harris J, Blanke CD, Demetri GD, Heinrich MC, Watson JC, et al. Phase II trial of neoadjuvant/adjuvant imatinib mesylate (IM) for advanced primary and metastatic/recurrent operable gastrointestinal stromal tumor (GIST): Early results of RTOG 0132/ACRIN 6665. J Surg Oncol [Internet]. 2009 Jan 1 [cited 2022 Jan 14];99(1):42–7. Available from: https://pubmed.ncbi.nlm.nih.gov/18942073/
49. Poveda A, García del Muro X, López-Guerrero JA, Cubedo R, Martínez V, Romero I, et al. GEIS guidelines for gastrointestinal sarcomas (GIST) [Internet]. Vol. 55, Cancer Treatment Reviews. Elsevier; 2017 [cited 2022 Jan 14]. p. 107–19. Available from:

http://www.cancertreatmentreviews.com/article/S0305737216301360/fulltext

50. Heinrich MC, Corless CL, Demetri GD, Blanke CD, Von Mehren M, Joensuu H, et al. Kinase mutations and imatinib response in patients with metastatic gastrointestinal stromal tumor. J Clin Oncol [Internet]. 2003 Dec 1 [cited 2022 Jan 14];21(23):4342–9. Available from: https://pubmed.ncbi.nlm.nih.gov/14645423/
51. Debiec-Rychter M, Dumez H, Judson I, Wasag B, Verweij J, Brown M, et al. Use of c-KIT/PDGFRA mutational analysis to predict the clinical response to imatinib in patients with advanced gastrointestinal stromal tumours entered on phase I and II studies of the EORTC Soft Tissue and Bone Sarcoma Group. Eur J Cancer [Internet]. 2004 Mar [cited 2022 Jan 14];40(5):689–95. Available from: https://pubmed.ncbi.nlm.nih.gov/15010069/
52. Debiec-Rychter M, Sciot R, Le Cesne A, Schlemmer M, Hohenberger P, van Oosterom AT, et al. KIT mutations and dose selection for imatinib in patients with advanced gastrointestinal stromal tumours. Eur J Cancer [Internet]. 2006 May [cited 2022 Jan 14];42(8):1093–103. Available from: https://pubmed.ncbi.nlm.nih.gov/16624552/
53. Heinrich MC, Maki RG, Corless CL, Antonescu CR, Harlow A, Griffith D, et al. Primary and secondary kinase genotypes correlate with the biological and clinical activity of sunitinib in imatinib-resistant gastrointestinal stromal tumor. J Clin Oncol [Internet]. 2008 Nov 20 [cited 2022 Jan 14];26(33):5352–9. Available from: https://pubmed.ncbi.nlm.nih.gov/18955458/
54. Corless CL, Schroeder A, Griffith D, Town A, McGreevey L, Harrell P, et al. PDGFRA mutations in gastrointestinal stromal tumors: Frequency, spectrum and in vitro sensitivity to imatinib. J Clin Oncol [Internet]. 2005 [cited 2022 Jan 14];23(23):5357–64. Available from: https://pubmed.ncbi.nlm.nih.gov/15928335/
55. Heinrich MC, Corless CL, Blanke CD, Demetri GD, Joensuu H, Roberts PJ, et al. Molecular correlates of imatinib resistance in gastrointestinal stromal tumors. J Clin Oncol. 2006 Oct 10;24(29):4764–74.
56. Liegl B, Kepten I, Le C, Zhu M, Demetri GD, Heinrich MC, et al. Heterogeneity of kinase inhibitor resistance mechanisms in GIST. J Pathol [Internet]. 2008 Sep [cited 2022 Jan 14];216(1):64–74. Available from: https://pubmed.ncbi.nlm.nih.gov/18623623/
57. Serrano C, Fletcher JA. Overcoming heterogenity in imatinib-resistant gastrointestinal stromal tumor [Internet]. Vol. 10, Oncotarget. Impact Journals, LLC; 2019 [cited 2022 Jan 14]. p. 6586–7. Available from: /pmc/articles/PMC6824868/
58. Pilco-Janeta DF, García-Valverde A, Gomez-Peregrina D, Serrano C. Emerging drugs for the treatment of gastrointestinal stromal tumors [Internet]. Vol. 26, Expert Opinion on Emerging Drugs. Expert Opin Emerg Drugs; 2021 [cited 2022 Jan 14]. p. 53–62. Available from: https://pubmed.ncbi.nlm.nih.gov/33645383/
59. Serrano C, Mariño-Enríquez A, Tao DL, Ketzer J, Eilers G, Zhu M, et al. Complementary activity of tyrosine kinase inhibitors against secondary kit mutations in imatinib-resistant gastrointestinal stromal tumours. Br J Cancer [Internet]. 2019 Mar 19 [cited 2022 Jan 14];120(6):612–20. Available from: https://pubmed.ncbi.nlm.nih.gov/30792533/
60. Serrano C, George S. Gastrointestinal Stromal Tumor: Challenges and Opportunities for a New Decade [Internet]. Vol. 26, Clinical Cancer Research. American Association for Cancer Research; 2020 [cited 2022 Jan 14]. p. 5078–85. Available from: https://clincancerres.aacrjournals.org/content/26/19/5078

61. Demetri GD, van Oosterom AT, Garrett CR, Blackstein ME, Shah MH, Verweij J, et al. Efficacy and safety of sunitinib in patients with advanced gastrointestinal stromal tumour after failure of imatinib: a randomised controlled trial. Lancet [Internet]. 2006 Oct 14 [cited 2022 Jan 14];368(9544):1329–38. Available from: https://pubmed.ncbi.nlm.nih.gov/17046465/
62. George S, Blay JY, Casali PG, Le Cesne A, Stephenson P, DePrimo SE, et al. Clinical evaluation of continuous daily dosing of sunitinib malate in patients with advanced gastrointestinal stromal tumour after imatinib failure. Eur J Cancer [Internet]. 2009 Jul [cited 2022 Jan 14];45(11):1959–68. Available from: https://pubmed.ncbi.nlm.nih.gov/19282169/
63. Demetri GD, Reichardt P, Kang YK, Blay JY, Rutkowski P, Gelderblom H, et al. Effi cacy and safety of regorafenib for advanced gastrointestinal stromal tumours after failure of imatinib and sunitinib (GRID): An international, multicentre, randomised, placebo-controlled, phase 3 trial. Lancet [Internet]. 2013 [cited 2022 Jan 14];381(9863):295–302. Available from: https://pubmed.ncbi.nlm.nih.gov/23177515/
64. Smith BD, Kaufman MD, Lu WP, Gupta A, Leary CB, Wise SC, et al. Ripretinib (DCC-2618)Is a Switch Control Kinase Inhibitor of a Broad Spectrum of Oncogenic and Drug-Resistant KIT and PDGFRA Variants. Cancer Cell [Internet]. 2019;35(5):738-751.e9. Available from: https://doi.org/10.1016/j.ccell.2019.04.006
65. Blay JY, Serrano C, Heinrich MC, Zalcberg J, Bauer S, Gelderblom H, et al. Ripretinib in patients with advanced gastrointestinal stromal tumours (INVICTUS): a double-blind, randomised, placebo-controlled, phase 3 trial. Lancet Oncol [Internet]. 2020 Jul 1 [cited 2022 Jan 14];21(7):923–34. Available from: /pmc/articles/PMC8383051/
66. Nemunaitis J, Bauer S, Blay JY, Choucair K, Gelderblom H, George S, et al. Intrigue: Phase III study of ripretinib versus sunitinib in advanced gastrointestinal stromal tumor after imatinib. Futur Oncol [Internet]. 2019 [cited 2022 Jan 14];16(1):4251–64. Available from: https://pubmed.ncbi.nlm.nih.gov/31755321/
67. Deciphera Pharmaceuticals Announces Top-Line Results from the INTRIGUE Phase 3 Clinical Study | Business Wire [Internet]. [cited 2022 Jan 14]. Available from: https://www.businesswire.com/news/home/20211105005311/en/Deciphera-Pharmaceuticals-Announces-Top-Line-Results-from-the-INTRIGUE-Phase-3-Clinical-Study
68. Evans EK, Gardino AK, Kim JL, Hodous BL, Shutes A, Davis A, et al. A precision therapy against cancers driven by KIT/PDGFRA mutations. Sci Transl Med [Internet]. 2017 Nov 1 [cited 2022 Jan 14];9(414). Available from: https://pubmed.ncbi.nlm.nih.gov/29093181/
69. Gebreyohannes YK, Wozniak A, Zhai ME, Wellens J, Cornillie J, Vanleeuw U, et al. Robust Activity of Avapritinib, Potent and Highly Selective Inhibitor of Mutated KIT, in Patient-derived Xenograft Models of Gastrointestinal Stromal Tumors. Clin Cancer Res [Internet]. 2019 Jan 15 [cited 2022 Jan 14];25(2):609–18. Available from: https://pubmed.ncbi.nlm.nih.gov/30274985/
70. Heinrich MC, Jones RL, von Mehren M, Schöffski P, Serrano C, Kang YK, et al. Avapritinib in advanced PDGFRA D842V-mutant gastrointestinal stromal tumour (NAVIGATOR): a multicentre, open-label, phase 1 trial. Lancet Oncol [Internet]. 2020 Jul 1 [cited 2022 Jan 14];21(7):935–46. Available from: https://pubmed.ncbi.nlm.nih.gov/32615108/
71. Kang YK, George S, Jones RL, Rutkowski P, Shen L, Mir O, et al. Avapritinib versus regorafenib in locally advanced unresectable or metastatic GI stromal tumor: A randomized, open-label phase III study. J Clin Oncol [Internet]. 2021 Oct 1 [cited 2022 Jan 14];39(28):3128–39. Available from:

https://pubmed.ncbi.nlm.nih.gov/34343033/

72. Grunewald S, Klug LR, Mühlenberg T, Lategahn J, Falkenhorst J, Town A, et al. Resistance to avapritinib in pdgfra-driven gist is caused by secondary mutations in the pdgfra kinase domain. Cancer Discov [Internet]. 2021 Jan 1 [cited 2022 Jan 14];11(1):108–25. Available from: https://cancerdiscovery.aacrjournals.org/content/11/1/108
73. Mol CD, Dougan DR, Schneider TR, Skene RJ, Kraus ML, Scheibe DN, et al. Structural basis for the autoinhibition and STI-571 inhibition of c-Kit tyrosine kinase. J Biol Chem. 2004;279(30):31655–63.
74. Mol CD, Dougan DR, Schneider TR, Skene RJ, Kraus ML, Scheibe DN, et al. Structural basis for the autoinhibition and STI-571 inhibition of c-Kit tyrosine kinase. J Biol Chem [Internet]. 2004 [cited 2020 Nov 1];279(30):31655–63. Available from: http://www.rcsb.org/
75. Corless CL, McGreevey L, Town A, Schroeder A, Bainbridge T, Harrell P, et al. KIT gene deletions at the intron 10-exon 11 boundary in GI stromal tumors. J Mol Diagnostics. 2004;6(4):366–70.
76. Wardelmann E, Losen I, Hans V, Neidt I, Speidel N, Bierhoff E, et al. Deletion of Trp-557 and Lys-558 in the juxtamembrane domain of the c-kit protooncogene is associated with metastatic behavior of gastrointestinal stromal tumors. Int J Cancer [Internet]. 2003 Oct 10 [cited 2022 Jan 14];106(6):887–95. Available from: https://pubmed.ncbi.nlm.nih.gov/12918066/
77. Martín J, Poveda A, Llombart-Bosch A, Ramos R, López-Guerrero JA, García Del Muro J, et al. Deletions affecting codons 557-558 of the c-KIT gene indicate a poor prognosis in patients with completely resected gastrointestinal stromal tumors: A study by the Spanish Group for Sarcoma Research (GEIS). J Clin Oncol [Internet]. 2005 [cited 2022 Jan 14];23(25):6190–8. Available from: https://pubmed.ncbi.nlm.nih.gov/16135486/
78. Yuzawa S, Opatowsky Y, Zhang Z, Mandiyan V, Lax I, Schlessinger J. Structural Basis for Activation of the Receptor Tyrosine Kinase KIT by Stem Cell Factor. Cell [Internet]. 2007 Jul 27 [cited 2022 Jan 14];130(2):323–34. Available from: https://pubmed.ncbi.nlm.nih.gov/17662946/
79. Antonescu CR, Viale A, Sarran L, Tschernyavsky SJ, Gonen M, Segal NH, et al. Gene expression in gastrointestinal stromal tumors is distinguished by KIT genotype and anatomic site. Clin Cancer Res. 2004;10(10):3282–90.
80. Lasota J, Corless CL, Heinrich MC, Debiec-Rychter M, Sciot R, Wardelmann E, et al. Clinicopathologic profile of gastrointestinal stromal tumors (GISTs) with primary KIT exon 13 or exon 17 mutations: A multicenter study on 54 cases. Mod Pathol. 2008;21(4):476–84.
81. Heinrich MC, Corless CL, Duensing A, McGreevey L, Chen CJ, Joseph N, et al. PDGFRA activating mutations in gastrointestinal stromal tumors. Science (80-). 2003;299(5607):708–10.
82. Pauls K, Merkelbach-Bruse S, Thal D, Büttner R, Wardelmann E. PDGFRα- and c-kit-mutated gastrointestinal stromal tumours (GISTs) are characterized by distinctive histological and immunohistochemical features. Histopathology [Internet]. 2005 Feb [cited 2022 Jan 14];46(2):166–75. Available from: https://pubmed.ncbi.nlm.nih.gov/15693889/
83. Cassier PA, Fumagalli E, Rutkowski P, Schöffski P, Van Glabbeke M, Debiec-Rychter M, et al. Outcome of patients with platelet-derived growth factor receptor alpha-mutated gastrointestinal stromal tumors in the tyrosine kinase inhibitor era. Clin Cancer Res [Internet]. 2012 Aug 15 [cited 2022 Jan 14];18(16):4458–64. Available from: https://pubmed.ncbi.nlm.nih.gov/22718859/
84. Duensing A, Medeiros F, McConarty B, Joseph NE, Panigrahy D, Singer S, et al. Mechanisms of oncogenic KIT signal transduction in primary gastrointestinal stromal tumors (GISTs). Oncogene.

2004;23(22):3999–4006.

85. Letouzé E, Martinelli C, Loriot C, Burnichon N, Abermil N, Ottolenghi C, et al. SDH Mutations Establish a Hypermethylator Phenotype in Paraganglioma. Cancer Cell [Internet]. 2013 Jun 10 [cited 2022 Jan 14];23(6):739–52. Available from: https://pubmed.ncbi.nlm.nih.gov/23707781/
86. Killian JK, Kim SY, Miettinen M, Smith C, Merino M, Tsokos M, et al. Succinate dehydrogenase mutation underlies global epigenomic divergence in gastrointestinal stromal tumor. Cancer Discov [Internet]. 2013 [cited 2022 Jan 14];3(6):648–57. Available from: https://pubmed.ncbi.nlm.nih.gov/23550148/
87. Janeway KA, Liegl B, Harlow A, Le C, Perez-Atayde A, Kozakewich H, et al. Pediatric KIT-wild-type and platelet-derived growth factor receptor α-wild-type gastrointestinal stromal tumors share KIT activation but not mechanisms of genetic progression with adult gastrointestinal stromal tumors. Cancer Res [Internet]. 2007 Oct 1 [cited 2022 Jan 14];67(19):9084–8. Available from: https://pubmed.ncbi.nlm.nih.gov/17909012/
88. Miettinen M, Wang ZF, Sarlomo-Rikala M, Osuch C, Rutkowski P, Lasota J. Succinate dehydrogenase-deficient GISTs: A clinicopathologic, immunohistochemical, and molecular genetic study of 66 gastric GISTs with predilection to young age. Am J Surg Pathol [Internet]. 2011 Nov [cited 2022 Jan 14];35(11):1712–21. Available from: https://pubmed.ncbi.nlm.nih.gov/21997692/
89. Wagner AJ, Remillard SP, Zhang YX, Doyle LA, George S, Hornick JL. Loss of expression of SDHA predicts SDHA mutations in gastrointestinal stromal tumors. Mod Pathol [Internet]. 2013 Feb [cited 2022 Jan 14];26(2):289–94. Available from: https://pubmed.ncbi.nlm.nih.gov/22955521/
90. Brems H, Beert E, de Ravel T, Legius E. Mechanisms in the pathogenesis of malignant tumours in neurofibromatosis type 1 [Internet]. Vol. 10, The Lancet Oncology. Lancet Oncol; 2009 [cited 2022 Jan 14]. p. 508–15. Available from: https://pubmed.ncbi.nlm.nih.gov/19410195/
91. Serrano C, Wang Y, Mariño-Enríquez A, Lee JC, Ravegnini G, Morgan JA, et al. KRAS and KIT gatekeeper mutations confer polyclonal primary imatinib resistance in GI stromal tumors: Relevance of concomitant phosphatidylinositol 3-kinase/AKT dysregulation. J Clin Oncol [Internet]. 2015 Aug 1 [cited 2022 Jan 14];33(22):e93–6. Available from: /pmc/articles/PMC4559610/
92. Agaram NP, Wong GC, Guo T, Maki RG, Singer S, DeMatteo RP, et al. Novel V600E BRAF mutations in imatinib-naive and imatinib-resistant gastrointestinal stromal tumors. Genes Chromosom Cancer [Internet]. 2008 Oct [cited 2022 Jan 14];47(10):853–9. Available from: https://pubmed.ncbi.nlm.nih.gov/18615679/
93. El-Rifai W, Sarlomo-Rikala M, Andersson LC, Knuutila S, Miettinen M. DNA sequence copy number changes in gastrointestinal stromal tumors: Tumor progression and prognostic significance. Cancer Res. 2000;60(14):3899–903.
94. Fukasawa T, Chong JM, Sakurai S, Koshiishi N, Ikeno R, Tanaka A, et al. Allelic loss of 14q and 22q, NF2 mutation, and genetic instability occur independently of c-kit mutation in gastrointestinal stromal tumor. Japanese J Cancer Res [Internet]. 2000 [cited 2022 Jan 14];91(12):1241–9. Available from: https://pubmed.ncbi.nlm.nih.gov/11123422/
95. Heinrich MC, Rubin BP, Longley BJ, Fletcher JA. Biology and genetic aspects of gastrointestinal stromal tumors: KIT activation and cytogenetic alterations. Hum Pathol. 2002 May 1;33(5):484–95.
96. Kim NG, Kim JJ, Ahn JY, Seong CM, Noh SH, Kim CB, et al. Putative chromosomal deletions on 9p, 9q and 22q occur preferentially in malignant gastrointestinal stromal tumors. Int J Cancer. 2000;85(5):633–8.

97. Ylipää A, Hunt KK, Yang J, Lazar AJF, Torres KE, Lev DC, et al. Integrative genomic characterization and a genomic staging system for gastrointestinal stromal tumors. Cancer [Internet]. 2011 Jan 15 [cited 2022 Jan 15];117(2):380–9. Available from: https://onlinelibrary.wiley.com/doi/full/10.1002/cncr.25594
98. Schaefer IM, Wang Y, Liang CW, Bahri N, Quattrone A, Doyle L, et al. MAX inactivation is an early event in GIST development that regulates p16 and cell proliferation. Nat Commun [Internet]. 2017 Mar 8 [cited 2021 Oct 4];8(1):1–6. Available from: https://www.nature.com/articles/ncomms14674
99. Pang Y, Xie F, Cao H, Wang C, Zhu M, Liu X, et al. Mutational inactivation of mTORC1 repressor gene DEPDC5 in human gastrointestinal stromal tumors. Proc Natl Acad Sci U S A [Internet]. 2019 Nov 5 [cited 2021 Oct 4];116(45):22746–53. Available from: https://pubmed.ncbi.nlm.nih.gov/31636198/
100. Schneider-Stock R, Boltze C, Lasota J, Miettinen M, Peters B, Pross M, et al. High prognostic value of p16INK4 alterations in gastrointestinal stromal tumors. J Clin Oncol [Internet]. 2003 May 1 [cited 2022 Jan 15];21(9):1688–97. Available from: https://pubmed.ncbi.nlm.nih.gov/12721243/
101. Ricci R, Arena V, Castri F, Martini M, Maggiano N, Murazio M, et al. Role of p16/INK4a in Gastrointestinal Stromal Tumor Progression. Am J Clin Pathol [Internet]. 2004 Jul 1 [cited 2022 Jan 15];122(1):35–43. Available from: https://pubmed.ncbi.nlm.nih.gov/15272528/
102. Sabah M, Cummins R, Leader M, Kay E. Loss of heterozygosity of chromosome 9p and loss of p16INK4A expression are associated with malignant gastrointestinal stromal tumors. Mod Pathol [Internet]. 2004 Jun 4 [cited 2022 Jan 15];17(11):1364–71. Available from: https://www.nature.com/articles/3800199
103. Schneider-Stock R, Boltze C, Lasota J, Peters B, Corless CL, Ruemmele P, et al. Loss of p16 protein defines high-risk patients with gastrointestinal stromal tumors: A tissue microarray study. Clin Cancer Res. 2005;11(2 I):638–45.
104. Wang Y, Marino-Enriquez A, Bennett RR, Zhu M, Shen Y, Eilers G, et al. Dystrophin is a tumor suppressor in human cancers with myogenic programs. Nat Genet [Internet]. 2014 May 4 [cited 2021 Oct 4];46(6):601–6. Available from: https://www.nature.com/articles/ng.2974
105. Rubin BP, Singer S, Tsao C, Duensing A, Lux ML, Ruiz R, et al. KIT activation is a ubiquitous feature of gastrointestinal stromal tumors. Cancer Res. 2001;61(22):8118–21.
106. Duensing A, Joseph NE, Medeiros F, Smith F, Hornick JL, Heinrich MC, et al. Protein kinase C θ (PKC θ) expression and constitutive activation in gastrointestinal stromal tumors (GISTs). Cancer Res [Internet]. 2004 Aug 1 [cited 2022 Jan 16];64(15):5127–31. Available from: https://pubmed.ncbi.nlm.nih.gov/15289315/
107. Rossi F, Ehlers I, Agosti V, Socci ND, Viale A, Sommer G, et al. Oncogenic Kit signaling and therapeutic intervention in a mouse model of gastrointestinal stromal tumor. Proc Natl Acad Sci U S A [Internet]. 2006 Aug 22 [cited 2022 Jan 16];103(34):12843–8. Available from: /pmc/articles/PMC1568935/
108. Zhu MJ, Ou WB, Fletcher CDM, Cohen PS, Demetri GD, Fletcher JA. KIT oncoprotein interactions in gastrointestinal stromal tumors: Therapeutic relevance. Oncogene. 2007;26(44):6386–95.
109. Mahadevan D, Cooke L, Riley C, Swart R, Simons B, Della Croce K, et al. A novel tyrosine kinase switch is a mechanism of imatinib resistance in gastrointestinal stromal tumors. Oncogene [Internet]. 2007 Feb 26 [cited 2021 Oct 5];26(27):3909–19. Available from: https://www.nature.com/articles/1210173

110. Chi P, Chen Y, Zhang L, Guo X, Wongvipat J, Shamu T, et al. ETV1 is a lineage survival factor that cooperates with KIT in gastrointestinal stromal tumours. Nature [Internet]. 2010;467(7317):849–53. Available from: http://dx.doi.org/10.1038/nature09409
111. Ran L, Sirota I, Cao Z, Murphy D, Chen Y, Shukla S, et al. Combined inhibition of MAP kinase and KIT signaling synergistically destabilizes ETV1 and suppresses GIST tumor growth. Cancer Discov. 2015;5(3):304–15.
112. Li F, Hung H, Li X, Ruddy DA, Wang Y, Ong R, et al. FGFR-mediated reactivation of MAPK signaling attenuates antitumor effects of imatinib in gastrointestinal stromal tumors. Cancer Discov. 2015;5(4):438–51.
113. Rosenbaum E, Kelly C, D'Angelo SP, Dickson MA, Gounder M, Keohan ML, et al. A Phase I Study of Binimetinib (MEK162) Combined with Pexidartinib (PLX3397) in Patients with Advanced Gastrointestinal Stromal Tumor. Oncologist [Internet]. 2019 Oct 1 [cited 2022 Jan 16];24(10):1309-e983. Available from: https://pubmed.ncbi.nlm.nih.gov/31213500/
114. Chi P, Qin L-X, Nguyen B, Kelly CM, D'Angelo SP, Dickson MA, et al. Phase II Trial of Imatinib Plus Binimetinib in Patients With Treatment-Naive Advanced Gastrointestinal Stromal Tumor. J Clin Oncol [Internet]. 2022 Jan 18 [cited 2022 Mar 1]; Available from: https://pubmed.ncbi.nlm.nih.gov/35041493/
115. Gupta A, Singh J, García-Valverde A, Serrano C, Flynn DL, Smith BD. Ripretinib and MEK inhibitors synergize to induce apoptosis in preclinical models of GIST and systemic mastocytosis. Mol Cancer Ther [Internet]. 2021 Jul 1 [cited 2022 Jan 16];20(7):1234–45. Available from: https://mct.aacrjournals.org/content/20/7/1234
116. Bosbach B, Rossi F, Yozgat Y, Loo J, Zhang JQ, Berrozpe G, et al. Direct engagement of the PI3K pathway by mutant KIT dominates oncogenic signaling in gastrointestinal stromal tumor. Proc Natl Acad Sci U S A [Internet]. 2017 Oct 3 [cited 2022 Jan 16];114(40):E8448–57. Available from: https://pubmed.ncbi.nlm.nih.gov/28923937/
117. Bauer S, Duensing A, Demetri GD, Fletcher JA. KIT oncogenic signaling mechanisms in imatinib-resistant gastrointestinal stromal tumor: PI3-kinase/AKT is a crucial survival pathway. Oncogene [Internet]. 2007 Nov 29 [cited 2022 Jan 16];26(54):7560–8. Available from: https://pubmed.ncbi.nlm.nih.gov/17546049/
118. Van Looy T, Wozniak A, Floris G, Sciot R, Li H, Wellens J, et al. Phosphoinositide 3-kinase inhibitors combined with imatinib in patient-derived xenograft models of gastrointestinal stromal tumors: Rationale and efficacy. Clin Cancer Res [Internet]. 2014 Dec 1 [cited 2022 Jan 16];20(23):6071–82. Available from: https://pubmed.ncbi.nlm.nih.gov/25316817/
119. Floris G, Wozniak A, Sciot R, Li H, Friedman L, Van Looy T, et al. A potent combination of the novel PI3K inhibitor, GDC-0941, with imatinib in gastrointestinal stromal tumor xenografts: Long-lasting responses after treatment withdrawal. Clin Cancer Res. 2013;19(3):620–30.
120. Dolly SO, Wagner AJ, Bendell JC, Kindler HL, Krug LM, Seiwert TY, et al. Phase I study of apitolisib (GDC-0980), dual phosphatidylinositol-3-kinase and mammalian target of rapamycin kinase inhibitor, in patients with advanced solid tumors. Clin Cancer Res [Internet]. 2016 Jun 15 [cited 2019 May 9];22(12):2874–84. Available from: http://www.ncbi.nlm.nih.gov/pubmed/26787751
121. NIH/U.S. National Library of Medicine. A dose-finding study of a combi- nation of imatinib and BKM120 in the treatment of 3rd line GIST patients. [Internet]. Available from:

https://www.clinicaltrials.gov/ct2/show/NCT01735968

122. NIH/U.S. National Library of Medicine. A dose-finding study of a combination of imatinib and BYL719 in the treatment of 3rd line GIST patients.
123. García-Valverde A, Rosell J, Serna G, Valverde C, Carles J, Nuciforo P, et al. Preclinical activity of PI3K inhibitor copanlisib in gastrointestinal stromal tumor. Mol Cancer Ther [Internet]. 2020 Jun 1 [cited 2022 Jan 16];19(6):1289–97. Available from: https://mct.aacrjournals.org/content/19/6/1289
124. Jokinen E, Koivunen JP. MEK and PI3K inhibition in solid tumors: Rationale and evidence to date [Internet]. Vol. 7, Therapeutic Advances in Medical Oncology. Ther Adv Med Oncol; 2015 [cited 2022 Jan 17]. p. 170–80. Available from: https://pubmed.ncbi.nlm.nih.gov/26673580/
125. Azaro A, Marino D, Garrido-Castro A, Cruz C, Alsina M, Perez J, et al. 386 PI3K and MEK inhibitor combination toxicities and relative dose intensity: Vall d'Hebron experience. Eur J Cancer [Internet]. 2014 Nov 1 [cited 2022 Jan 17];50:124. Available from: http://www.ejcancer.com/article/S095980491470512X/fulltext
126. Bardia A, Gounder M, Rodon J, Janku F, Lolkema MP, Stephenson JJ, et al. Phase Ib Study of Combination Therapy with MEK Inhibitor Binimetinib and Phosphatidylinositol 3-Kinase Inhibitor Buparlisib in Patients with Advanced Solid Tumors with RAS/RAF Alterations. Oncologist [Internet]. 2020 Jan 1 [cited 2022 Jan 18];25(1):e160–9. Available from: https://pubmed.ncbi.nlm.nih.gov/31395751/
127. Kaestner KH, Knöchel W, Martínez DE. Unified nomenclature for the winged helix/forkhead transcription factors [Internet]. Vol. 14, Genes and Development. Cold Spring Harbor Laboratory Press; 2000 [cited 2022 Jan 20]. p. 142–6. Available from: http://genesdev.cshlp.org/content/14/2/142.full
128. Brunet A, Bonni A, Zigmond MJ, Lin MZ, Juo P, Hu LS, et al. Akt promotes cell survival by phosphorylating and inhibiting a forkhead transcription factor. Cell [Internet]. 1999 Mar 19 [cited 2022 Jan 20];96(6):857–68. Available from: https://pubmed.ncbi.nlm.nih.gov/10102273/
129. Stitt TN, Drujan D, Clarke BA, Panaro F, Timofeyva Y, Kline WO, et al. The IGF-1/PI3K/Akt pathway prevents expression of muscle atrophy-induced ubiquitin ligases by inhibiting FOXO transcription factors. Mol Cell. 2004 May 7;14(3):395–403.
130. Webb AE, Brunet A. FOXO transcription factors: Key regulators of cellular quality control [Internet]. Vol. 39, Trends in Biochemical Sciences. NIH Public Access; 2014 [cited 2022 Jan 19]. p. 159–69. Available from: /pmc/articles/PMC4021867/
131. Greer EL, Oskoui PR, Banko MR, Maniar JM, Gygi MP, Gygi SP, et al. The energy sensor AMP-activated protein kinase directly regulates the mammalian FOXO3 transcription factor. J Biol Chem [Internet]. 2007 Oct 12 [cited 2022 Jan 20];282(41):30107–19. Available from: https://pubmed.ncbi.nlm.nih.gov/17711846/
132. Essers MAG, Weijzen S, De Vries-Smits AMM, Saarloos I, De Ruiter ND, Bos JL, et al. FOXO transcription factor activation by oxidative stress mediated by the small GTPase Ral and JNK. EMBO J [Internet]. 2004 Dec 8 [cited 2022 Jan 20];23(24):4802–12. Available from: https://pubmed.ncbi.nlm.nih.gov/15538382/
133. Yang JY, Zong CS, Xia W, Yamaguchi H, Ding Q, Xie X, et al. ERK promotes tumorigenesis by inhibiting FOXO3a via MDM2-mediated degradation. Nat Cell Biol [Internet]. 2008 Feb [cited 2022 Jan 20];10(2):138–48. Available from: https://pubmed.ncbi.nlm.nih.gov/18204439/
134. Consolaro F, Ghaem-Maghami S, Bortolozzi R, Zona S, Khongkow M, Basso G, et al. FOXO3a

and posttranslational modifications mediate glucocorticoid sensitivity in B-ALL. Mol Cancer Res [Internet]. 2015 Dec 1 [cited 2022 Jan 20];13(12):1578–90. Available from: https://pubmed.ncbi.nlm.nih.gov/26376801/

135. Marzi L, Combes E, Vié N, Ayrolles-Torro A, Tosi D, Desigaud D, et al. FOXO3a and the MAPK p38 are activated by cetuximab to induce cell death and inhibit cell proliferation and their expression predicts cetuximab efficacy in colorectal cancer. Br J Cancer [Internet]. 2016 Nov 8 [cited 2022 Jan 20];115(10):1223–33. Available from: https://pubmed.ncbi.nlm.nih.gov/27685445/
136. Chapuis N, Park S, Leotoing L, Tamburini J, Verdier F, Bardet V, et al. IκB kinase overcomes PI3K/Akt and ERK/MAPK to control FOXO3a activity in acute myeloid leukemia. Blood [Internet]. 2010 Nov 18 [cited 2022 Jan 20];116(20):4240–50. Available from: https://pubmed.ncbi.nlm.nih.gov/20671123/
137. Roy SK, Srivastava RK, Shankar S. Inhibition of PI3K/AKT and MAPK/ERK pathways causes activation of FOXO transcription factor, leading to cell cycle arrest and apoptosis in pancreatic cancer. J Mol Signal [Internet]. 2010 Jul 19 [cited 2022 Jan 20];5. Available from: https://pubmed.ncbi.nlm.nih.gov/20642839/
138. Gordon PM, Fisher DE. Role for the proapoptotic factor BIM in mediating imatinib-induced apoptosis in a c-KIT-dependent gastrointestinal stromal tumor cell line. J Biol Chem [Internet]. 2010 May 7 [cited 2022 Jan 20];285(19):14109–14. Available from: https://pubmed.ncbi.nlm.nih.gov/20231287/
139. Kelly CM, Shoushtari AN, Qin LX, D'Angelo SP, Dickson MA, Gounder MM, et al. A phase Ib study of BGJ398, a pan-FGFR kinase inhibitor in combination with imatinib in patients with advanced gastrointestinal stromal tumor. Invest New Drugs [Internet]. 2019 Apr 15 [cited 2022 Jan 17];37(2):282–90. Available from: https://pubmed.ncbi.nlm.nih.gov/30101387/
140. Cohen NA, Zeng S, Seifert AM, Kim TS, Sorenson EC, Greer JB, et al. Pharmacological inhibition of KIT activates MET signaling in gastrointestinal stromal tumors. Cancer Res [Internet]. 2015 May 15 [cited 2022 Jan 17];75(10):2061–70. Available from: /pmc/articles/PMC4467991/
141. Schöffski P, Mir O, Kasper B, Papai Z, Blay JY, Italiano A, et al. Activity and safety of the multi-target tyrosine kinase inhibitor cabozantinib in patients with metastatic gastrointestinal stromal tumour after treatment with imatinib and sunitinib: European Organisation for Research and Treatment of Cancer phase II tri. Eur J Cancer. 2020 Jul 1;134:62–74.
142. Tu Y, Zuo R, Ni N, Eilers G, Wu D, Pei Y, et al. Activated tyrosine kinases in gastrointestinal stromal tumor with loss of KIT oncoprotein expression. Cell Cycle [Internet]. 2018 Dec 2 [cited 2022 Jan 17];17(23):2577–92. Available from: https://pubmed.ncbi.nlm.nih.gov/30488756/
143. Miller MA, Oudin MJ, Sullivan RJ, Wang SJ, Meyer AS, Im H, et al. Reduced proteolytic shedding of receptor tyrosine kinases is a post-translational mechanism of kinase inhibitor resistance. Cancer Discov [Internet]. 2016 Apr 1 [cited 2022 Jan 17];6(4):383–99. Available from: https://cancerdiscovery.aacrjournals.org/content/6/4/382
144. Weiss F, Lauffenburger D, Friedl P. Towards targeting of shared mechanisms of cancer metastasis and therapy resistance. Nat Rev Cancer [Internet]. 2022 Jan 10 [cited 2022 Jan 17]; Available from: https://pubmed.ncbi.nlm.nih.gov/35013601/
145. Liu Y, Perdreau SA, Chatterjee P, Wang L, Kuan SF, Duensing A. Imatinib mesylate induces quiescence in gastrointestinal stromal tumor cells through the CDH1-SKP2-p27Kip1 signaling axis. Cancer Res [Internet]. 2008 Nov 1 [cited 2022 Jan 17];68(21):9015–23. Available from:

https://pubmed.ncbi.nlm.nih.gov/18974147/

146. Boichuk S, Parry JA, Makielski KR, Litovchick L, Baron JL, Zewe JP, et al. The DREAM complex mediates GIST cell quiescence and is a novel therapeutic target to enhance imatinib-induced apoptosis. Cancer Res [Internet]. 2013 Aug 15 [cited 2022 Jan 17];73(16):5120–9. Available from: https://pubmed.ncbi.nlm.nih.gov/23786773/
147. Gupta A, Roy S, Lazar AJF, Wang WL, McAuliffe JC, Reynoso D, et al. Autophagy inhibition and antimalarials promote cell death in gastrointestinal stromal tumor (GIST). Proc Natl Acad Sci U S A [Internet]. 2010 Aug 10 [cited 2022 Jan 17];107(32):14333–8. Available from: https://pubmed.ncbi.nlm.nih.gov/20660757/
148. Diaz LA, Williams RT, Wu J, Kinde I, Hecht JR, Berlin J, et al. The molecular evolution of acquired resistance to targeted EGFR blockade in colorectal cancers. Nature [Internet]. 2012 Jun 13 [cited 2022 Jan 17];486(7404):537–40. Available from: https://www.nature.com/articles/nature11219
149. Russo M, Crisafulli G, Sogari A, Reilly NM, Arena S, Lamba S, et al. Adaptive mutability of colorectal cancers in response to targeted therapies. Science (80-) [Internet]. 2019 Dec 20 [cited 2022 Jan 17];366(6472):1473–80. Available from: https://pubmed.ncbi.nlm.nih.gov/31699882/
150. Cipponi A, Goode DL, Bedo J, McCabe MJ, Pajic M, Croucher DR, et al. MTOR signaling orchestrates stress-induced mutagenesis, facilitating adaptive evolution in cancer. Science (80-) [Internet]. 2020 Jun 5 [cited 2022 Jan 17];368(6495):1127–31. Available from: https://pubmed.ncbi.nlm.nih.gov/32499442/
151. Shen M, Schmitt S, Buac D, Dou QP. Targeting the ubiquitin-proteasome system for cancer therapy [Internet]. Vol. 17, Expert Opinion on Therapeutic Targets. Expert Opin Ther Targets; 2013 [cited 2022 Jan 17]. p. 1091–108. Available from: https://pubmed.ncbi.nlm.nih.gov/23822887/
152. Rausch JL, Ali AA, Lee DM, Gebreyohannes YK, Mehalek KR, Agha A, et al. Differential antitumor activity of compounds targeting the ubiquitin-proteasome machinery in gastrointestinal stromal tumor (GIST) cells. Sci Rep [Internet]. 2020 Mar 20 [cited 2022 Jan 17];10(1):1–14. Available from: https://www.nature.com/articles/s41598-020-62088-7
153. Park J, Cho J, Song EJ. Ubiquitin–proteasome system (UPS) as a target for anticancer treatment [Internet]. Vol. 43, Archives of Pharmacal Research. Arch Pharm Res; 2020 [cited 2022 Jan 17]. p. 1144–61. Available from: https://pubmed.ncbi.nlm.nih.gov/33165832/
154. Gupta I, Singh K, Varshney NK, Khan S. Delineating crosstalk mechanisms of the ubiquitin proteasome system that regulate apoptosis. Vol. 6, Frontiers in Cell and Developmental Biology. Frontiers Media S.A.; 2018. p. 11.
155. Lorick KL, Jensen JP, Fang S, Ong AM, Hatakeyama S, Weissman AM. RING fingers mediate ubiquitin-conjugating enzyme (E2)-dependent ubiquitination. Proc Natl Acad Sci U S A [Internet]. 1999 Sep 28 [cited 2022 Jan 17];96(20):11364–9. Available from: https://pubmed.ncbi.nlm.nih.gov/10500182/
156. Lydeard JR, Schulman BA, Harper JW. Building and remodelling Cullin-RING E3 ubiquitin ligases [Internet]. Vol. 14, EMBO Reports. EMBO Rep; 2013 [cited 2022 Jan 17]. p. 1050–61. Available from: https://pubmed.ncbi.nlm.nih.gov/24232186/
157. Wang D, Ma L, Wang B, Liu J, Wei W. E3 ubiquitin ligases in cancer and implications for therapies. Cancer Metastasis Rev [Internet]. 2017 Dec 1 [cited 2022 Jan 17];36(4):683–702. Available from: https://pubmed.ncbi.nlm.nih.gov/29043469/
158. Whitesell L, Lindquist SL. HSP90 and the chaperoning of cancer [Internet]. Vol. 5, Nature Reviews

Cancer. Nat Rev Cancer; 2005 [cited 2022 Jan 17]. p. 761–72. Available from: https://pubmed.ncbi.nlm.nih.gov/16175177/

159. Bauer S, Yu LK, Demetri GD, Fletcher JA. Heat shock protein 90 inhibition in imatinib-resistant gastrointestinal stromal tumor. Cancer Res. 2006;66(18):9153–61.
160. Floris G, Sciot R, Wozniak A, Van Looy T, Wellens J, Faa G, et al. The novel HSP90 inhibitor, IPI-493, is highly effective in human gastrostrointestinal stromal tumor xenografts carrying heterogeneous KIT mutations. Clin Cancer Res [Internet]. 2011 Sep 1 [cited 2022 Jan 17];17(17):5604–14. Available from: https://pubmed.ncbi.nlm.nih.gov/21737509/
161. Floris G, Debiec-Rychter M, Wozniak A, Stefan C, Normant E, Faa G, et al. The heat shock protein 90 inhibitor IPI-504 induces KIT degradation, tumor shrinkage, and cell proliferation arrest in xenograft models of gastrointestinal stromal tumors. Mol Cancer Ther [Internet]. 2011 Oct [cited 2022 Jan 17];10(10):1897–908. Available from: https://pubmed.ncbi.nlm.nih.gov/21825009/
162. Smyth T, Van Looy T, Curry JE, Rodriguez-Lopez AM, Wozniak A, Zhu M, et al. The HSP90 Inhibitor, AT13387, Is Effective against Imatinib-Sensitive and -Resistant Gastrointestinal Stromal Tumor Models. Mol Cancer Ther [Internet]. 2012;11(8):1799–808. Available from: http://mct.aacrjournals.org/cgi/doi/10.1158/1535-7163.MCT-11-1046
163. Wagner AJ, Chugh R, Rosen LS, Morgan JA, George S, Gordon M, et al. A phase i study of the HSP90 inhibitor retaspimycin hydrochloride (IPI-504) in patients with gastrointestinal stromal tumors or soft-tissue sarcomas. Clin Cancer Res [Internet]. 2013 Nov 1 [cited 2022 Jan 18];19(21):6020–9. Available from: https://pubmed.ncbi.nlm.nih.gov/24045182/
164. Dickson MA, Okuno SH, Keohan ML, Maki RG, D'Adamo DR, Akhurst TJ, et al. Phase II study of the HSP90-inhibitor BIIB021 in gastrointestinal stromal tumors. Ann Oncol [Internet]. 2013 Jan [cited 2022 Jan 18];24(1):252–7. Available from: https://pubmed.ncbi.nlm.nih.gov/22898035/
165. Shapiro GI, Kwak E, Dezube BJ, Yule M, Ayrton J, Lyons J, et al. First-in-human phase i dose escalation study of a second-generation non-ansamycin HSP90 inhibitor, AT13387, in patients with advanced solid tumors. Clin Cancer Res [Internet]. 2015 Jan 1 [cited 2022 Jan 18];21(1):87–97. Available from: https://pubmed.ncbi.nlm.nih.gov/25336693/
166. Wagner AJ, Agulnik M, Heinrich MC, Mahadevan D, Riedel RF, Von Mehren M, et al. Dose-escalation study of a second-generation non-ansamycin HSP90 inhibitor, onalespib (AT13387), in combination with imatinib in patients with metastatic gastrointestinal stromal tumour. In: European Journal of Cancer [Internet]. Eur J Cancer; 2016 [cited 2022 Jan 18]. p. 94–101. Available from: https://pubmed.ncbi.nlm.nih.gov/27156227/
167. Chiang N-J, Yeh K-H, Chiu C-F, Chen J-S, Yen C-C, Lee K-D, et al. Results of Phase II trial of AUY922, a novel heat shock protein inhibitor in patients with metastatic gastrointestinal stromal tumor (GIST) and imatinib and sunitinib therapy. J Clin Oncol. 2016 Feb 1;34(4_suppl):134–134.
168. Demetri GD, Heinrich MC, Chmielowski B, Morgan JA, George S, Bradley R, et al. An open-label phase II study of the Hsp90 inhibitor ganetespib (STA-9090) in patients (pts) with metastatic and/or unresectable GIST. J Clin Oncol. 2011 May 20;29(15_suppl):10011–10011.
169. Liu Y, Tseng M, Perdreau SA, Rossi F, Antonescu C, Besmer P, et al. Histone H2AX is a mediator of gastrointestinal stromal tumor cell apoptosis following treatment with imatinib mesylate. Cancer Res. 2007;67(6):2685–92.
170. Bauer S, Parry JA, Mühlenberg T, Brown MF, Seneviratne D, Chatterjee P, et al. Proapoptotic activity of bortezomib in gastrointestinal stromal tumor cells. Cancer Res [Internet]. 2010 [cited

2020 Jan 23];70(1):150–9. Available from: http://cancerres.aacrjournals.org/

171. Maki RG, Kraft AS, Scheu K, Yamada J, Wadler S, Antonescu CR, et al. A multicenter phase II study of bortezomib in ecurrent or metastatic sarcomas. Cancer [Internet]. 2005 Apr 1 [cited 2022 Jan 18];103(7):1431–8. Available from: https://pubmed.ncbi.nlm.nih.gov/15739208/
172. Bahleda R, Le Deley MC, Bernard A, Chaturvedi S, Hanley M, Poterie A, et al. Phase I trial of bortezomib daily dose: safety, pharmacokinetic profile, biological effects and early clinical evaluation in patients with advanced solid tumors. Invest New Drugs [Internet]. 2018 Aug 1 [cited 2022 Jan 18];36(4):619–28. Available from: https://pubmed.ncbi.nlm.nih.gov/29094232/
173. Deming DA, Ninan J, Bailey HH, Kolesar JM, Eickhoff J, Reid JM, et al. A Phase i study of intermittently dosed vorinostat in combination with bortezomib in patients with advanced solid tumors. Invest New Drugs [Internet]. 2014 [cited 2022 Jan 18];32(2):323–9. Available from: https://pubmed.ncbi.nlm.nih.gov/24114123/
174. Papandreou CN, Daliani DD, Nix D, Yang H, Madden T, Wang X, et al. Phase I trial of the proteasome inhibitor bortezomib in patients with advanced solid tumors with observations in androgen-independent prostate cancer. J Clin Oncol [Internet]. 2004 [cited 2022 Jan 18];22(11):2108–21. Available from: https://pubmed.ncbi.nlm.nih.gov/15169797/
175. Rausch JL, Ali AA, Lee DM, Gebreyohannes YK, Mehalek KR, Agha A, et al. Differential antitumor activity of compounds targeting the ubiquitin-proteasome machinery in gastrointestinal stromal tumor (GIST) cells. Sci Rep [Internet]. 2020 Mar 20 [cited 2022 Jan 18];10(1):1–14. Available from: https://www.nature.com/articles/s41598-020-62088-7
176. Gomes MD, Lecker SH, Jagoe RT, Navon A, Goldberg AL. Atrogin-1, a muscle-specific F-box protein highly expressed during muscle atrophy. Proc Natl Acad Sci U S A [Internet]. 2001 Dec 4 [cited 2022 Jan 18];98(25):14440–5. Available from: https://pubmed.ncbi.nlm.nih.gov/11717410/
177. Kipreos ET, Pagano M. The F-box protein family [Internet]. Vol. 1, Genome Biology. Genome Biol; 2000 [cited 2022 Jan 18]. p. XIX–XX. Available from: https://pubmed.ncbi.nlm.nih.gov/11178263/
178. Yuan L, Han J, Meng Q, Xi Q, Zhuang Q, Jiang Y, et al. Muscle-specific E3 ubiquitin ligases are involved in muscle atrophy of cancer cachexia: An in vitro and in vivo study. Oncol Rep. 2015 May 1;33(5):2261–8.
179. Mota R, Rodríguez JE, Bonetto A, O'Connell TM, Asher SA, Parry TL, et al. Post-translationally modified muscle-specific ubiquitin ligases as circulating biomarkers in experimental cancer cachexia. Am J Cancer Res [Internet]. 2017 [cited 2022 Jan 18];7(9):1948–58. Available from: /pmc/articles/PMC5622228/
180. Milan G, Romanello V, Pescatore F, Armani A, Paik JH, Frasson L, et al. Regulation of autophagy and the ubiquitin-proteasome system by the FoxO transcriptional network during muscle atrophy. Nat Commun [Internet]. 2015 Apr 10 [cited 2022 Jan 18];6(1):1–14. Available from: https://www.nature.com/articles/ncomms7670
181. Reed SA, Sandesara PB, Senf SM, Judge AR. Inhibition of FoxO transcriptional activity prevents muscle fiber atrophy during cachexia and induces hypertrophy. FASEB J [Internet]. 2012 Mar [cited 2022 Jan 18];26(3):987–1000. Available from: https://pubmed.ncbi.nlm.nih.gov/22102632/
182. Zhang G, Jin B, Li YP. C/EBPβ mediates tumour-induced ubiquitin ligase atrogin1/MAFbx upregulation and muscle wasting. EMBO J [Internet]. 2011 Oct 19 [cited 2022 Jan 18];30(20):4323–35. Available from: /pmc/articles/PMC3199382/
183. Lagirand-Cantaloube J, Offner N, Csibi A, Leibovitch MP, Batonnet-Pichon S, Tintignac LA, et al.

The initiation factor eIF3-f is a major target for Atrogin1/MAFbx function in skeletal muscle atrophy. EMBO J [Internet]. 2008 Apr 23 [cited 2022 Jan 18];27(8):1266–76. Available from: /pmc/articles/PMC2367397/

184. Tintignac LA, Lagirand J, Batonnet S, Sirri V, Leibovitch MP, Leibovitch SA. Degradation of MyoD mediated by the SCF (MAFbx) ubiquitin ligase. J Biol Chem [Internet]. 2005 Jan 28 [cited 2022 Jan 18];280(4):2847–56. Available from: http://www.jbc.org/article/S0021925820763362/fulltext
185. Lagirand-Cantaloube J, Cornille K, Csibi A, Batonnet-Pinchon S, Leibovitch MP, Leibovitch SA. Inhibition of atrogin-1/MAFbx mediated MyoD proteolysis prevents skeletal muscle atrophy in vivo. PLoS One [Internet]. 2009 Mar 25 [cited 2022 Jan 18];4(3). Available from: /pmc/articles/PMC2656614/
186. Lokireddy S, Wijesoma IW, Sze SK, McFarlane C, Kambadur R, Sharma M. Identification of atrogin-1-targeted proteinsθδ during the myostatin-induced skeletal muscle wasting. Am J Physiol - Cell Physiol [Internet]. 2012 [cited 2022 Jan 18];303(5). Available from: https://pubmed.ncbi.nlm.nih.gov/22673621/
187. Sandri M, Sandri C, Gilbert A, Skurk C, Calabria E, Picard A, et al. Foxo transcription factors induce the atrophy-related ubiquitin ligase atrogin-1 and cause skeletal muscle atrophy. Cell [Internet]. 2004 Apr 30 [cited 2022 Jan 18];117(3):399–412. Available from: https://pubmed.ncbi.nlm.nih.gov/15109499/
188. Chou JL, Su HY, Chen LY, Liao YP, Hartman-Frey C, Lai YH, et al. Promoter hypermethylation of FBXO32, a novel TGF-B/SMAD4 target gene and tumor suppressor, is associated with poor prognosis in human ovarian cancer. Lab Investig [Internet]. 2010 Mar [cited 2022 Jan 18];90(3):414–25. Available from: https://pubmed.ncbi.nlm.nih.gov/20065949/
189. Li HH, Willis MS, Lockyer P, Miller N, McDonough H, Glass DJ, et al. Atrogin-1 inhibits Akt-dependent cardiac hypertrophy in mice via ubiquitin-dependent coactivation of Forkhead proteins. J Clin Invest [Internet]. 2007 Nov 1 [cited 2022 Jan 18];117(11):3211–23. Available from: https://pubmed.ncbi.nlm.nih.gov/17965779/
190. Guo W, Zhang M, Guo Y, Shen S, Guo X, Dong Z. FBXO32, a new TGF-β/Smad signaling pathway target gene, is epigenetically inactivated in gastric cardia adenocarcinoma. Neoplasma. 2015;62(4):646–57.
191. Mei Z, Zhang D, Hu B, Wang J, Shen X, Xiao W. FBXO32 targets c-Myc for proteasomal degradation and inhibits c-Myc activity. J Biol Chem [Internet]. 2015 Jun 26 [cited 2022 Jan 18];290(26):16202–14. Available from: https://pubmed.ncbi.nlm.nih.gov/25944903/
192. Tan J, Yang X, Zhuang L, Jiang X, Chen W, Puay LL, et al. Pharmacologic disruption of polycomb-repressive complex 2-mediated gene repression selectively induces apoptosis in cancer cells. Genes Dev [Internet]. 2007 May 1 [cited 2022 Jan 18];21(9):1050–63. Available from: https://pubmed.ncbi.nlm.nih.gov/17437993/
193. Wu Z, Lee ST, Qiao Y, Li Z, Lee PL, Lee YJ, et al. Polycomb protein EZH2 regulates cancer cell fate decision in response to DNA damage. Cell Death Differ [Internet]. 2011 Nov [cited 2022 Jan 18];18(11):1771–9. Available from: https://pubmed.ncbi.nlm.nih.gov/21546904/
194. Ciarapica R, De Salvo M, Carcarino E, Bracaglia G, Adesso L, Leoncini PP, et al. The Polycomb group (PcG) protein EZH2 supports the survival of PAX3-FOXO1 alveolar rhabdomyosarcoma by repressing FBXO32 (Atrogin1/MAFbx). Oncogene [Internet]. 2014 Aug 7 [cited 2022 Jan 18];33(32):4173–84. Available from: https://pubmed.ncbi.nlm.nih.gov/24213577/

195. Taylor BS, Barretina J, Maki RG, Antonescu CR, Singer S, Ladanyi M. Advances in sarcoma genomics and new therapeutic targets [Internet]. Vol. 11, Nature Reviews Cancer. Nat Rev Cancer; 2011 [cited 2022 Jan 30]. p. 541–57. Available from: https://pubmed.ncbi.nlm.nih.gov/21753790/
196. Serrano C, Mariño-Enríquez A, Tao DL, Ketzer J, Eilers G, Zhu M, et al. Complementary activity of tyrosine kinase inhibitors against secondary kit mutations in imatinib-resistant gastrointestinal stromal tumours. Br J Cancer. 2019 Mar 19;120(6):612–20.
197. Taguchi T, Sonobe H, Toyonaga SI, Yamasaki I, Shuin T, Takano A, et al. Conventional and molecular cytogenetic characterization of a new human cell line, GIST-T1, established from gastrointestinal stromal tumor. Lab Investig [Internet]. 2002 May 1 [cited 2022 Jan 18];82(5):663–5. Available from: https://www.nature.com/articles/3780461
198. Garner AP, Gozgit JM, Anjum R, Vodala S, Schrock A, Zhou T, et al. Ponatinib inhibits polyclonal drug-resistant KIT oncoproteins and shows therapeutic potential in heavily pretreated gastrointestinal stromal tumor (GIST) patients. Clin Cancer Res [Internet]. 2014 Nov 15 [cited 2022 Jan 18];20(22):5745–55. Available from: https://clincancerres.aacrjournals.org/content/20/22/5745
199. Schindelin J, Arganda-Carreras I, Frise E, Kaynig V, Longair M, Pietzsch T, et al. Fiji: An open-source platform for biological-image analysis [Internet]. Vol. 9, Nature Methods. Nature Publishing Group; 2012 [cited 2022 Jan 18]. p. 676–82. Available from: https://www.nature.com/articles/nmeth.2019
200. Maurel J, López-Pousa A, Calabuig S, Bagué S, del Muro XG, Sanjuan X, et al. Phosphorylated-insulin growth factor I receptor (p-IGF1R) and metalloproteinase-3 (MMP3) expression in advanced gastrointestinal stromal tumors (GIST). A GEIS 19 study. Clin Sarcoma Res [Internet]. 2016 Dec [cited 2022 Jan 18];6(1). Available from: https://pubmed.ncbi.nlm.nih.gov/27358721/
201. Vitiello GA, Bowler TG, Liu M, Medina BD, Zhang JQ, Param NJ, et al. Differential immune profiles distinguish the mutational subtypes of gastrointestinal stromal tumor. J Clin Invest [Internet]. 2019 May 1 [cited 2022 Jan 18];129(5):1863–77. Available from: https://pubmed.ncbi.nlm.nih.gov/30762585/
202. Wang D, Zhang Q, Blanke CD, Demetri GD, Heinrich MC, Watson JC, et al. Phase II trial of neoadjuvant/adjuvant imatinib mesylate for advanced primary and metastatic/recurrent operable gastrointestinal stromal tumors: Long-term follow-up results of radiation therapy oncology group 0132. Ann Surg Oncol [Internet]. 2012 Apr [cited 2022 Jan 18];19(4):1074–80. Available from: https://pubmed.ncbi.nlm.nih.gov/22203182/
203. Ritchie ME, Phipson B, Wu D, Hu Y, Law CW, Shi W, et al. Limma powers differential expression analyses for RNA-sequencing and microarray studies. Nucleic Acids Res [Internet]. 2015 Jan 6 [cited 2022 Jan 18];43(7):e47. Available from: https://pubmed.ncbi.nlm.nih.gov/25605792/
204. Frolov A, Chahwan S, Ochs M, Arnoletti JP, Pan ZZ, Favorova O, et al. Response markers and the molecular mechanisms of action of gleevec in gastrointestinal stromal tumors. Mol Cancer Ther. 2003 Aug;2(8):699–709.
205. Van Der Horst A, Burgering BMT. Stressing the role of FoxO proteins in lifespan and disease [Internet]. Vol. 8, Nature Reviews Molecular Cell Biology. Nat Rev Mol Cell Biol; 2007 [cited 2022 Jan 18]. p. 440–50. Available from: https://pubmed.ncbi.nlm.nih.gov/17522590/
206. Yang JY, Zong CS, Xia W, Yamaguchi H, Ding Q, Xie X, et al. ERK promotes tumorigenesis by inhibiting FOXO3a via MDM2-mediated degradation. Nat Cell Biol [Internet]. 2008 Feb [cited 2022

Jan 18];10(2):138–48. Available from: https://pubmed.ncbi.nlm.nih.gov/18204439/

207. Tenbaum SP, Ordóñez-Morán P, Puig I, Chicote I, Arqués O, Landolfi S, et al. β-Catenin confers resistance to PI3K and AKT inhibitors and subverts FOXO3a to promote metastasis in colon cancer. Nat Med [Internet]. 2012 Jun [cited 2022 Jan 18];18(6):892–901. Available from: https://pubmed.ncbi.nlm.nih.gov/22610277/
208. Cardozo T, Pagano M. The SCF ubiquitin ligase: Insights into a molecular machine [Internet]. Vol. 5, Nature Reviews Molecular Cell Biology. Nature Publishing Group; 2004 [cited 2022 Jan 18]. p. 739–51. Available from: https://www.nature.com/articles/nrm1471
209. Hyer ML, Milhollen MA, Ciavarri J, Fleming P, Traore T, Sappal D, et al. A small-molecule inhibitor of the ubiquitin activating enzyme for cancer treatment. Nat Med [Internet]. 2018 Jan 15 [cited 2022 Jan 18];24(2):186–93. Available from: https://www.nature.com/articles/nm.4474
210. Jin J, Li X, Gygi SP, Harper JW. Dual E1 activation systems for ubiquitin differentially regulate E2 enzyme charging. Nature [Internet]. 2007 Jun 28 [cited 2022 Jan 18];447(7148):1135–8. Available from: https://pubmed.ncbi.nlm.nih.gov/17597759/
211. Hemming ML, Lawlor MA, Zeid R, Lesluyes T, Fletcher JA, Raut CP, et al. Gastrointestinal stromal tumor enhancers support a transcription factor network predictive of clinical outcome. Proc Natl Acad Sci [Internet]. 2018;115(25):E5746–55. Available from: http://www.pnas.org/lookup/doi/10.1073/pnas.1802079115
212. Serrano C, Leal A, Kuang Y, Morgan JA, Barysauskas CM, Phallen J, et al. Phase I study of rapid alternation of sunitinib and regorafenib for the treatment of tyrosine kinase inhibitor refractory gastrointestinal stromal tumors. Clin Cancer Res. 2019;25(24):7287–93.
213. Bauer S, Duensing A, Demetri GD, Fletcher JA. KIT oncogenic signaling mechanisms in imatinib-resistant gastrointestinal stromal tumor: PI3-kinase/AKT is a crucial survival pathway. Oncogene [Internet]. 2007 Nov 29 [cited 2020 Nov 1];26(54):7560–8. Available from: www.nature.com/onc
214. Bosbach B, Rossi F, Yozgat Y, Loo J, Zhang JQ, Berrozpe G, et al. Direct engagement of the PI3K pathway by mutant KIT dominates oncogenic signaling in gastrointestinal stromal tumor. Proc Natl Acad Sci [Internet]. 2017;201711449. Available from: http://www.pnas.org/lookup/doi/10.1073/pnas.1711449114
215. Jia S, Liu Z, Zhang S, Liu P, Zhang L, Lee SH, et al. Essential roles of PI(3)K-p110β in cell growth, metabolism and tumorigenesis. Nature [Internet]. 2008 Aug 7 [cited 2022 Jan 30];454(7205):776–9. Available from: https://pubmed.ncbi.nlm.nih.gov/18594509/
216. Ali K, Bilancio A, Thomas M, Pearce W, Gilfillan AM, Tkaczyk C, et al. Essential role for the p110δ phosphoinositide 3-kinase in the allergic response. Nature [Internet]. 2004 Oct 21 [cited 2022 Jan 30];431(7011):1007–11. Available from: https://pubmed.ncbi.nlm.nih.gov/15496927/
217. She QB, Chandarlapaty S, Ye Q, Lobo J, Haskell KM, Leander KR, et al. Breast tumor cells with P13K mutation or HER2 amplification are selectively addicted to Akt signaling. PLoS One [Internet]. 2008 Aug 26 [cited 2022 Jan 30];3(8). Available from: /pmc/articles/PMC2516933/
218. Prahallad A, Sun C, Huang S, Di Nicolantonio F, Salazar R, Zecchin D, et al. Unresponsiveness of colon cancer to BRAF(V600E) inhibition through feedback activation of EGFR. Nature [Internet]. 2012 Mar 1 [cited 2022 Jan 30];483(7387):100–4. Available from: https://pubmed.ncbi.nlm.nih.gov/22281684/
219. Will M, Qin ACR, Toy W, Yao Z, Rodrik-Outmezguine V, Schneider C, et al. Rapid induction of apoptosis by PI3K inhibitors is dependent upon their transient inhibition of RAS-ERK signaling.

Cancer Discov [Internet]. 2014 [cited 2022 Jan 30];4(3):334–48. Available from: /pmc/articles/PMC4049524/

220. Manning BD, Toker A. AKT/PKB Signaling: Navigating the Network [Internet]. Vol. 169, Cell. Cell; 2017 [cited 2022 Jan 30]. p. 381–405. Available from: https://pubmed.ncbi.nlm.nih.gov/28431241/
221. Ran L, Chen Y, Sher J, Wong EWP, Murphy D, Zhang JQ, et al. FOXF1 defines the core-regulatory circuitry in gastrointestinal stromal tumor. Cancer Discov [Internet]. 2018 [cited 2020 Feb 13];8(2):234–51. Available from: www.aacrjournals.org
222. Chou JL, Su HY, Chen LY, Liao YP, Hartman-Frey C, Lai YH, et al. Promoter hypermethylation of FBXO32, a novel TGF-B/SMAD4 target gene and tumor suppressor, is associated with poor prognosis in human ovarian cancer. Lab Investig [Internet]. 2010 Mar [cited 2021 Nov 11];90(3):414–25. Available from: https://pubmed.ncbi.nlm.nih.gov/20065949/
223. Guo W, Zhang M, Shen S, Guo Y, Kuang G, Yang Z, et al. Aberrant methylation and decreased expression of the TGF-β/Smad target gene FBXO32 in esophageal squamous cell carcinoma. Cancer [Internet]. 2014 Aug 15 [cited 2022 Jan 18];120(16):2412–23. Available from: https://pubmed.ncbi.nlm.nih.gov/24798237/
224. Zhou H, Liu Y, Zhu R, DIng F, Wan Y, Li Y, et al. FBXO32 suppresses breast cancer tumorigenesis through targeting KLF4 to proteasomal degradation. Oncogene [Internet]. 2017 Jun 8 [cited 2022 Jan 30];36(23):3312–21. Available from: https://pubmed.ncbi.nlm.nih.gov/28068319/
225. Meshram SN, Paul D, Manne R, Choppara S, Sankaran G, Agrawal Y, et al. FBXO32 activates NF-κB through IκBα degradation in inflammatory and genotoxic stress. Int J Biochem Cell Biol [Internet]. 2017 Nov 1 [cited 2022 Feb 7];92:134–40. Available from: https://pubmed.ncbi.nlm.nih.gov/28970077/
226. Sahu SK, Tiwari N, Pataskar A, Zhuang Y, Borisova M, Diken M, et al. FBXO32 promotes microenvironment underlying epithelial-mesenchymal transition via CtBP1 during tumour metastasis and brain development. Nat Commun [Internet]. 2017;8(1):1–18. Available from: http://dx.doi.org/10.1038/s41467-017-01366-x
227. Zheng N, Wang Z, Wei W. Ubiquitination-mediated degradation of cell cycle-related proteins by F-box proteins [Internet]. Vol. 73, International Journal of Biochemistry and Cell Biology. NIH Public Access; 2016 [cited 2022 Mar 2]. p. 99–110. Available from: /pmc/articles/PMC4798898/
228. Kannt A, Đikić I. Expanding the arsenal of E3 ubiquitin ligases for proximity-induced protein degradation. Vol. 28, Cell Chemical Biology. Cell Press; 2021. p. 1014–31.